

WIND TUNNEL STUDY OF DOWNWASH AT THE
BAY SHORE POWER STATION

by

R. L. Petersen¹⁾ and J. E. Cermak²⁾

for

The Toledo Edison Company
300 Madison Avenue
Toledo, Ohio 43652

Fluid Mechanics and Wind Engineering Program
Fluid Dynamics and Diffusion Laboratory
Department of Civil Engineering
Colorado State University
Fort Collins, Colorado 80523

April 1979

1) Research Assistant Professor, Fluid Dynamics
Diffusion Laboratory

2) Professor-in-Charge, Fluid Mechanics and
Wind Engineering Program

ABSTRACT

The proposed Environmental Protection Agency stack height regulation gives regional administrators the authority to require a field or fluid modeling demonstration of an air quality problem due to downwash, wakes or eddies at existing sources. If the demonstration indicates the existence of an air quality problem then an existing source which increases its stack height may employ an empirical equation to determine the stack height credit it will receive. Since Toledo Edison is replacing its existing four stacks at the Bay Shore Power Station with one taller single stack, the requirement of the regulation seemingly must be satisfied before credit for the new stack is obtained.

Toledo Edison contracted Colorado State University to conduct a fluid modeling investigation of the effect of structural generated downwash, wakes or eddies upon ground level concentrations. The tests were conducted using state of the art wind-tunnel testing procedures. Visualization and concentration measurements of the simulated plumes from the Bay Shore Power Station stacks were obtained for eight wind directions, three plant load conditions and one wind speed. For comparison several tests were run without the plant structure present.

The results of the study show that the maximum concentration is in excess of the national ambient air quality standard for SO_2 and is at least 40 percent in excess of the maximum concentration experienced in the absence of downwash, wakes, and eddy effects produced by nearby structures. The maximum concentration excess observed was approximately 650 percent.

TABLE OF CONTENTS

<u>Chapter</u>		<u>Page</u>
	ABSTRACT	i
	LIST OF TABLES	iii
	LIST OF FIGURES	iv
	LIST OF SYMBOLS	ix
1	INTRODUCTION	1
2	SUMMARY AND CONCLUSION	3
3	WIND-TUNNEL SIMILARITY REQUIREMENTS	5
4	EXPERIMENTAL PROGRAM	14
	4.1 Summary	14
	4.2 Scale Models and Wind Tunnel	15
	4.3 Flow Visualization	16
	4.4 Gas Tracer Technique	17
	4.5 Velocity and Temperature Measurements	22
5	WIND DISTRIBUTIONS AT BAY SHORE VICINITY	27
6	RESULTS	30
	6.1 Visualization	30
	6.2 Concentration Measurements	30
	6.3 Velocity Measurements	36
	REFERENCES	40
	TABLES	42
	FIGURES	54
	APPENDIX A--Concentration Data Tabulations	82
	APPENDIX B--NUS Corporation Analysis of Davis-Besse Nuclear Power Plant Wind Data	132

LIST OF TABLES

Table		Page
4.1	Model operating parameters for the Bay Shore Power Station	43
4.2	Bay Shore Power Station operating parameters	44
4.3	Description of photographic and concentration tests	45
4.4	Horizontal coordinate key	46
4.5	Vertical coordinate key	47
6.1	Maximum dimensionless concentration K and corresponding SO_2 concentration at each downwind sampling location	49
6.2	Summary of visualization and concentration results including the maximum SO_2 concentration for each case	50
6.3	Velocity profiles--data tabulation	51
6.4	Summary of velocity profile analysis	52
6.5	Values of the surface roughness parameter z_o	53

LIST OF FIGURES

<u>Figure</u>		<u>Page</u>
4.2-1	Photograph of model Bay Shore Power Station (BSPS)	55
4.2-2	Photograph of prototype Bay Shore Power Station . .	56
4.2-3	Perspective view of model Bay Short Power Station from north corner giving important dimensions . . .	57
4.2-4	Industrial wind tunnel	58
4.2-5	Wind tunnel set-up	59
4.4-1	Sampling rake used for obtaining horizontal and vertical concentration profiles	60
4.4-2	Equipment set-up for gas sampling	61
4.4-3	Schematic of gas sampling equipment set-up	62
4.5-1	Hot-film calibration curve used for obtaining velocity profiles	63
5.1-1	Map showing location of Bay Shore Power Station, the Toledo Airport and Davis-Besse Nuclear Power Plant	64
5.1-2	Percent of time wind velocity exceeds indicated level--based on Davis-Besse 76.2 m wind for periods 8/4/74-12/16/75 and 4/22/77-12/31/78; based on Davis-Besse 10.7 m wind for period 8/4/74-8/31/75	65
6.1-1	Plume visualization of BSPS for 100 percent load with the building present and wind directions of a) north, b)northeast, c) east, d) southeast, e) south, f) southwest, g) west, and h) northwest	66
6.1-2	Plume visualization of BSPS for 100 percent load cases without the building present for wind directions of a) southwest, and b) northwest	68
6.2-1a-d	Horizontal profiles of dimensionless concentration at the indicated height, z, above the tunnel floor for 100 percent load and a) northwest wind direction without buildings, b) southwest wind direction without buildings, c) southeast wind direction without buildings, and d) south wind direction with the buildings	69

<u>Figure</u>	<u>Page</u>
6.2-2a-d Vertical profiles of dimensionless concentration at the indicated downwind distance for 100 percent load and a) northwest wind direction without the buildings, b) southwest wind direction without the buildings, c) southeast wind direction with the buildings, and d) south wind direction with buildings	73
6.2-3 Atmospheric horizontal dispersion rate for neutral stability in comparison to wind tunnel results	77
6.2-4 Atmospheric vertical dispersion rate for neutral stability in comparison to wind tunnel results	78
6.2-5 Plots of K versus x/H_b for three wind directions with the buildings, one case without the buildings and one case from Huber (1976)	79
6.3-1 Vertical profiles of dimensionless velocity with the building present $[(\frac{u}{u_\infty})_w]$ and the difference in dimensionless velocity $[(\frac{u}{u_\infty})_w - (\frac{u}{u_\infty})_{w0}]$	80
6.3-2 Vertical profiles of turbulence intensity with the building $[(i_x)_w]$ and turbulence intensity difference $[(i_x)_w - (i_x)_{w0}]$	81

LIST OF SYMBOLS

<u>Symbol</u>	<u>Definition</u>	<u>Units</u>
A	Hot film calibration constant	(-)
B	Hot film calibration constant	(-)
C_p	Specific heat at constant pressure	$(m^2 s^{-2} \circ K^{-1})$
d	Diameter of hot film	(m)
D	Stack diameter	(m)
E	Hot-film voltage	(V)
E_c	Eckert number $[u_o^2 / (C_{p_o} \Delta T_o)]$	(-)
F_L	Lagrangian spectral function	(s)
Fr	Stack Froude number $[\frac{u_s}{\sqrt{g\gamma D}}]$	(-)
g	Acceleration due to gravity	(ms^{-2})
Gr	Grashof number $[\frac{gd^3(T_w - T_g)}{v_g^2 T_g}]$	(-)
h	Height of stack	(m)
H_b	Height of building	(m)
H	Effective plume altitude	(m)
$i_{x,y,z}$	Turbulence intensity in x, y or z direction [$u'/u, v'/u, w'/u$]	(1)
I	Current through wire	(a)
k	Thermal conductivity	$(Wm^{-1} \circ K^{-1})$
K	Dimensionless concentration $[\frac{x_u H_b^2}{x_o V}]$ or $[\frac{x_u H_b^2}{Q}]$	(-)
ℓ	Length	(m)
L	Length scale or Monin Obukhov length scale	(m)
n	Frequency, Power Law exponent or King's Law exponent	(varies)
Nu	Nusselt number	(-)

<u>Symbol</u>	<u>Definition</u>	<u>Units</u>
P	Pressure	(mb)
Pr	Prandtl number $\left[\frac{\nu_o \rho_o C_{p_o}}{k_a} \right]$	(-)
Q	Emission rate	(g/s)
R	Velocity ratio $[u_s/u_h]$	(-)
R _c	Hot resistance at calibration conditions	(Ω)
Re	Reynolds number $\left[\frac{L_o u_o}{\nu_o} \right]$	(-)
R _H	Film hot resistance	(Ω)
Ri	Richardson number $\frac{g}{T} \left[\frac{\frac{\partial \theta}{\partial z}}{\frac{\partial u^2}{\partial z}} \right]$	(-)
Ro	Rossby number $\left[\frac{L_o \Omega_o}{u_o} \right]$	(-)
R _o	Film resistance at reference conditions	(-)
R(τ)	Autocorrelation	(-)
t, τ, ξ	Time or time scales	(s)
T, θ	Temperature or potential temperature	(°K)
t ₁	Center of gravity of autocorrelation curve	(s)
t _o	Integral time scale	(s)
u	Ambient velocity	(m/s)
u _h	Ambient velocity at stack height, h	(m/s)
u _s	Stack exit velocity	(m/s)
u _*	Friction velocity	(m/s)
V	Volume flow	(m ³ s ⁻¹)
x, y, z	Cartesian coordinates	(-)
\bar{z}	Center of mass	(m)

Greek Symbols

<u>Symbol</u>	<u>Definition</u>	<u>Units</u>
α	Thermal coefficients of resistance	($\Omega/^{\circ}\text{K}$)
χ	Concentration	(ppm)
χ_0	Source strength	(ppm)
γ	Density ratio $[\frac{\rho_a - \rho_s}{\rho_a}]$	(-)
Λ	Length scale	(m)
ν	Kinematic viscosity	($\text{m}^2 \text{s}^{-1}$)
Ω	Angular velocity	(s^{-1})
ϕ^*	Dissipation term	(-)
ρ	Density	(gm^{-3})
σ_z, σ_y	Vertical and horizontal standard deviation of concentration distribution	(m)

Subscripts

<u>Symbol</u>	<u>Definition</u>
a	Pertaining to ambient conditions
h	Pertaining to reference height h
i,j,k	Tensor or summation indices
m	Model
o	General reference quantity or initial condition
p	Prototype
r	Reference quantity
s	Pertaining to stack exit conditions
w _o	Without building present
w	With building present
∞	Free stream

Superscripts

'	Root-mean-square of quantity
*	Dimensionless parameter

1. INTRODUCTION

The Toledo Edison Company is in the process of upgrading its emission exhaust system at the Bay Shore Power Station (BSPS) by replacing the existing four stacks with one new taller stack. The emission limit for the new stack will be set by numerical modeling using as an input the "good engineering practice" (GEP) stack height as defined in Section 123 of the 1977 Clean Air Act Amendment for stack height (Public Law 95-95) and proposed revisions to the regulations posted in the Federal Register, Volume 44, Number 9 (Friday, January 12, 1979, page 2608-2614). Section 123 defines GEP stack height to be

"the height necessary to insure that emissions from the stack do not result in excessive concentrations of any air pollutant in the immediate vicinity of the source as a result of atmospheric downwash, eddies, and wakes which may be created by the source itself nearby structures or nearby terrain...."

The GEP height will be used to support the state implementation plan revision request and will be used in the computer modeling to be conducted by Enviroplan, Inc.

The proposed regulation further defines GEP stack height, H_g , using the following equation.

$$H_g = H + 1.5 L$$

where

H = height of structure or nearby structure

L = lesser dimension (height or width) of the structure or nearby structure.

However, the proposed regulation also states that for existing sources with stacks below GEP, as is the Bay Shore Power Station (BSPS), "the Administrator may require a field or fluid modeling demonstration of an air quality problem attributable to downwash wakes or eddies

affecting such sources as justification for the use of the equation based GEP height."

Hence the purpose of this study is to demonstrate through physical modeling in a wind tunnel that the plumes from the existing BSPS stacks are adversely affected by the wakes, eddies or downwash of the adjacent building and also demonstrate that this effect creates an air quality problem.

Included in this report are a summary, a description of the similarity requirements for wind tunnel modeling, the experimental methods employed, and a discussion of results. A complete set of photographs and motion picture supplement this report.

2. SUMMARY AND CONCLUSIONS

The effect of the wakes, eddies and downwash due to the BSPS structure upon the plumes emitted from the four existing stacks was studied in a wind tunnel. A scale model of the plant was constructed and a metered quantity of tracer gas was released from the stacks. The resulting concentration distributions were measured for eight wind directions, one wind speed and three simulated plant load conditions (100, 85 and 70%). In addition measurements of the dispersion were also made without the building present so as to demonstrate the effect of the building upon plume dispersion. A visual record of all cases was also obtained. A series of velocity measurements were obtained to document the flow field in the wind tunnel for comparison with the profiles expected for the atmosphere.

The results of the measurement program can be summarized as follows:

- The horizontal and vertical dispersion parameters observed in the wind tunnel compared favorably with those expected for a similar stability and surface roughness in the atmosphere.
- The maximum ground level SO_2 concentration with the building present was predicted to be $4930 \mu\text{g}/\text{m}^3$ for the range of conditions studied.
- The percentage increase in maximum concentration with the building present as compared to the maximum without the building was observed to be greater than 40 percent for numerous cases and as high as 650 percent.
- The dimensionless velocity profile in the wind tunnel compares favorably with that expected for the BSPS vicinity.

The wind velocity and directions used in the wind tunnel study were verified to actually occur in the geographic area nearby BPS by analysis of actual meteorological measurements.

In conclusion the results above clearly demonstrate that the wakes, eddies and downwash generated by the BPS structures adversely affect the dispersion of the plumes from the existing stacks. The effect is of such a magnitude that 1) air quality standards are exceeded, and 2) the percent increase in ground level concentrations due to the structure is greater than 40 percent. Items 1 and 2 above are the necessary criteria that must be met according to the stack height regulations before Toledo Edison can receive credit for that portion of their new stack that is "good engineering practice."

3 WIND-TUNNEL SIMILARITY REQUIREMENTS

The basic equations governing atmospheric and plume motion (conservation of mass, momentum and energy) may be expressed in the following dimensionless form (Cermak, 1974; Snyder, 1972).

$$\frac{\partial \rho^*}{\partial t^*} + \frac{\partial(\rho^* u_i^*)}{\partial x_i^*} = 0, \quad 3.1$$

$$\begin{aligned} \frac{\partial u_i^*}{\partial t^*} + u_j^* \frac{\partial u_i^*}{\partial x_j^*} - \left[\frac{L_o \Omega_o}{u_o} \right] 2\epsilon_{ijk} \Omega_j^* u_k^* = \\ - \frac{\partial p^*}{\partial x_i^*} - \left[\frac{\Delta T_o L_o g_o}{T_o u_o^2} \right] \Delta T^* g^* \delta_{i3} \\ + \left[\frac{v_o}{u_o L_o} \right] \frac{\partial^2 u_i^*}{\partial x_k^* \partial x_k^*} + \frac{\partial}{\partial x_j^*} - \overline{u_i^* u_j^*} \end{aligned} \quad 3.2$$

and

$$\begin{aligned} \frac{\partial T^*}{\partial t^*} + u_i^* \frac{\partial T^*}{\partial x_i^*} = \left[\frac{k_o}{\rho_o C_{p_o} v_o} \right] \left[\frac{v_o}{L_o u_o} \right] \frac{\partial^2 T^*}{\partial x_k^* \partial x_k^*} \\ + \frac{\partial}{\partial x_i^*} \overline{\theta_i^* u_i^*} + \left[\frac{v_o}{u_o L_o} \right] \left[\frac{u_o^2}{C_{p_o} (\Delta T)_o} \right] \phi^* . \end{aligned} \quad 3.3$$

The dependent and independent variables have been made dimensionless (indicated by an asterisk) by choosing appropriate reference values.

For exact similarity, the bracketed quantities and boundary conditions must be the same in the wind tunnel and in the plume as they are in the corresponding full-scale case. The complete set of requirements for similarity is:

- 1) Undistorted geometry
- 2) Equal Rossby number: $Ro = u_o / (L_o \Omega_o)$

- 3) Equal gross Richardson number: $Ri = \Delta T_o g L_o / T_o u_o^2$
- 4) Equal Reynolds number: $Re = u_o L_o / \nu_o$
- 5) Equal Prandtl number: $Pr = (\nu_o \rho_o C_{p_o}) / k_o$
- 6) Equal Eckert number: $Ec = u_o^2 / [C_{p_o} (\Delta T)_o]$
- 7) Similar surface-boundary conditions
- 8) Similar approach-flow characteristics

All of the above requirements cannot be simultaneously satisfied in the model and prototype. However, some of the quantities are not important for the simulation of many flow conditions. The parameters which can be neglected for this study and those which are important will now be discussed in detail.

- Neglected Parameters

For this study equal Reynolds number for model and prototype is not possible since the least scaling is 1:500 and unreasonably high wind tunnel speeds would be required. This inequality is not a serious limitation. The Reynolds number related to the stack exit is defined by

$$Re_s = \frac{u_s D}{\nu_s} .$$

Hoult and Weil (1972) reported that plumes appear to be fully turbulent for exit Reynolds numbers greater than 300. Their experimental data show that the plume trajectories are similar for Reynolds numbers above this critical value. In fact, the trajectories appear similar down to $Re_s = 28$ if only the buoyancy dominated position of the plume trajectory is considered. Hoult and Weil's study was in a laminar cross flow (water tank) with low ambient turbulence levels and hence the rise and

dispersion of the plume would be predominantly dominated by the plume's own self-generated turbulence. These arguments for Reynolds number independence only apply to plumes in low ambient turbulence or to the initial stage of plume rise where the plume's self-generated turbulence dominates.

For similarity in the region dominated by ambient turbulence consider Taylor's (1921) relation for diffusion in a stationary homogeneous turbulence

$$\sigma_z^2(t) = \overline{w'^2} \int_0^\xi \int_0^t R(\xi) d\xi dt \quad 3.4$$

which can be simplified to (see Csanady, 1973)

$$\sigma_z^2(t) \cong \overline{w'^2} t^2 \cong i_z^2 x^2 \quad 3.5$$

for short travel times; or,

$$\sigma_z(t) = \overline{w'^2} t_0 (t-t_1) ; \quad 3.6$$

for long travel times where

$$t_0 = \int_0^\infty R(\tau) d\tau \quad 3.7$$

is an integral time scale and

$$t_1 = \frac{1}{t_0} \int_0^\infty \tau R(\tau) d\tau \quad 3.8$$

is the center of gravity of the autocorrelations curve. Hence for geometric similarity at short travel times,

$$\frac{[\sigma_z^2]_m}{[\sigma_z^2]_p} = \frac{[L^2]_m}{[L^2]_p} = \frac{[i_z^2 x^2]_m}{[i_z^2 x^2]_p}$$

or,

$$[i_z]_m = [i_z]_p \quad . \quad 3.9$$

For similarity at long travel times

$$\begin{aligned} \frac{L_m^2}{L_p^2} &= \frac{[\sigma_z^2]_m}{[\sigma_z^2]_p} = \frac{[\overline{w'^2 t_o(t-t_1)}]_m}{[\overline{w'^2 t_o(t-t_1)}]_p} \\ &= \frac{[i_z^2]_m}{[i_z^2]_p} \frac{[t_o(t-t_1)/u^2]_m}{[t_o(t-t_1)/u^2]_p} = \frac{[Li_z^2 \Lambda]_m}{[Li_z^2 \Lambda]_p} \end{aligned}$$

if it is assumed $t_1 \ll t$, $t_o/u = \Lambda$ and $t/u = L$. Thus the turbulence length scales must scale as the ratio of the model to prototype length scaling if $(i_z)_m = (i_z)_p$ or,

$$\frac{L_m}{L_p} = \frac{\Lambda_m}{\Lambda_p} \quad . \quad 3.10$$

An alternate way of evaluating the similarity requirement is by putting 3.4 in spectral form or (Snyder, 1972),

$$\sigma_z^2 = \overline{w'^2} t^2 \int_0^\infty F_L(n) \left[\frac{\sin \pi n t}{\pi n t} \right]^2 dn = \overline{w'^2} t^2 I \quad 3.11$$

where

$$I = \int_0^\infty F_L(n) \left[\frac{\sin \pi n t}{\pi n t} \right]^2 dn$$

F_L = Langrangian spectral function

The quantity in brackets is a filter function the form of which can be seen in Pasquill (1974). In brief for $n > \frac{1}{t}$ the filter function is very small and for $n < \frac{1}{10t}$ virtually unity.

For geometric similarity of the plume the following must be true:

$$\frac{L_m^2}{L_p^2} = \frac{[\sigma_z^2]_m}{[\sigma_z^2]_p} = \frac{[\overline{w'^2 t^2 I}]_m}{[\overline{w'^2 t^2 I}]_p} = \frac{[L^2 i_z^2]_m}{[L^2 i_z^2]_p}$$

or

$$\frac{[i_z^2 I]_m}{[i_z^2 I]_p} = 1 \quad 3.12$$

If $[i_z]_m = [i_z]_p$ the requirement is $I_m = I_p$. For short travel times the filter function is essentially equal to one; hence,

$I_m = I_p = 1$ and the same similarity requirement as previously deduced for short travel times is obtained (equation 3.9).

For long travel times the larger scales (smaller frequencies) of turbulence progressively dominate the dispersion process. If the spectra in the model and prototype are of a similar shape then similarity would be achieved. However for a given turbulent flow a decrease in Reynolds number (hence wind velocity) decreases the range (or energy) of the high frequency end of the spectrum. Fortunately, due to the nature of the filter function, the high frequency (small wavelength) components do not contribute significantly to the dispersion. There would be, however, some critical Reynolds number below which too much of the high frequency turbulence is lost. If a study is run with a Reynolds number in this range similarity may be impaired. To evaluate whether geometric similarity of the plumes was achieved for this study the σ_y and σ_z

values obtained in the wind tunnel were compared with those quoted as being representative of atmospheric dispersion rates (Pasquill, 1976). If the model σ_y and σ_z values compare well for the corresponding atmospheric flow the inference is that Reynolds number independence was achieved.

The ambient flow field affects the plume trajectories and consequently similarity of this field between model and prototype is required. The mean flow field will become independent of Reynolds if the flow is fully turbulent. The critical Reynolds number for this criteria to be met is based on the work of Nikuradse as summarized by Schlichting (1968) and Sutton (1953) and is given by

$$(\text{Re})_{k_s} = \frac{k_s u^*}{\nu} > 75.$$

or assuming $k_s = 30 z_o$

$$\text{Re}_{z_o} = \frac{z_o u^*}{\nu} > 2.5.$$

In this relation k_s is a uniform sand grain height and z_o is the surface roughness factor. Re_{z_o} values were computed and will be discussed in Section 6.

The Rossby number Ro is a quantity which indicates the effect of the earth's rotation on the flow field. In the wind tunnel equal Rossby numbers between model and prototype cannot be achieved. The effect of the earth's rotation becomes significant if the distance scale is large. Snyder (1972) puts a conservative cutoff point at 5 km for diffusion studies. He states that for length scales above this value the Rossby number should be considered. For this particular study, the

maximum range over which the plume is transported is less than 5 km in the horizontal and 1 km in the vertical. Hence, neglecting the earth's rotation effect is justified.

When equal Richardson numbers are achieved, equality of the Eckert number between model and prototype cannot be attained. This is not a serious compromise since the Eckert number is equivalent to a Mach number squared. Consequently, the Eckert number is small compared to unity for laboratory and atmospheric flows.

- Relevant Parameters

Since air is a transport medium in the wind tunnel and the atmosphere, near equality of the Prandtl number is assured. To assure equality of the plume transport between model and prototype the plume height, \bar{z} in the model must equal that in the prototype divided by the scale factor or

$$\frac{(\bar{z})_m}{(\bar{z})_p} = \frac{(L)_m}{(L)_p}$$

where L is an arbitrary length scale. For this particular study $(L)_m/(L)_p = 1/500$; hence $(\bar{z})_m/(\bar{z})_p = 1/500$. The relevant parameters giving this equality can be derived from Briggs (1974) plume rise equations. Near the source where momentum effects are predominant Briggs gives the following equation for plume rise (\bar{z}) :

$$\bar{z} = C_1 \left[\frac{F_m}{u_a} t \right]^{1/3}$$

where

$$F_m = \frac{\rho_s u_s^2 r^2}{\rho_a}$$

C_1 = constant incorporating entrainment

If it is assumed that $t = \frac{x}{u_a}$ the equation can be reduced to the following dimensionless form

$$\frac{\bar{z}}{D} = C_1 [M]^{1/3} \left(\frac{x}{D}\right)^{1/3} .$$

where $M = \frac{\rho_s u_s^2}{\rho_a u_a^2}$ and is referred to as the momentum ratio. For

similarity of plume rise in this region undistorted length scaling is required as well as the requirement that

$$M_m = M_p$$

In the region where the plume has leveled off and buoyancy forces begin to dominate the rise Briggs presents the following equation

$$\bar{z} = C_2 \left(\frac{F}{u} t^2 \right)^{1/3}$$

where

$$F = g \frac{(T_s - T_a) r^2 u_s}{T_s}$$

$C_2 =$ a constant incorporating entrainment

This equation can be rearranged and nondimensionalized to give

$$\frac{\bar{z}}{D} = C_2 (B)^{1/3} \left(\frac{x}{D}\right)^{2/3}$$

where

$$B = \frac{R^3}{Fr^2}$$

$$R = u_s / u_a$$

$$Fr = \frac{u_s}{\sqrt{g\gamma D}}$$

$$\gamma = \frac{T_s - T_a}{T_s} = \frac{\rho_a - \rho_s}{\rho_a}$$

Thus for similarity in the buoyancy dominated region the requirement is

$$B_m = B_p .$$

Using this type of analysis to obtain the scaling laws for plume rise gives different relations than used by Halitsky (1979), Cermak (1974) and Petersen (1976). They find the requirement that $\gamma_m = \gamma_p$, $Fr_m = Fr_p$ and $R_m = R_p$. If in the present analysis γ_m and γ_p are set equal then $Fr_m = Fr_p$ and $R_m = R_p$ and the same scaling laws as used by Halitsky, Cermak and Petersen result. The relations above were used because higher wind tunnel operating speeds were desired. To achieve a high speed relaxation of the γ equality is often employed. Ludwig and Skinner (1974) showed that this technique gives acceptable agreement between a similar case with $\gamma_m = \gamma_p$.

In summary the following scaling criteria were applied for this study:

- 1) $B_m = B_p$; $B = \frac{R^3}{Fr^2}$
- 2) $M_m = M_p$; $M = (1-\gamma)R^2$
- 3) $Re_s > 300$; $Re_s = \frac{u_s D}{\nu_s}$
- 4) $Re_{z_0} > 2.5$; $Re_{z_0} = \frac{u^* z_0}{\nu_a}$
- 5) Similar geometric dimensions
- 6) Equality of dimensionless boundary conditions

4 EXPERIMENTAL PROGRAM

4.1 Summary

The objective of this study is to evaluate the adverse aerodynamic effect of the nearby structural obstacles upon the transport and diffusion of the plumes emitted from the four Bay Shore Power Station (BSPS) stacks. To meet this objective a 1:500 scale model of BSPS was constructed and placed in the CSU Industrial Wind Tunnel. A neutral boundary layer was developed naturally over an aerodynamically rough wind-tunnel surface and tracer gas releases were made through the model stacks simulating 100, 85 and 70 percent load conditions for one wind speed and eight wind directions.

The model operating conditions are given in Table 4.1 and for reference the full-scale plant conditions are enumerated in Table 4.2. A total of 30 test conditions were simulated in the wind tunnel. The run number, building configuration, wind direction and percent load for each test is given in Table 4.3. The tunnel operating conditions for the 85 percent and 70 percent load cases were determined by multiplying the volume flow (V), exit velocity (u_s) and source strength (Q) by the percentage load reduction.

All tests were conducted in a similar manner. A neutral boundary layer characteristic of the BSPS vicinity was established and measurements of velocity were made directly upwind and downwind of the plant. The profiles were analyzed to 1) assess the effect of the building upon the flow field, 2) to verify that the boundary layer was not growing significantly in the region where measurements were performed, and 3) document the shape of the approach velocity profile.

After completing the velocity measurements a metered quantity of buoyant gas was allowed to flow from the model stacks at three speeds simulating 100, 85 and 70 percent load conditions. Aerial distributions of the resulting plume were made at three locations for select cases with and without the building to document the dispersion patterns in the wind tunnel. For all tests 30 ground-level samples were obtained to establish the maximum ground level concentration.

To qualitatively document the flow pattern the plumes were made visible by passing the gas mixture through titanium tetrachloride prior to emission from the stacks. Stills (color and black and white) and motion pictures of the tests in Table 4.3 were obtained.

A more detailed description of every facet of the study will now be given.

4.2 Scale Models and Wind Tunnel

- Scale Model

A 1:500 scale model of the BSPS was constructed to be positioned in the industrial wind tunnel. A photograph of the model from two angles is shown in Figure 4.2-1 and a view of the prototype BSPS is shown in Figure 4.2-2. A three dimensional sketch of the model is shown in Figure 4.2-3 and gives the important building dimensions. The stacks are not shown in the sketch but each stack is 15.3 cm above the base of the building.

- Wind Tunnel

The industrial wind tunnel (IWT) shown in Figure 4.2-4 was used for this study. This wind tunnel, especially designed to study atmospheric and industrial flow phenomena, incorporates special features such as an adjustable ceiling, a rotating turntable, and a long test

section to permit adequate reproduction of micrometeorological behavior. Mean wind speeds of 0.1 to 39.6 m/s in the IWT can be obtained. Boundary layer thicknesses up to 1.2 m can be developed naturally over the downstream 6.1 m of the IWT test section.

For this study four vortex generators and a uniform surface roughness distribution were employed to reproduce the flow characteristics in the vicinity of the BSPS. Figure 4.2-5 shows the wind-tunnel test setup including the location of vortex generators, surface roughness, concentration sampling grid and BSPS.

4.3 Flow Visualization

The purpose of this phase of study is to visually assess the transport of the plumes released from the BSPS stacks. The data collected consist of a series of photographs of the smoke emitted from the stacks for the different tests numerated in Table 4.3.

The smoke was produced by passing the required gas mixture through a container of titanium tetrachloride located outside the wind tunnel and transported through the tunnel wall by means of a tygon tube terminating at the stack inlets. The plume was illuminated with high intensity lamps and a visible record was obtained by means of black and white photographs taken with two supergraphics cameras (lens focal length 127 mm) and color slides taken with one Retina camera (focal length 28 mm). The two supergraphics cameras were positioned such that overlapping field of views were obtained so as to extend the downwind field of observation. The shutter speed for the black and white photographs was 1/25 of a second and for the color slides 1/30 of a second. The black and white photographs are actually a composite of four superimposed pictures taken consecutively. This procedure was performed to obtain an average plume trajectory and not lose the detail of the turbulent

motion as happens at longer shutter speeds. The black and white and color photographs were taken at an angle perpendicular to the tunnel such that the field of view extended from the stack to approximately 2.5 km downwind.

A series of 16 mm motion pictures were taken of all tests. A Bolex movie camera was used with a speed of 24 ft per second. The movies consisted of taking an initial close-up of the smoke release after which the camera was moved parallel to the tunnel from the model BSPS to approximately 2.5 km downwind in the prototype.

4.4 Gas Tracer Technique

The purpose of this phase of the experimental study is to provide quantitative information on the transport and dispersion of the plume emitted from the BSPS stacks with and without the building present. Specifically this phase must demonstrate the magnitude of the SO_2 concentration produced with the building present and also the ratio of maximum concentration with and without the building. To meet this goal a comprehensive set of concentration measurements were taken. The data obtained included ground level samples, a horizontal array of samples elevated above the ground and an array of samples along the center of the tunnel in the vertical direction.

An array of 30 sampling tubes was fastened to the tunnel floor as depicted in Figure 4.2-5. For each test all 30 tubes were sampled consecutively. The maximum values in each downwind array was sampled four times and averaged together so that an average concentration representative of the true mean could be obtained.¹ A sampling rake shown in Figure 4.4-1 with 50 tubes in the vertical and 50 in a vertically

¹From analyzing several samples that were repeated from 7 to 14 times, the ratio of the standard deviation to the mean was estimated to be 0.15. Using the student t test showed there is a 67 percent probability that the mean of four samples is within 10 percent of the true mean.

traversing horizontal array was also used for the four runs indicated in Table 4.3. A vertical distribution of the plume was obtained using from 12 to 15 of the sampling tubes at three downwind locations. Each sample was repeated at least two times at the 91.5 cm location and at least three times at the other downwind positions. Thereafter a horizontal distribution was obtained at the height of maximum concentration using from 12 to 14 of the sampling tubes. The coordinates of the horizontal and vertical samples for each run are given in Tables 4.4 and 4.5.

The test procedure consisted of: 1) setting the proper tunnel wind speed, 2) releasing a metered mixture of source gas (ethane, nitrogen and helium) of the required density from the release probe, 3) withdraw samples of air from the tunnel at the locations designated, and 4) analyze the samples with a flame ionization gas chromatograph (FIGC). A photograph of the sampling system and gas chromatograph are shown in Figure 4.4-2. A schematic of the test setup is shown in Figure 4.4-3.

The procedure for analyzing air samples from the tunnel was as follows: 1) a 2 cc sample volume (represents approximately a 2 second averaging time) drawn from the wind tunnel is introduced into the flame ionization detector (FID), 2) the output from the electrometer (in millivolts) is sent to the Fluid Dynamics and Diffusion Laboratory (FDDL) dedicated minicomputer system, 3) the analog signal is converted to a digital record at a rate of 208 values per second which are then averaged in groups of 16, 4) a digital record is integrated and an ethane concentration determined by multiplying the integrated signal (mvs) times a calibration factor (ppm/mvs), 5) the ethane concentration is stored in the computer for subsequent use, and 6) a summary of the computer analysis (ethane concentration, peak height, integrated voltage, etc.) is printed out on the remote terminal at the wind tunnel. Prior

to any data collection a known concentration of ethane is introduced into the FID to determine the calibration factor. This factor is input into the computer for use in converting the data.

The FID operates on the principal that the electrical conductivity of a gas is directly proportional to the concentration of charged particles within the gas. The ions in this case are formed by the effluent gas being mixed in the FID with hydrogen and then burned in air. The ions and electrons formed enter an electrode gap and decrease the gap resistance. The resulting voltage drop is amplified by an electrometer and fed to the FDDL computer. When no effluent gas is flowing, a carrier gas flows (nitrogen) through the FID. Due to certain impurities in the carrier some ions and electrons are formed creating a background voltage or zero shift. When the effluent gas enters the FID the voltage increases above this zero shift in proportion to the degree of ionization or correspondingly the amount of tracer gas present. Since the chromatograph² used in this study features a temperature control on the flame and electrometer; there is very low zero drift. In case of any zero drift the computer program which integrates the effluent peak also subtracts out the zero drift.

The lower limit of measurement (approximately 5 ppm or an equivalent SO₂ concentration of approximately 0.02 ppm) is imposed by the instrument sensitivity and the background concentration of ethane within the air in the wind tunnel. Background concentrations were measured and subtracted from all data quoted herein.

The wind-tunnel concentration data for all tests in this report are presented in the following dimensionless form

²Two different FID gas chromatographs were used in this study. Runs 1-10 and 20-30 used a Baseline Industries GC and Runs 11-19 used a Hewlett-Packard GC.

$$K = \frac{\chi u_h H_b^2}{\chi_o V} \quad 4.1$$

where χ is the observed concentration and χ_o is the source strength of the tracer gas. The tracer gas source strength was measured during the period of measurement and the appropriate observed value was used in tabulating the data.

To determine a corresponding full-scale concentration from the model K values the K-model (K_m) is set equal to K-prototype (K_p). Equality of these two parameters can be verified by considering the equation for conservation of mass, or,

$$\left[\int_{-\infty}^{\infty} \int \frac{\chi u}{Q} dy dz \right]_m = \left[\int_{-\infty}^{\infty} \int \frac{\chi u}{Q} dy dz \right]_p = 1.$$

Since $(dy)_m = \frac{(H_b)_m}{(H_b)_p} (dy)_p$ and $(dz)_m = \frac{(H_b)_m}{(H_b)_p} (dz)_p$, the equation can be rearranged to give

$$\int_{-\infty}^{\infty} \int \left[\left(\frac{\chi u}{Q} \right)_p - \left(\frac{\chi u}{Q} \right)_m \frac{(H_b)_m^2}{(H_b)_p^2} \right] (dy dz)_p = 1$$

For this equality to be true requires

$$\left(\frac{\chi u}{Q} \right)_p = \left(\frac{\chi u}{Q} \right)_m \frac{(H_b)_m^2}{(H_b)_p^2}$$

or

$$\left(\frac{\chi u H_b^2}{Q} \right)_m = \left(\frac{\chi u H_b^2}{Q} \right)_p$$

Solving for χ_p and letting $u = u_h$ yields the following equation which is used in this report to calculate prototype concentrations

$$\chi_p = K_m \left[\frac{Q}{u_h H_b^2} \right]_p \quad 4.2$$

The concentration data was computer processed to obtain the center of mass (\bar{z}) and the standard deviation (σ_z or σ_y). The parameters were determined by numerically integrating the following equations over the height (and width, where appropriate) of the concentration profiles:

$$Q' = \int_0^h Kdz \quad 4.3$$

$$\bar{z} = 1/Q' \int_0^h zKdz \quad 4.4$$

$$\sigma_z^2 = 1/Q' \int_0^h (z-\bar{z})^2 Kdz \quad 4.5$$

The numerical integration was obtained using the trapezoidal rule.

To determine the averaging time for the predicted concentrations from wind-tunnel experiments the dispersion parameters-- σ_y and σ_z -- for the undisturbed flow in the wind tunnel were compared to those used for numerical modeling studies in the atmosphere. The dispersion rates used in the atmosphere are referred to as the Pasquill-Gifford curves and are given in Turner (1968) and modified values are given in Pasquill (1974). The results of this comparison as discussed in Section 6 showed that the σ_y and σ_z values in the wind tunnel compare (when multiplied by the length scaling factor 500) with the Pasquill-Gifford D stability line. Hence the method used for converting numerical model predictions to different averaging times should also be used for converting the wind-tunnel tests. The EPA guideline series for evaluating new stationary sources

(Budney, 1977) conservatively assumes that the Pasquill-Gifford σ_y and σ_z values represent 1-hour average values. To convert to a 3-hour concentration the document recommends multiplying the 1-hour value by 0.9 ± 0.1 and if aerodynamic disturbances are a problem the factor should be as high as 1. Huber (1979) recommended using the wind-tunnel predictions of SO_2 concentration as a 3-hour value. To be consistent with EPA recommendations the results presented herein will be assumed to represent 3-hour average SO_2 concentrations.

4.5 Velocity and Temperature Measurements

Mean and turbulent velocity measurements were performed to 1) monitor and set flow conditions and 2) document the flow conditions in the wind tunnel. Instrumentation used for this study included 1) one Thermo-Systems, Inc. (TSI) 1050 series anemometer, 2) a TSI Model 1210 hot-film sensor, 3) a Model 1800 LV Datametric Linear Flow Meter and Probe, and 4) a Matheson Linear Mass Flow Meter and Controller for velocity calibration. Since all tests were conducted under neutral stratification no detailed temperature measurements were required. The techniques used to obtain the velocity data with this assortment of equipment and the data processing techniques will now be discussed in more detail.

- Hot-Film Anemometry--Principle of Operation and Calibration Technique

The transducer used for measuring velocities for this study was a Model 1210 hot-film sensor. The sensor consists of a platinum film on a single quartz fiber. The diameter of the sensor is 0.0025 cm. The sensor has the capability of resolving one component of velocity in turbulent flow fields.

The basic theory of operation is based on the physical principle that the heat transfer from the wire equals the heat supplied to the wire by the anemometer or in equation form (see Hinze, 1975),

$$I^2 R_H = \pi \ell k_g (T_w - T_g) Nu \quad 4.6$$

where

I = current through wire

k_g = heat conductivity of gas

ℓ = length of wire

T_w = temperature of wire

T_g = temperature of gas

Nu = Nusselt number

$$= F(\text{Re}, \text{Pr}, \text{Gr} \frac{T_w - T_g}{T_g}, \frac{\ell}{d})$$

$$\text{Re} = \frac{ud}{v_g}$$

$$\text{Pr} = \frac{C_p \mu_g}{k_g}$$

$$\text{Gr} = \frac{gd^3 (T_w - T_g)}{v_g^2 T_g}$$

d = diameter of wire

R_H = operating resistance of wire

For most wind-tunnel applications an empirical equation evolved by Kramers as reported in Hinze (1975) is adequate for representing Nu for a Reynolds number range $0.01 < \text{Re} < 1000$, or

$$Nu = 0.42 \text{Pr}^{0.2} + 0.56 \text{Pr}^{0.33} \text{Re}^{0.5} .$$

Free convection from the wire can be neglected for $\text{Re} > 0.5$ when

$$\text{GrPr} < 10^{-4} .$$

Alternately buoyancy may be neglected when

$$\text{Gr} < \text{Re}^3 .$$

The temperature dependence of the resistance of the wire is assumed to follow the ensuing relation

$$R_H = R_O [1 + b_1(T_w - T_O) + b_2(T_w - T_O)^2 + \dots]$$

where b_i are temperature coefficients. Normally the higher order terms are neglected and

$$R_w = R_O [1 + b_1(T_w - T_O)].$$

Substituting the appropriate relations yields the following equation

$$\frac{I^2 R_w}{R_w - R_c} = A + B(\rho_c u)^n \quad 4.7$$

where

R_c = resistance of wire at calibration temperature

ρ_c = density of air at calibration temperature

$$A = \frac{\pi \ell k_f}{b_1 R_O} 0.42 (\text{Pr})^{0.2}$$

$$B = \frac{\pi \ell k_f}{b_1 R_O} 0.57 (\text{Pr})^{0.33} \left(\frac{d}{\mu}\right)^{0.5} .$$

For this study A , B and u were obtained by calibrating the wire over a range of known velocities and determining A , B and n by a least-squares analysis. Since the calibration temperature of the wire is nearly equal to the temperature in the wind tunnel no corrections for temperature were applied and the following equation was used to calculate the instantaneous velocity:

$$u = \left[\frac{I^2 R_w}{\frac{R_w - R_c}{B} - A} \right]^{1/n} \quad 4.8$$

Calibration of the hot film was performed with the Matheson Linear Flow Meter (MLFR). A special flow chamber was attached to the MLFR with a specially constructed orifice which gave a uniform velocity profile upon exit. With this device velocities over the range of 0.09 to 2 m/s could be obtained. Accuracy of this system is quoted to be 1 percent of full-scale range or ± 0.02 m/s. A typical calibration curve is shown in Figure 4.5-1. A calibration was performed at the beginning of each day's measurement.

After the wire was calibrated, the desired flow condition was set in the wind tunnel. The free-stream velocity was monitored with the Model 800 LV Datametric Flow Meter and Probe. Once the desired condition at the reference height was obtained the Datametrics setting was recorded and used to monitor and set the tunnel conditions for all remaining tests. During all subsequent velocity measurements care was taken to ensure the Datametrics probe reading remained constant.

- Data Collection

Velocity and temperature profiles were measured at three locations with and without the building. The profiles were taken at locations 1.25 meters upwind of the plant and 1.5 and 2.8 meters downwind. The manner of collecting the data was as follows: 1) the hot film was attached to a carriage, 2) the bottom height of the profile was set to be 0.64 cm, 3) a vertical distribution of velocity was obtained using a vertically traversing mechanism which gave a voltage output corresponding to the height of the wire above the ground, 4) the signals

from the hot film and potentiometer device indicating height were fed directly to a Hewlett-Packard Series 1000 Real Time Executive Data Acquisition System, 5) samples were stored digitally in the computer at a rate of 500 samples/second, and 6) the computer program converted each voltage into a velocity (m/s) using the equation 4.3. At this point the program computes several useful quantities using the following equations:

$$\bar{u} = 1/N \sum_{i=1}^N u_i$$

4.9

$$\overline{u'^2} = \frac{1}{N-1} \sum_{i=1}^N (u_i - \bar{u})^2$$

where N is the number of velocities considered (a 15-second average was taken, hence 7500 samples were obtained). The mean velocity and turbulence intensity at each measurement height were stored on a file in addition to being returned to the operator at the wind tunnel on a remote terminal.

5. WIND DISTRIBUTION AT BAY SHORE VICINITY

In order to determine the representativeness of the wind speeds and wind directions studied in the wind tunnel, the 76.2 m wind data from the Davis-Besse Nuclear Power Plant were analyzed. A portion of the analysis was performed by NUS Corporation. Their results are given in Appendix B. The location of the Davis-Besse Plant in relation to BSPS and Toledo Express Airport is shown in Figure 5.1-1. In general it appears that the Davis-Besse site should give a more reasonable estimate of the winds at BSPS than the Toledo Express Airport data. The Davis-Besse data are favored because 1) the quality assurance measures for all nuclear power plant data are high, 2) the wind speeds were measured at a height nearly equal to the BSPS existing stack height (76.2 m), and 3) both the BSPS and Davis-Besse Nuclear Power Plant are located within 2 km of the Lake Erie shoreline. On the other hand, the data collected at Toledo Express Airport were measured at a height of approximately 10 m and the site is 40 km inland.

The purpose of the wind data analysis is to 1) show that the wind speed chosen to simulate in the wind tunnel is reasonable, and 2) demonstrate that winds persist for three or more hours for the test speeds and wind directions studied. Figure 5.1-2 shows a graph depicting the percent the indicated wind speed is exceeded at 76.2 m and for comparison at 10.7 m. At 76.2 m (the height of the existing stacks) the ambient speed of 11.9 m/s, which was simulated in the wind tunnel, is exceeded 350 hours per year or 4 percent of the time. At 10.7 m this speed is only exceeded 65 hours per year or 0.75 percent of the time--an expected result due to the normal decrease in velocity with height. This result indicates that an ambient wind velocity of

11.9 m/s at stack top is realistic and is exceeded on numerous occasions.

Since the short-term SO₂ air quality standard is related to a 3-hour averaging time, the highest predicted concentrations for the cases modeled in the wind tunnel would be those cases for which the winds persist three or more hours.³⁾ At the end of Appendix B typical strip chart traces are shown for persistent wouth-southeast, east and east-southeast winds. As is indicative of a persistent wind, the wind direction and speed remain nearly constant throughout the period.

Table 2 in Appendix B shows that wind direction persisted at least three hours for every wind direction category. Numerous cases with the wind direction persisting longer than 20 hours are also tabulated. Table 6 shows the number of occurrences of wind direction persistence for D stability class and wind speeds greater than 9 m/s (20 mph). At least three hours of persistence were observed for every wind direction except southeast, south-southeast and south. Table 1-1 in Appendix B shows wind direction persistence for speeds between 11 and 13 m/s. At least three hours of persistence were observed for every wind direction except north, east-northeast, southeast, south-southeast, south, south-southwest and southwest. One year of data were available to be analyzed for this report, hence, cases of persistence for the above wind directions may also be observed when a longer period of record is assessed.

³⁾A higher 3-hour average concentration could result with only one hour of persistence if a wind speed different than that modeled gave a concentration at least three times greater than that measured in the wind tunnel.

In summary the results of the analysis of wind in the Bay Shore vicinity shows that 1) the test design speed of 11.9 m/s is reasonable and occurs frequently at BSPS, and 2) cases occur with winds persisting three or more hours from a fixed wind direction with a speed between 11 and 13 m/s.

6. RESULTS

6.1 Visualization

The visualization of plume dispersion from the model stack was performed to qualitatively assess the downwash effects of the building. Figure 6-1.1 shows the visualization for the 100 percent load cases with the buildings present for all wind directions studied. For comparative purposes Figure 6.1-2 shows a plume visualization without the building for 100 percent load and two wind directions.

The most pronounced downwash effect is observed for the east, southeast and south wind directions (Figures 6.1-1c, d and e). These are the wind directions for which the plant structure is upwind of the stacks. The wind directions showing the least effect are the northeast (Figure 6.1-1b) and southwest (Figure 6.1-1f) wind directions. These are the two wind directions for which the plant structure is not upwind and the stacks are aligned parallel to the wind. In summary, the pictures clearly demonstrate that the building is adversely affecting the dispersion of the plume from the stack for the conditions studied. The effect on ground level concentrations will be discussed in the next section.

6.2 Concentration Measurements

The purpose of this phase of the study is to quantify the magnitude of the SO₂ concentrations downwind of BSPS. This was done by releasing a metered quantity of tracer gas (ethane) from a scale model of the BSPS stacks in the industrial wind tunnel. The resulting concentrations were measured with and without the building to comply with the EPA Stack Height credit regulation requirement. Normally for an existing source to be able to raise their stack heights to a GEP stack height,

the owner or operator (Toledo Edison) must first demonstrate that air quality standards or PSP limits are exceeded and second that the maximum concentration with the building is at least 40 percent in excess of that without the building.

Hence this section of the report will discuss 1) the wind tunnel dispersion characteristics, 2) ground level concentrations, and 3) implication of results on GEP stack height.

- Dispersion Characteristics

To determine whether the wind tunnel dispersion parameters (σ_y and σ_z) agree with those for the atmosphere, the vertical and horizontal concentration profiles (see Appendix A for data listing) were analyzed to determine σ_y , σ_z and \bar{z} as discussed in section 4.4. The model values were then scaled to prototype values by multiplying by the length scaling factor (500). The results for each vertical and horizontal profile are tabulated on the profile plots which are given in Figures 6-2-1 and 6-2-2.

The atmospheric values for σ_y and σ_z are often assumed to follow the Pasquill-Gifford curves as given in Turner (1969). However, Pasquill (1976) has recommended a different method for computing these parameters. For σ_y Pasquill recommends the following formula for sampling times up to one hour

$$\sigma_y = i_y \cdot x \cdot f(x)$$

where $f(x)$ is defined as follows

x(km)	0.1	0.2	0.4	1.0	2.0	4.0
f(x)	0.8	0.7	0.65	0.6	0.5	0.4

For this study i_y was not measured only the intensity of turbulence in the longitudinal direction i_x . It will be assumed here that

$i_y = i_x = 0.1$. The 0.1 is based on the velocity measurements which are discussed in Section 6.3. For σ_z Pasquill (1976) recommends using the Turner Workbook curves when the surface roughness is 3 cm. For other roughness he recommends using nomograms or equations in Pasquill (1974). The equation used here for σ_z is

$$\sigma_z = 0.040 x^{0.74}$$

where x is in kilometers and the constants 0.040 and 0.74 were derived from Pasquill (1974) assuming $z_0 = 20$ cm.

Figure 6.2-3 shows the expected σ_y dispersion rate for the atmosphere in comparison to that observed in the wind tunnel. At 0.5 km the wind tunnel σ_y values are higher than expected whereas at 2.1 km the values are low. At 1.2 km the wind tunnel σ_y values compare closely with those estimated for the atmosphere. The highest σ_y values at 0.5 km (solid symbols) are higher due to the stacks being aligned perpendicular to the wind. The low values at 2.1 km may be explained by the fact that the horizontal concentration distribution measured in the wind tunnel did not go down to zero on one side. In other words the computation for σ_y did not include enough of the plume concentration resulting in a low estimate for σ_y . Overall the agreement appears acceptable for the variation of σ_y with distance. In addition, the σ_y 's with and without the building compared favorably for a similar stack orientation with respect to wind direction in agreement with Huber (1976).

Figure 6.2-4 shows the expected variation of σ_z and that observed in the wind tunnel. For those cases without the building the agreement between laboratory and atmosphere is good. As expected the σ_z values are larger when the building is present.

The vertical concentration distributions in Figure 6.2-2 show clearly the effect of the building on ground level concentrations. Figures 6.2-2a and 2b show the vertical distribution without the building. As can be seen the plume center remains elevated above the ground and continues to rise with distance from the stack top. The concentration at the ground are low until the plume becomes almost uniformly mixed at the farthest downwind distance. Figures 6.2-2c and 2d show a marked difference due to the presence of the building. The plume center of mass is lowered and the distribution of material below the plume center quickly becomes uniformly mixed due to the high turbulence in the wake of the building.

- Ground-level Concentrations

The ground level concentration measurements for each run are given in Appendix A. The location of each sample can be ascertained by referring to Figure 4.2-5. The maximum values at each downwind location, which represent an average of four independent samples, are summarized in Table 6.1. Two topics of interest are relevant to this data namely the maximum ground level SO_2 concentration, and 2) the difference between the maximum value with and without the building.

Table 6.2 summarizes for each run the 1) maximum dimensionless concentration, K , 2) the maximum SO_2 concentration, 3) the downwind distance of the maximum concentration, and 4) the downwind distance where the plume was first observed to touch down. The SO_2 concentration was computed using K , equation 4-2 and the prototype data given in Table 4.2. The maximum concentrations of 4615, 4930 and 4671 $\mu\text{g}/\text{m}^3$ are associated with the east wind direction and respective plant loads of 100, 85 and 70 percent. The second highest set of SO_2 concentrations

are predicted to be 3233 and 3056 $\mu\text{g}/\text{m}^3$ for the south wind direction and respective loads of 85 and 70 percent. These two wind directions (south and east) represent cases where the ambient flow is approximately perpendicular to a building diagonal. This case has been observed by others (Barrett et al., 1978; and Robins and Castro, 1977) to produce the highest ground concentrations for a stack positioned downwind of a building.

The lowest concentrations were observed for the southwest and northeast wind direction. For these two directions the stacks are aligned parallel to the flow and the building is neither up nor downwind. In fact the concentrations for these cases are nearly equal to the no building cases.

To assess the difference between the concentrations with and without the building, Figure 6.2-5 was prepared. This figure shows a plot of K versus x/H_b for three wind directions with the building present, one case without the building and a case from Huber (1976). Reference to this figure shows that the magnitude of the concentration with the building present is from 2.5 to 7.1 times greater than that without the building. The Huber (1976) case corresponds closely to the case with flow perpendicular to the building face (southwest wind direction). The K value for the two cases are very similar but the Huber maximum is greater and closer to the stack. This can be explained by a lower velocity ratio (0.7) for Huber's case. The low velocity ratio will act to lower the plume rise thus increasing the maximum ground level concentration and bringing the maximum closer to the source.

- Implication of Results on GEP Stack Height

As stated earlier, for Toledo Edison to raise their stacks to a GEP stack height two criteria must be met according to the EPA stack height credit regulation. They are 1) the source must demonstrate air quality standards are exceeded, and 2) the maximum concentration with the building must be at least 40 percent in excess of that without the building. Since the maximum concentration predicted from the wind tunnel test was $4930 \mu\text{g}/\text{m}^3$ and ambient standard is $1300 \mu\text{g}/\text{m}^3$ criteria one above is met. In addition criteria 2 is satisfied since the ratio of maximum concentration with and without the building was found to range from at least a 150 to 650 percent increase in concentration due to the building. Hence Toledo Edison has met the criteria as stated in the stack height regulation to use the EPA formula to determine a GEP stack height for the new stack.

It must also be noted that criteria 1 was met without further consideration of the added concentration due to background and also without consideration of interaction of other sources in the vicinity of the Bay Shore Power Station. Further there were several instances (different wind direction and/or exit velocities) where there were exceedances all of which would normally occur with the meteorological conditions that exist in the Bay Shore area.

6.3 Velocity Measurements

Velocity measurements were obtained to: 1) establish the correct operating speeds in the tunnel, 2) assess the representativeness of the wind tunnel velocity profile in comparison to those observed in the atmosphere and 3) document the flow conditions in the wind tunnel. To meet this objective a total of five vertical profiles of horizontal wind speed and turbulence intensity were obtained. One profile was taken 1.25 m upwind of the plant site, two were taken 1.5 m downwind (one with and one without the building) and two were taken 2.8 m downwind (one with and one without the building). The data for each profile is listed in Table 6.3.

To assess the flow characteristics in the wind tunnel and to aid in comparing to atmospheric flows the velocity profiles were analyzed to obtain the boundary layer thickness (δ), the surface roughness factor (z_0), the friction velocity (u_*), the turbulent Reynolds number (Re_{z_0}), and the power law exponent (n). The estimated values for each profile are given in Table 6.4. The values of z_0 and u^* were determined by finding the z_0 and u^* which gave the best fit (by least squares) to the following equation which is characteristic of atmospheric (Businger, 1972) and wind tunnel flows (Cermak, 1974).

$$\frac{u}{u_*} = \frac{1}{k} \ln \frac{z}{z_0} .$$

The expected value for z_0 in the vicinity of the BSPS can be estimated by referring to Table 6.5 from Engineering Science Data Unit, 1972.

The BSPS site can be characterized somewhere between "outskirts of towns" and "many trees, hedges, few buildings" giving an expected z_0 range of 20 to 50 cm. For wind tunnel similarity the model z_0 should equal the atmospheric value divided by the scale factor of 500. This results

in desired values for a model z_o from 0.040 to 0.100 cm. As can be seen from Table 6.4, the range of values for the wind-tunnel profiles was from 0.047 to 0.117 cm in good agreement with the required range for the BSPS vicinity.

The power law exponent was computed by fitting the data by least squares to the following equation:

$$\frac{u}{u_r} = \left(\frac{z}{z_r} \right)^n .$$

Counihan (1975) presents the following equation for estimating n as a function of z_o

$$n = 0.096 \log_{10} z_o + 0.016 (\log_{10} z_o)^2 + 0.24 .$$

where z_o is in meters. Using the expected z_o range of 0.20 to 0.50 meters for the BSPS site gives an expected n range of 0.18 to 0.21. The exponent for the approach velocity profile is 0.20 as seen in Table 6.4. The exponents at the two downwind measurement locations without the building were 0.26 and 0.22. The increase in the exponent is due to the increased effective roughness due to the presence of the stacks (note: only the buildings were removed). When the buildings are present the exponent varies from 0.26 to 0.25 at the downwind measurement locations.

The turbulent Reynolds numbers in Table 6.4 range from 1.9 at the upwind profile to 11.2 at 1.5 m with the buildings present. The approach value of 1.9 is close to the critical value of 2.5 as discussed in Section 3 and implies Reynolds number independence may have been achieved especially since the Re_{z_o} values downwind of the source were all greater than 2.5. Reynolds number independence is also inferred due to

the close agreement between the atmospheric and laboratory dispersion rates as discussed in Section 6.2.

The boundary layer thickness was estimated from the velocity profiles by assuming the highest velocity (at 1 m) is the free stream value, u_{∞} . The boundary layer thickness is assumed to be the height where the free stream value is reduced by 10 percent. Assuming a power law wind profile:

$$\frac{u(\delta)}{u_{\infty}} = 0.9 = \left(\frac{\delta}{z_{\infty}}\right)^n.$$

Rearranging δ can be calculated as follows:

$$\delta = z_{\infty} (0.9)^{1/2}$$

where $z_{\infty} = 1$ m. The δ -values computed for the different n values are given in Table 6.4 and range from 295 to 335 m full-scale.

To compare the difference between the velocity and turbulence profiles with and without the building, Figures 6.3-1 and 6.3-2 were prepared. Figure 6.3-1 shows the velocity profile at each relative downwind location and a profile of the difference between the velocity with and without the building. At 1.5 m downwind the velocity with the building is reduced up to a height of approximately 20 cm or 2.1 building heights. At 2.8 m the velocity is still reduced when the building is present up to a height of 30 cm or 3.2 building heights.

The turbulence intensity profiles are displayed in a similar manner in Figure 6.3-2. The approach turbulence intensity profile varies from 12 percent near the floor to 6 percent at 1 m. The profile at 1.5 m downwind of the source shows a large turbulence intensity excess (10 percent) at building height which diminishes to zero at 30 cm or 3.2 building

heights. At 2.8 m downwind the turbulence intensity excess is close to zero at all heights except near the ground where a slight increase in turbulence without the building is noted.

In summary the velocity profiles show that the boundary layer in the wind tunnel closely approximates that expected for the BSPS vicinity. The profiles also show the expected trend of increased velocity and decreased turbulence in the wake of the building.

REFERENCES

- Barrett, C. F., D. J. Hall, and A. C. Simmonds, "Dispersion From Chimneys Downwind of Cubical Buildings - A Wind Tunnel Study," Paper presented at NATO/CCMS 9th International Meeting on Air Pollution Modeling and Its Application, Toronto, Canada, August 28-31, 1978.
- Briggs, G. A., "Plume Rise Predictions," Presented in Lectures on Air Pollution and Environmental Impact Analyses, Sponsored by American Meteorological Society, Sept. 29-Oct. 3, 1975, Boston, Mass.
- Budney, L. J., "Procedures for Evaluating Air Quality Impact of New Stationary Sources." Guidelines for Air Quality Maintenance Planning and Analysis, Volume 10 (OAQPS No. 1.2-029R) Environmental Protection Agency, Research Triangle Park, North Carolina, 27711, July 1977.
- Businger, J. A., "The Atmospheric Boundary Layer," Chapter 6 in Remote Sensing of the Troposphere, edited by V. E. Derr, U.S. Department of Commerce, National Oceanic and Atmospheric Administration, 1972.
- Cermak, J. E., "Applications of Fluid Mechanics to Wind Engineering," presented at Winter Annual Meeting of ASME, New York, November 17-21, 1974.
- Counihan, J., "Adiabatic Atmospheric Boundary Layers: A Review and Analysis of Data from the period 1880-1972," Atmospheric Environment, Vol. 9, pp. 871-905, 1975.
- Engineering Science Data Unit Item Number 72026, "Characteristic of Wind Speed in the Lower Layers of the Atmosphere near the Ground: Strong Winds (Neutral Atmosphere)," November 1972.
- Halitsky, J., "Wind Tunnel Modeling of Treated Stack Effluents in Disturbed Flows," Accepted for publication in Atmospheric Environment, 1979.
- Hinze, O. J., Turbulence, 2nd Edition, McGraw-Hill, Inc., 1975.
- Hoult, D. P. and J. Weil, "Turbulent Plume in a Laminar Cross Flow," Atmospheric Environment, 6:513-531, 1972.
- Huber, A. H. and W. H. Snyder, "Building Wake Effects on Short Stack Effluents," Third Symposium on Atmospheric Turbulence Diffusion and Air Quality, Raleigh, NC, p. 235-241, Oct. 19-22, 1976.
- Ludwig, G. T. and G. R. Skinner, "Physical Modeling of Dispersion in the Atmospheric Boundary Layer," Calspan Report No. 201, Buffalo, New York 14221, 1978.
- Pasquill, F., Atmospheric Diffusion, 2nd Edition, John Wiley and Sons, New York, 1974.

- Pasquill, F., "Atmospheric Dispersion Parameters in Gaussian Plume Modeling, Part II," EPA Report No. EPA-600/4/-76-0360, 1976.
- Petersen, R. L., J. E. Cermak, and R. N. Meroney, "Plume Rise and Dispersion-Effects of Exit Velocity and Atmospheric Stability, Technical Report for North American Weather Consultants, CER76-77RLP-JEC-RNM59, June 1977.
- Robins, A. G. and I. P. Castro, "A Wind Tunnel Investigation of Plume Dispersion in the Vicinity of a Surface Mounted Cube--I The Flow Field, II The Concentration Field." Atmospheric Environment, 17 pp. 291-311, 1977.
- Schlichting, H., Boundary Layer Theory, McGraw-Hill, Inc., New York, 1968.
- Snyder, W. H., "Similarity Criteria for the Application of Fluid Models to the Study of Air Pollution Meteorology," Boundary Layer Meteorology, Vol. 3, pp. 113-134, 1972.
- Sutton, O. G., Micrometeorology, McGraw-Hill, Inc., New York, 1953.
- Taylor, G. I., "Diffusion by Continuous Movements," Proceedings, London Meteorological Society, Vol. 20, pp. 196-211, 1921.
- Turner, P. B., Workbook of Atmospheric Dispersion Estimates, U.S. Department of Health, Education and Welfare, Public Health Service Publ. No. 999, Cincinnati, Ohio, AP-26, 88 p., 1969.

TABLES

Table 4.1. Model operating parameters for the Bay Shore Power Station.*

Parameter	Unit 1	Unit 2	Unit 3	Unit 4
1. Building height H_b (cm)			9.45	
2. Stack diameter D (cm)	0.74	0.74	0.74	0.86
3. Stack height h (cm)			15.24	
4. Exit temperature T_s ($^{\circ}$ K)			293.0	
5. Exit velocity u_s (m/s)	1.74	1.74	1.73	1.90
6. Volume flow V (cm ³ /s)	74.8	74.8	74.4	110.4
7. Ethane source strength χ_o (ppm)			80000	
8. Molecular weight of release gas mixture m_s (gms)			11.55	
9. Molecular weight of air m_a (gms)			28.9	
10. Ambient temperature T_a ($^{\circ}$ K)			293.0	
11. Ambient pressure P_a (mb)			850	
12. Ambient velocity at stack top u_h (m/s)			0.88	
13. Density ratio $\gamma \left(\frac{m_a - m_s}{m_a} \right)$			0.60	
14. Froude number $F_r \left(\frac{u_s}{\sqrt{g\gamma D}} \right)$	8.35	8.35	8.30	8.44
15. Velocity ratio $R \left(\frac{u_s}{u_a} \right)$	1.98	1.98	1.97	2.16
16. Momentum ratio $M[1-\gamma]R^2$	1.57	1.57	1.55	1.87
17. Buoyancy ratio $B \left(\frac{R^3}{Fr^2} \right)$	0.11	0.11	0.11	0.14
18. $Re_s \left(\frac{u_s D}{\nu_a} \right)$	858	858	853	1089

*This table assumes 100 percent operating load--wind-tunnel tests were also conducted at 85 and 70 percent load. For reduced load the values of u_s , V and Q_s are reduced by the appropriate percentage.

Table 4.2. Bay Shore Power Station operating parameters.

Parameter	Unit 1	Unit 2	Unit 3	Unit 4
1. Building height H_b (m)	46.95	46.95	46.95	46.95
2. Stack height h (m)	76.20	76.20	76.20	76.20
3. Stack diameter D (m)	3.66	3.66	3.66	4.27
4. Exit temperature T_s ($^{\circ}$ K)	400.0	400.0	400.0	398.0
5. Exit velocity u_s (m/s)	17.62	17.62	17.53	19.20
6. Volume flow V (m^3/s)	185.38	185.38	184.43	274.95
7. SO_2 emission rate Q_s (g/s)	182.05	185.38	185.74	284.00
8. Ambient temperature T_a ($^{\circ}$ K)		283.0		
9. Ambient pressure P_a (mb)		1000		
10. Surface roughness z_o (cm)		20-50		
11. Boundary layer height δ (m)		300-500		
12. Ambient velocity at u_h (m/s) stack top		11.9		
13. Density ratio $\gamma \left(\frac{T_s - T_a}{T_s} \right)$		0.29		
14. Froude number $F_r \left(\frac{u_s}{\sqrt{g\gamma D}} \right)$	5.46	5.46	5.44	5.51
15. Velocity ratio $R \left(\frac{u_s}{u_a} \right)$	1.48	1.48	1.47	1.61
16. Momentum ratio $M(\{1-\gamma\}R^2)$	1.56	1.56	1.53	1.84
17. Bouyancy ratio $B(R^3/Fr^2)$	0.11	0.11	0.11	0.14

*This table assumes 100 percent operating load--wind tunnel tests were also conducted at 85 and 70 percent load. For reduced load the values of u_s , V and Q_s are reduced by the appropriate percentage.

Table 4.3. Description of photographic and concentration tests.

Run No.	Building Configuration	Wind Direction	Percent Load
1	In	North	100
2			85
3			70
4		Northeast	100
5			85
6			70
7		East	100
8			85
9			70
10		Southeast	100
11			85
12			70
13		South	100
14			85
15			70
*16		Southwest	100
17			85
18			70
19		West	100
20			85
21			70
*22		Northwest	100
23			85
24			70
*25	Out	Southwest	100
26			85
27			70
*28		Northwest	100
29			85
30			70

*Runs for which horizontal and vertical concentration distributions were measured at downwind distances of 101, 244 and 427 cm.

Table 4.4. Horizontal coordinate key.

Sample No.	y (cm)	Files ^{1/}											
		<u>61-10,61-25,61-28</u>			<u>61-13</u>		<u>62-10</u>		<u>62-13</u>		<u>62-28,62-25</u>		<u>63-10</u>
		x (cm)	z (cm)	x (cm)	z (cm)	x (cm)	z (cm)	x (cm)	z (cm)	x (cm)	z (cm)	x (cm)	z (cm)
15	32.9	100.97	19.10	100.97	8.9	244.47	19.10	244.47	8.9	244.47	29.0	427.35	16.4
19	28.2												
23	22.8												
27	17.9												
31	12.7												
34	8.9												
37	5.2												
42	-5.0												
45	-8.4												
48	-12.6												
52	-17.7												
56	-22.9												
60	-27.8												
64	-32.9												

^{1/}The second number (61-10) corresponds to the run numbers given in Table 4.3.

Table 4.5. Vertical coordinate key.

FILES: 51-10, 51-13, 51-25, 51-28

<u>SAMPLE NO.</u>	<u>y(cm)</u>	<u>z(cm)</u>
GND	0.0	0.0
1	0.0	4.0
5	0.0	8.9
8	0.0	12.5
11	0.0	16.4
13	0.0	19.1
15	0.0	21.8
17	0.0	24.3
19	0.0	27.0
21	0.0	29.0
23	0.0	31.4
26	0.0	36.2

FILES: 52-10, 52-13, 52-25, 52-28

<u>SAMPLE NO.</u>	<u>y(cm)</u>	<u>z(cm)</u>
GND	0.0	0.0
1	0.0	4.0
5	0.0	8.9
8	0.0	12.5
11	0.0	16.4
13	0.0	19.1
15	0.0	21.8
17	0.0	24.3
19	0.0	27.0
21	0.0	29.0
23	0.0	31.4
26	0.0	36.2
29	0.0	40.1
32	0.0	44.2
36	0.0	49.5
40	0.0	54.7

Table 4.5 (continued)

FILES: 53-10, 53-28

<u>SAMPLE NO.</u>	<u>y (cm)</u>	<u>z (cm)</u>
GND	0.0	0.0
1	0.0	4.0
5	0.0	8.9
8	0.0	12.5
11	0.0	16.4
13	0.0	19.1
15	0.0	21.8
17	0.0	24.3
19	0.0	27.0
21	0.0	29.0
23	0.0	31.4
26	0.0	36.2
29	0.0	40.1
32	0.0	44.2
36	0.0	49.5
40	0.0	54.7

Table 6.1. Maximum dimensionless concentration K and corresponding SO₂ concentration at each downwind sampling location.

RUN	4.80		6.52		12.97		19.42		22.65		29.10		35.55		42.00	
	K _{max}	χ _{max}														
1	0.00524	163.38	0.0276	860.57	0.0726	2263.69	0.0583	1817.81	0.0507	1580.84	0.0570	1777.27	0.0311	969.71	0.0484	1509.12
2	0.0089	235.88	0.0246	651.97	0.0688	1823.41	0.0694	1839.31	0.0792	2099.04	0.0556	1473.57	0.0369	977.96	0.0458	1213.84
3	0.00939	204.95	0.0295	643.87	0.0916	1999.28	0.0690	1506.01	0.0775	1691.53	0.0630	1375.05	0.0457	997.46	0.0562	1226.63
4	0.00165	51.45	0.00251	78.26	0.00859	267.84	0.0147	458.35	0.0213	664.14	0.0275	857.46	0.0129	402.23	0.0176	548.77
5	0.00117	31.01	0.00195	51.68	0.00753	199.57	0.00400	106.01	0.0187	495.61	0.0202	535.36	0.0158	418.75	0.0155	410.80
6	0.00246	53.69	0.00306	66.79	0.0135	294.65	0.00850	185.52	0.0295	643.87	0.0299	652.60	0.0210	458.35	0.0238	519.46
7	0.0492	1534.07	0.112	3492.19	0.148	4614.68	0.137	4271.69	0.0990	3086.84	0.0867	2703.33	0.0756	2357.23	0.0506	1577.72
8	0.0835	2213.00	0.176	4664.53	0.186	4929.57	0.151	4001.96	0.125	3312.88	0.0936	2480.68	0.0844	2236.86	0.0563	1492.12
9	0.119	2597.32	0.201	4387.07	0.214	4670.81	0.140	3055.67	0.126	2750.10	0.100	2182.62	0.0867	1892.33	0.0520	1134.96
10	0.0352	1097.54	0.0532	1658.79	0.0712	2220.03	0.0533	1661.91	0.0607	1892.64	0.0542	1689.97	0.0327	1019.59	0.0354	1103.78
11	0.0552	2272.98	0.0625	1656.44	0.0523	1386.11	0.0580	1537.18	0.0587	1555.73	0.0556	1473.57	0.0336	890.50	-	-
12	0.0638	1392.51	0.0540	1178.62	0.0557	1215.72	0.0692	1510.37	0.0584	1274.65	0.0522	1139.33	0.0378	825.03	-	-
13	0.0138	430.28	0.0493	1537.17	0.0879	2740.72	0.110	3429.80	0.0887	2765.67	0.0814	2538.05	0.0593	1848.97	0.0585	1824.03
14	0.0377	999.16	0.0708	1876.42	0.0832	2205.05	0.122	3233.37	0.114	3021.35	0.101	2676.81	0.0688	1823.41	0.0718	1902.92
15	0.0607	1324.85	0.100	2182.62	0.132	2881.06	0.140	3055.67	0.130	2837.41	0.116	2531.84	0.0895	1953.45	0.0694	1514.74
16	0.00200	62.36	0.00101	31.49	0.0195	608.01	0.0283	882.40	0.0313	975.94	0.0260	810.69	0.0289	901.11	0.0310	966.59
17	0.00295	78.18	0.00852	225.81	0.0159	421.40	0.0216	572.47	0.0181	479.70	0.0235	622.82	0.0146	386.94	0.0234	620.17
18	0.00560	122.23	0.0150	327.39	0.0285	622.05	0.0279	608.95	0.0217	473.63	0.0299	652.60	0.0287	626.41	0.0262	571.85
19	0.0117	364.81	0.0248	773.27	0.0566	1764.80	0.0564	1758.57	0.0561	1749.21	0.0446	1390.64	0.0367	1144.31	0.0325	1013.36
20	0.0167	442.60	0.0381	1009.77	0.0755	2000.98	0.0657	1741.25	0.0564	1494.77	0.0521	1380.81	0.0469	1242.99	0.0337	893.15
21	0.0262	571.85	0.0488	1065.12	0.0798	1741.73	0.0816	1781.02	0.0608	1327.03	0.0559	1220.08	0.0423	923.25	0.0369	805.39
22	0.00420	130.96	0.0133	414.70	0.0379	1181.73	0.0456	1421.82	0.0476	1484.18	0.0331	1032.07	0.0315	982.18	0.0334	1041.42
23	0.00257	68.11	0.0178	471.75	0.0424	1123.73	0.0536	1420.56	0.0527	1396.71	0.0422	1118.43	0.0318	842.80	0.0330	874.60
24	0.00683	149.07	0.0318	694.07	0.0580	1265.92	0.0575	1255.01	0.0476	1038.93	0.0493	1076.03	0.0463	1010.55	0.0386	842.49
25	-	-	-	-	0.00542	169.00	0.00658	205.17	0.0122	380.40	0.0147	458.35	0.0158	49.26	0.0215	670.38
26	-	-	-	-	0.00204	54.07	0.0101	267.68	0.0190	503.56	0.0153	405.50	0.0236	625.47	0.0211	559.21
27	-	-	-	-	0.00601	131.18	0.0148	323.03	0.0165	360.13	0.0164	357.95	0.0153	333.94	0.0198	432.16
28	0.000675	21.05	0.00108	33.67	0.00300	93.54	0.00742	231.36	0.0144	449.00	0.0139	433.41	0.0222	692.20	0.0172	536.30
29	0.000939	24.89	0.00135	35.78	0.00198	52.48	0.00409	108.40	0.0211	559.21	0.0200	530.06	0.0260	689.08	0.0146	386.94
30	0.00076	16.59	0.00059	12.88	0.00198	43.22	0.00686	149.73	0.0252	550.02	0.0284	619.86	0.0186	405.97	0.0211	460.53

Table 6.2. Summary of visualization and concentration results including the maximum SO₂ concentration for each case.

Run No.	Building Configuration	Wind Direction	Load (%)	Observed Touch Down Prototype (m)	Prototype Distance to Maximum Concentration (m)	K _{max}	(x _p) _{max} ^{-SO₂*} (μg/m ³)
1	In	North	100	305	613	0.0726	2264
2			85	305	1070	0.0792	2099
3			75	274	613	M	M
4		Northeast	100	488	1375	0.0275	857
5			85	518	1375	0.0202	535
6			70	518	1375	0.0299	653
7		East	100	305	613	0.148	4615
8			85	244	613	0.186	4930
9			70	244	613	0.214	4671
10		Southeast	100	244	613	0.0712	2220
11			85	244	303	0.0625	1656
12			70	244	918	0.0692	1510
13		South	100	213	918	0.110	3430
14			85	213	918	0.122	3233
15			70	152	918	0.140	3056
16		Southwest	100	610	1984	0.0313	976
17			85	610	1375	0.0216	572
18			70	610	1680	0.0285	622
19		West	100	396	613	0.0566	1765
20			85	396	613	0.0755	2001
21			70	396	918	0.0816	1781
22		Northwest	100	610	918	0.0476	1484
23			85	549	918	0.0536	1421
24			70	579	918	0.0580	1266
25	Out	Southwest	100	1463	1984	0.0215	670
26			85	1372	1680	0.0236	625
27			70	1158	1070	0.0198	432
28		Northwest	100	1189	1680	0.0222	692
29			85	1158	1680	0.0260	689
30			70	914	1375	0.0284	620

*The 3-hour SO₂ standard is 1300 μg/m³.

Table 6.3. Velocity profiles*-data tabulation.

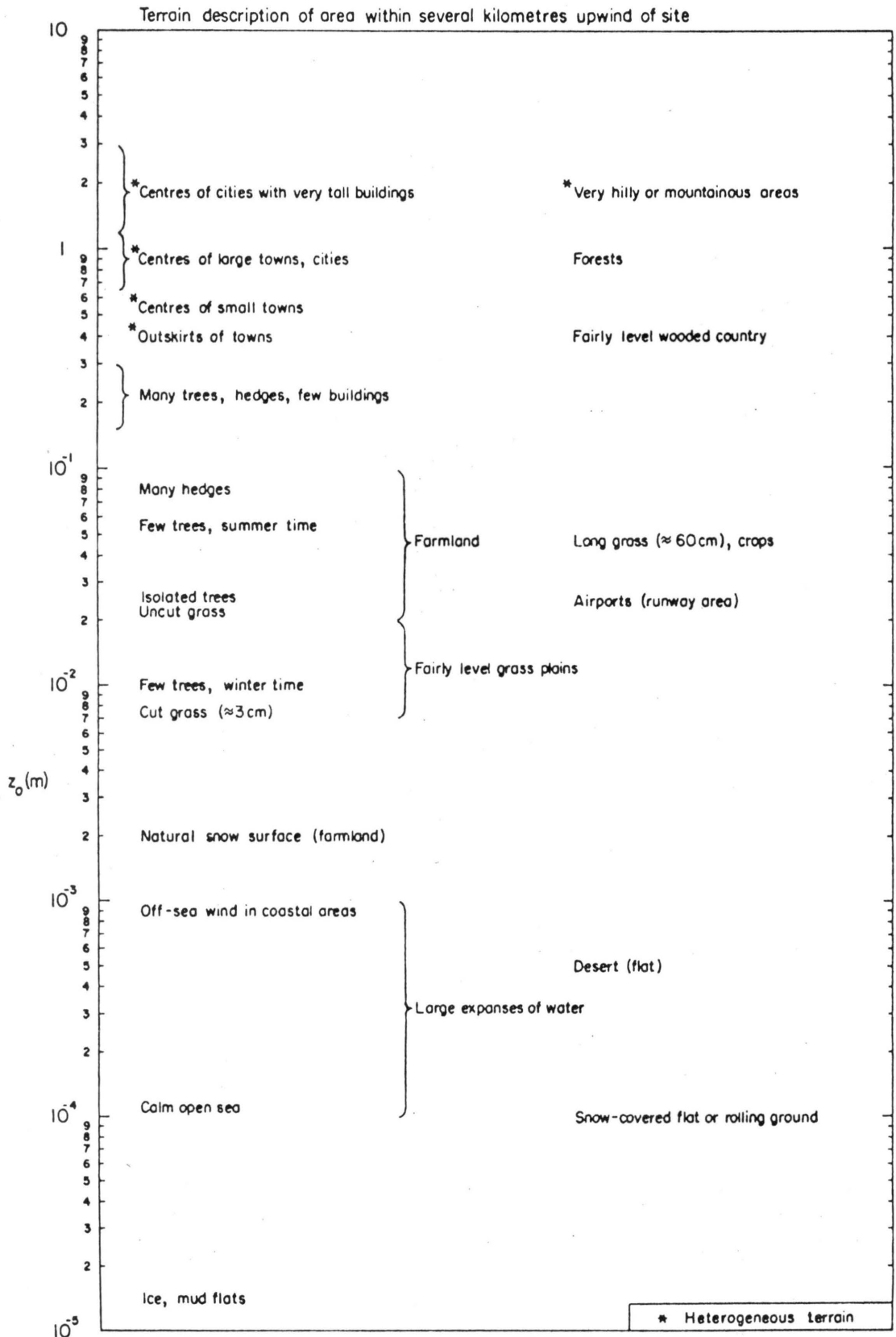
Location	Distance from Origin (cm)	Elevation-z (cm)	Velocity-u (m/s)	Turbulence Intensity i_x	Remarks
A	-125	0.97	0.48	22.15	With building present
		2.47	0.59	20.00	
		5.45	0.69	16.56	
		10.05	0.84	13.43	
		20.24	0.95	10.74	
		40.40	1.06	7.09	
		60.31	1.08	7.75	
		79.93	1.11	5.99	
B	150	1.01	0.40	28.83	With building present
		2.85	0.54	27.70	
		5.42	0.50	29.98	
		10.25	0.65	30.26	
		20.25	0.92	14.95	
		40.27	1.06	6.85	
		60.55	1.08	7.26	
		80.26	1.10	5.34	
B	150	0.99	0.37	23.15	With building removed
		2.86	0.45	18.17	
		5.36	0.59	19.90	
		9.77	0.69	14.47	
		20.02	0.92	9.85	
		39.79	1.01	9.51	
		60.01	1.05	8.09	
		80.32	1.04	5.77	
C	280	0.99	0.45	18.56	With building removed
		2.41	0.49	23.01	
		5.14	0.57	18.91	
		9.96	0.75	13.56	
		20.02	0.85	12.02	
		40.03	1.03	8.03	
		59.83	1.09	5.83	
		80.23	1.12	5.88	
C	280	1.01	0.40	20.42	With building present
		2.90	0.47	20.56	
		5.05	0.52	18.40	
		10.00	0.65	16.90	
		20.08	0.80	14.22	
		40.08	1.03	8.59	
		60.41	1.09	5.59	
		80.29	1.09	5.34	
	100.13	1.07	5.72		

*Sampling rate 500/sec for 15 sec.

Table 6.4. Summary of velocity profile analysis.

Distance from Origin (cm)	Buildings In	Boundary Layer Thickness - δ		Surface Roughness z_o		Friction Velocity u_* (cm/s)	Power Law Exponent-n	Turbulent Reynolds Number- Re_{z_o}
		model (cm)	prototype (cm)	model (cm)	prototype (cm)			
-125	YES	59	295	0.047	23.3	6.08	0.20	1.90
150	YES	67	335	0.167	83.5	7.10	0.26	7.90
150	NO	67	335	0.217	108.5	7.77	0.26	11.2
280	YES	62	310	0.116	58.3	6.77	0.22	5.3
280	NO	66	328	0.217	108.5	7.38	0.25	10.7

Table 6.5. Values of the surface roughness parameter z_0 .



FIGURES

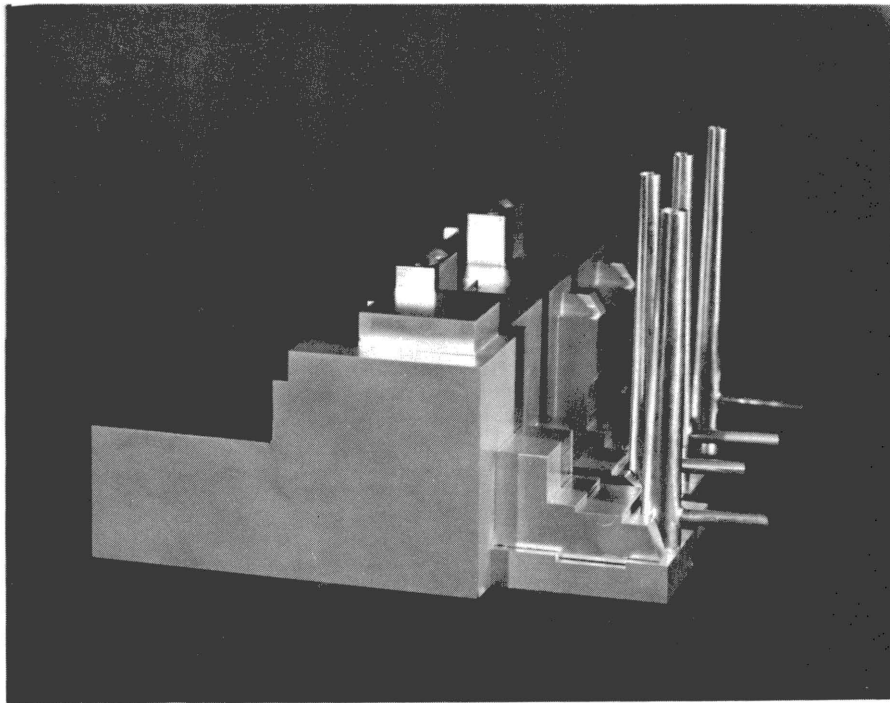
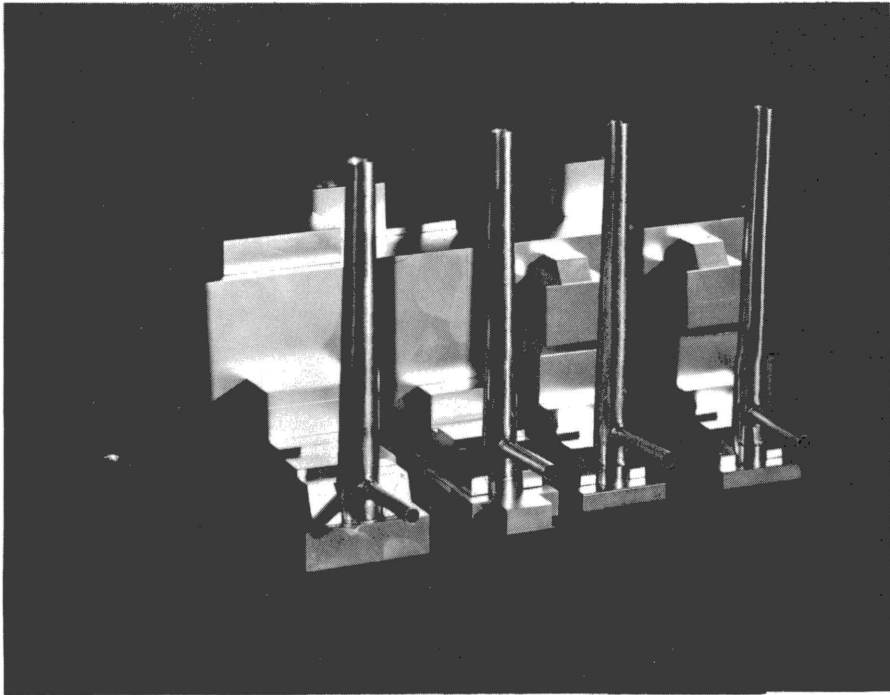


Figure 4.2-1. Photograph of model Bay Shore Power Station (BSPS).

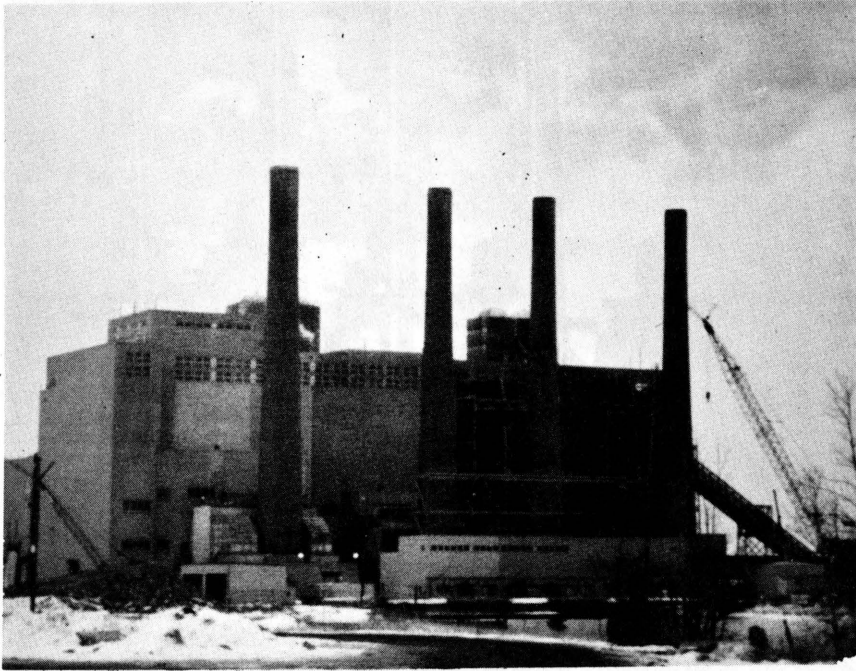
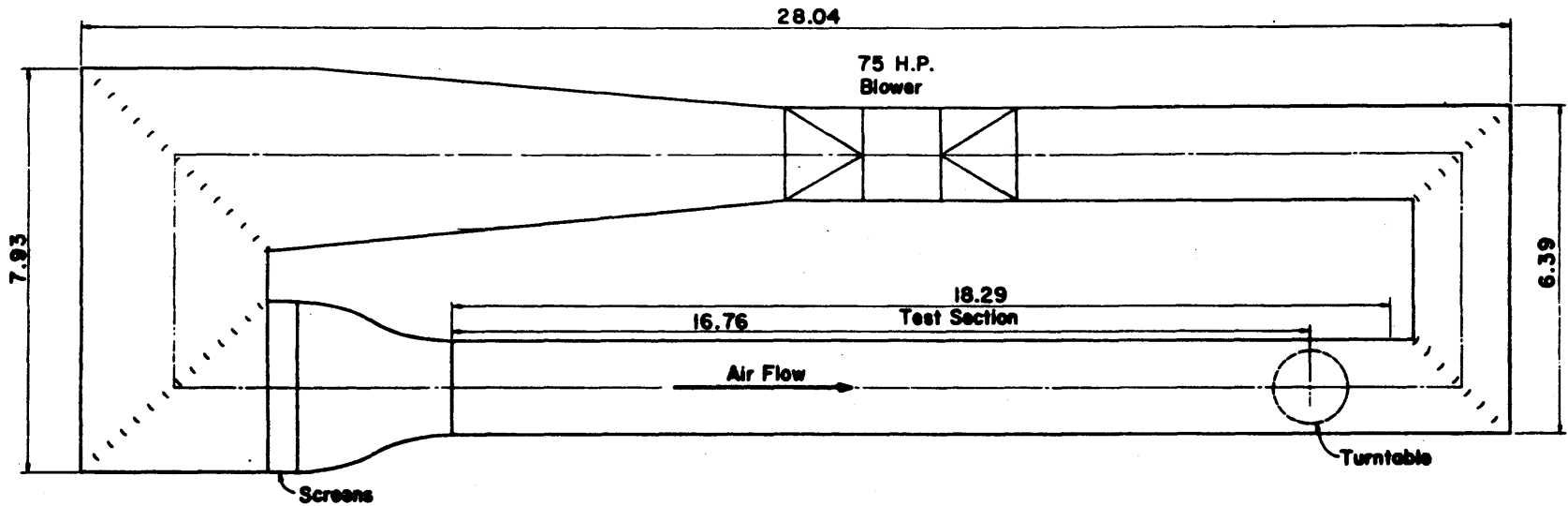


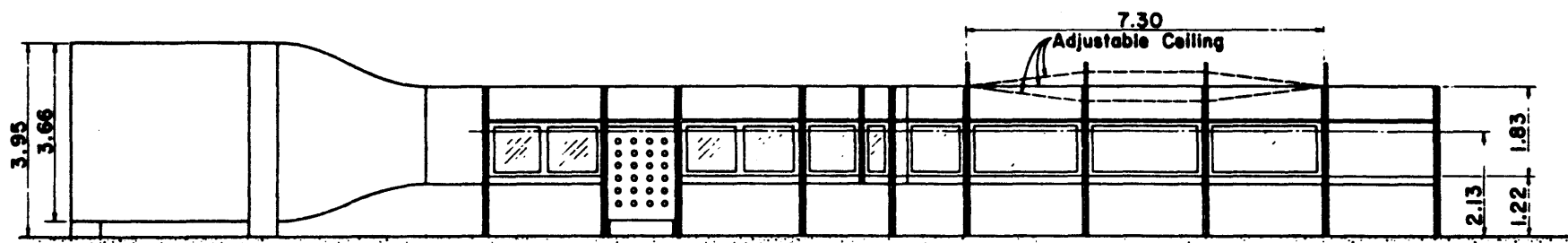
Figure 4.2-2. Photograph of prototype Bay Shore Power Station.



PLAN



58

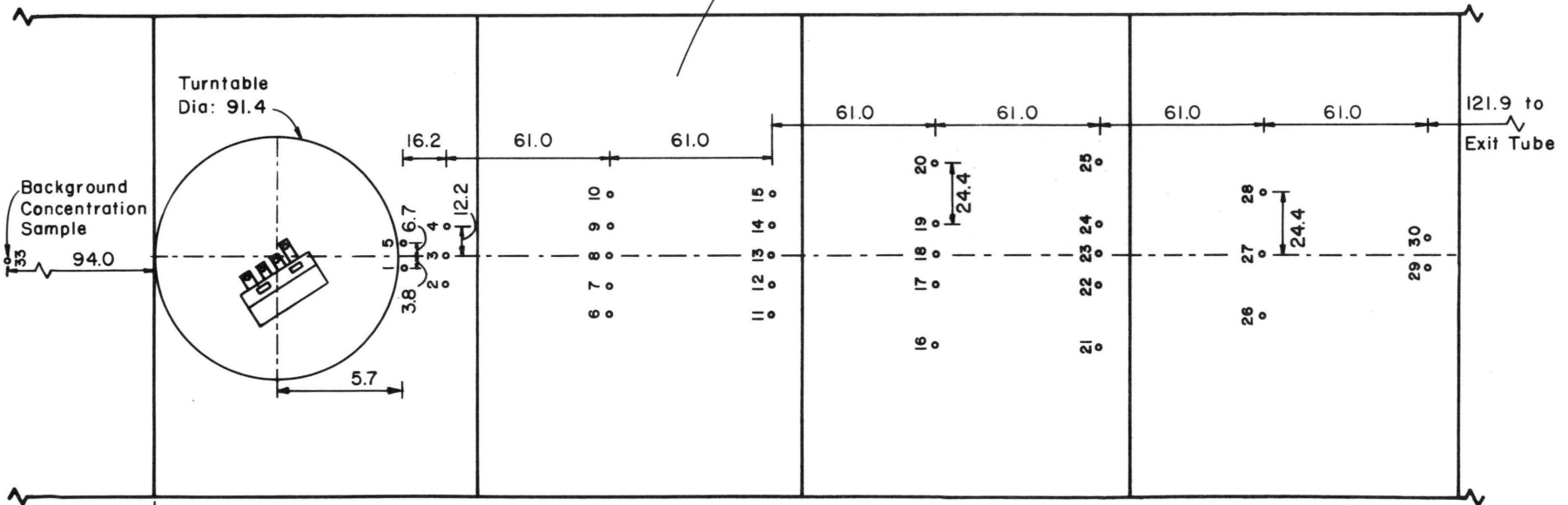
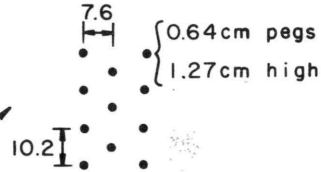


All Dimensions in m

ELEVATION

Figure 4.2-4. Industrial wind tunnel.

Roughness Pattern for each
121.9 x 182.9 Masonite Sheet -
a Total of 37 Sheets



Background
Concentration
Sample

Turntable
Dia: 91.4

121.9 to
Exit Tube

Distance
to Spires:
1097

975 to
Beginning of
Roughness

Note: All Dimensions in cm
Scale
Model

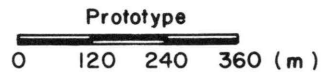


Figure 4.2-5. Wind tunnel set-up.

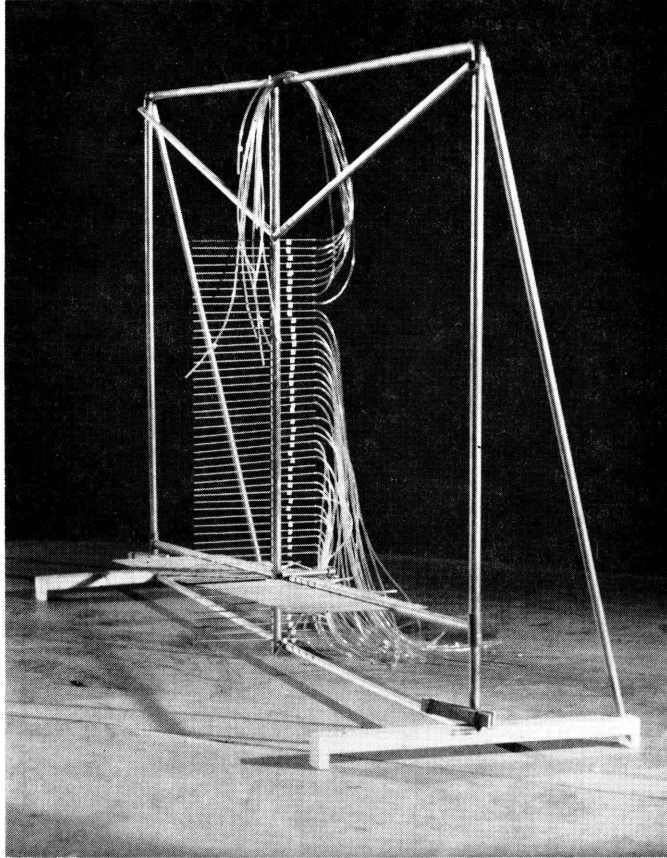


Figure 4.4-1. Sampling rake used for obtaining horizontal and vertical concentration profiles.

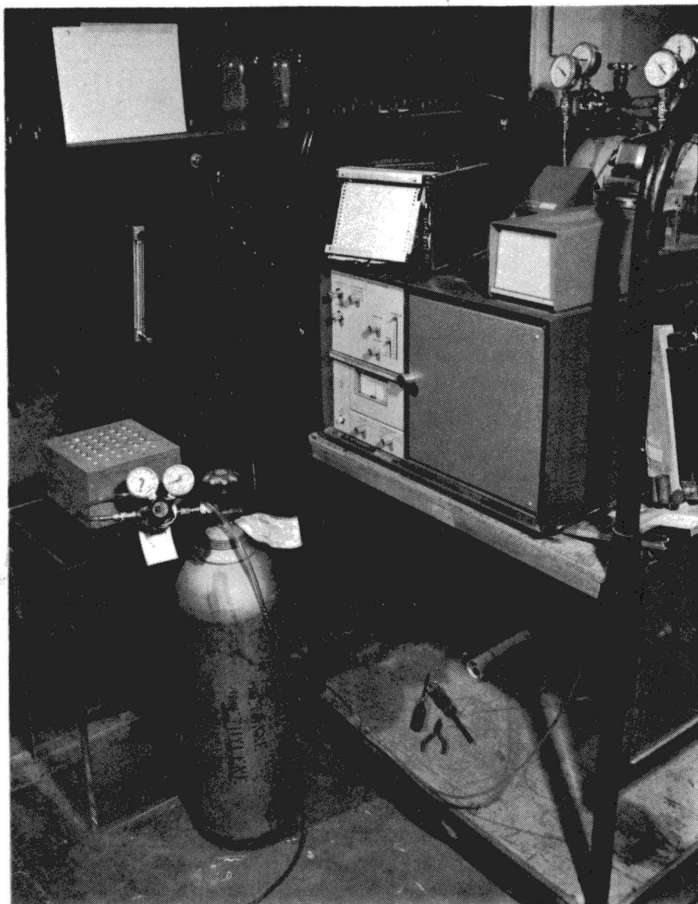


Figure 4.4-2. Equipment set-up for gas sampling. Shown in picture are Hewlett-Packard FID Gas Chromatograph, chart recorder, calibration gas cylinder, and sampling manifold.

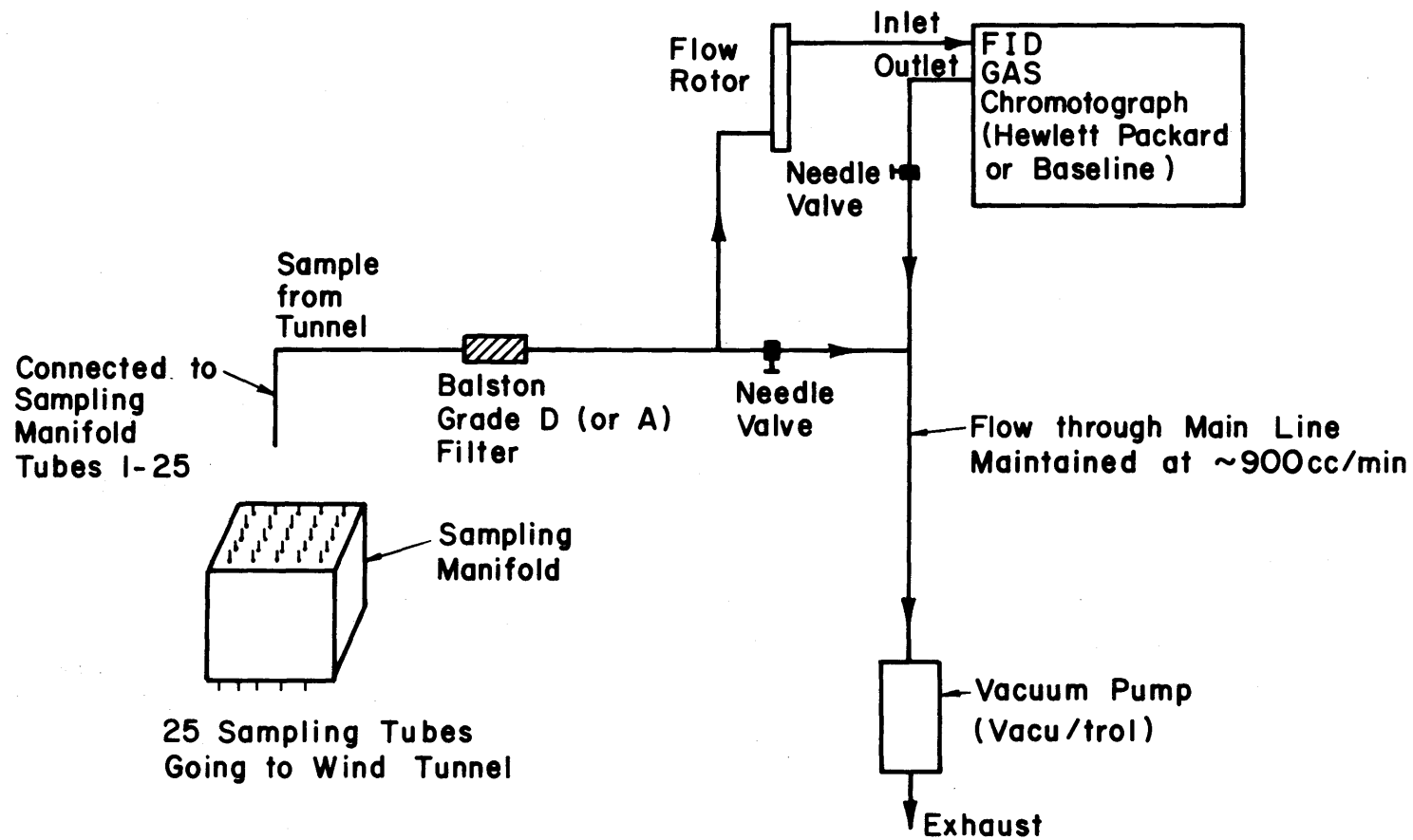


Figure 4.4-3. Schematic of gas sampling equipment set-up.

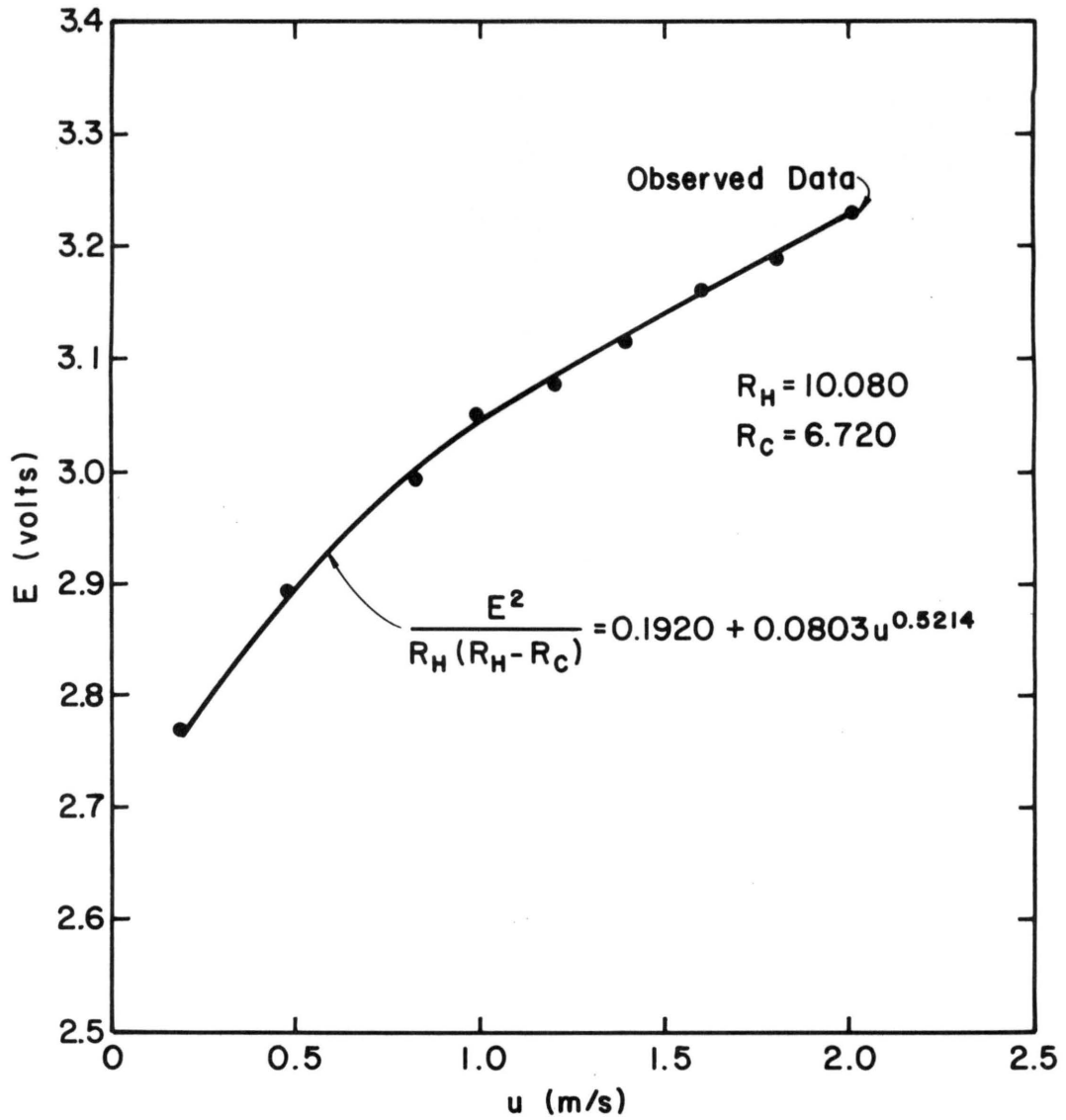
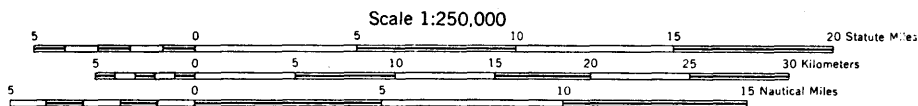
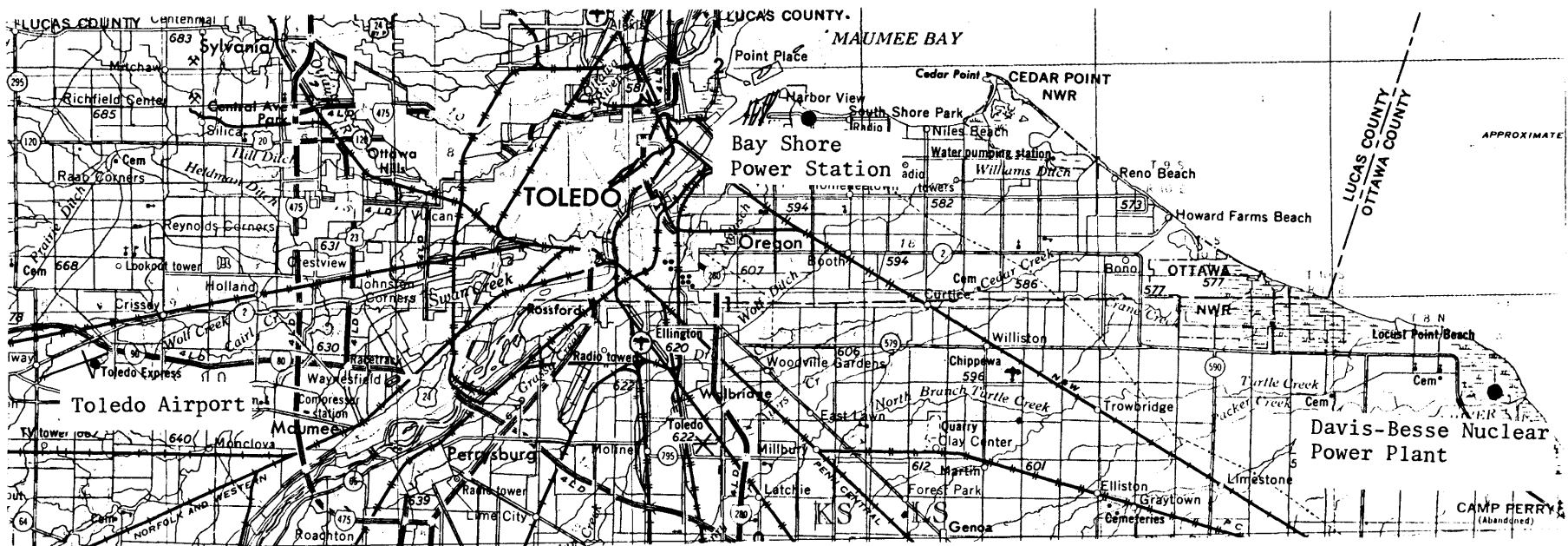


Figure 4.5-1. Hot-film calibration curve used for obtaining velocity profiles.



CONTOUR INTERVAL 50 FEET

TRANSVERSE MERCATOR PROJECTION

BLACK NUMBERED LINES INDICATE THE 10,000 METER UNIVERSAL TRANSVERSE MERCATOR GRID, ZONE 17

1985 MAGNETIC DECLINATION FROM TRUE NORTH VARIES FROM 2° (40 MILES) WESTERLY FOR THE CENTER OF THE WEST EDGE TO 3¼° (60 MILES) WESTERLY FOR THE CENTER OF THE EAST EDGE

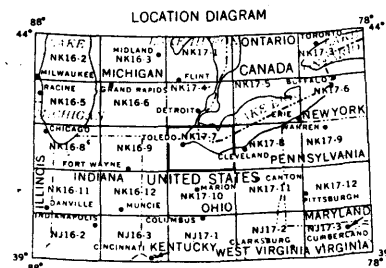


Figure 5.1-1. Map showing location of Bay Shore Power Station, the Toledo Airport and Davis-Besse Nuclear Power Plant.

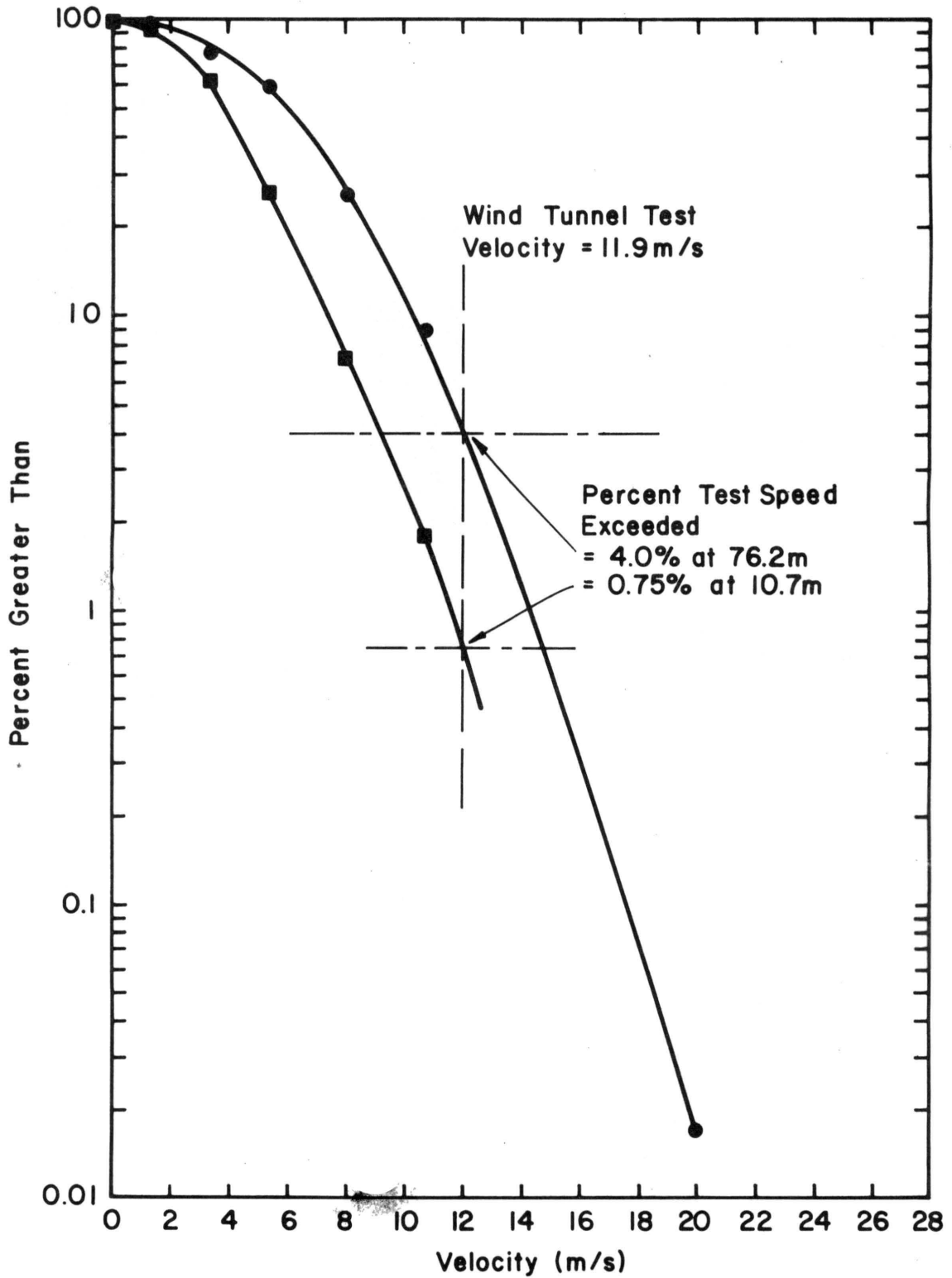
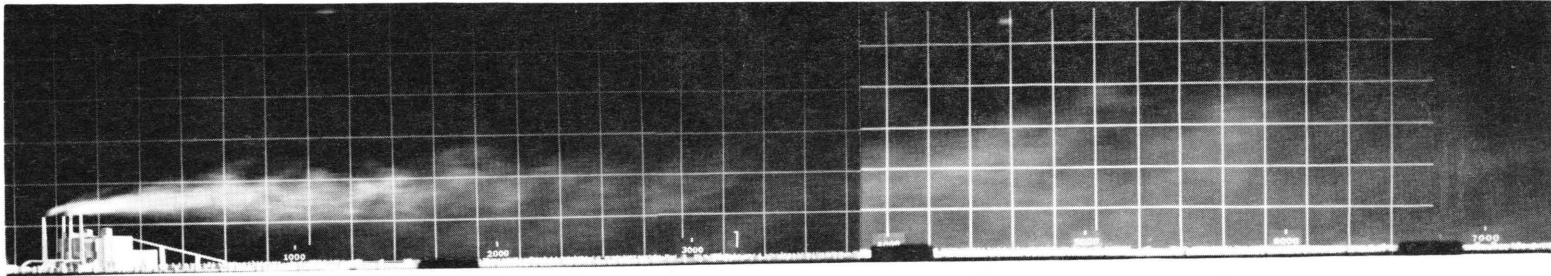
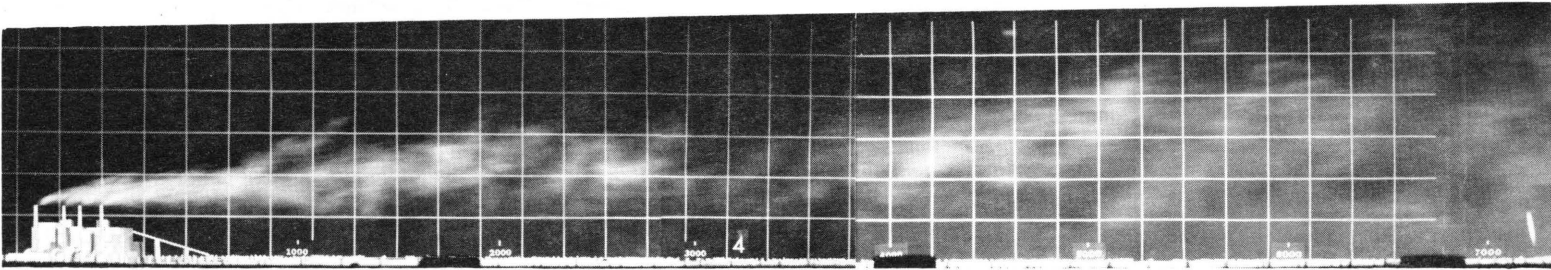


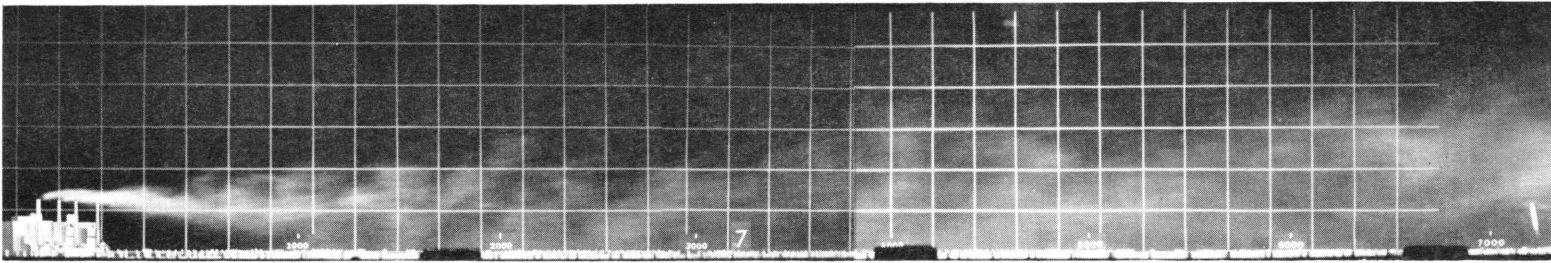
Figure 5.1-2. Percent of time wind velocity exceeds indicated level-- based on Davis-Besse 76.2 m wind for periods 8/4/74-12/16/75 and 4/22/77-12/31/78; based on Davis-Besse 10.7 m wind for period 8/4/74-8/31/75.



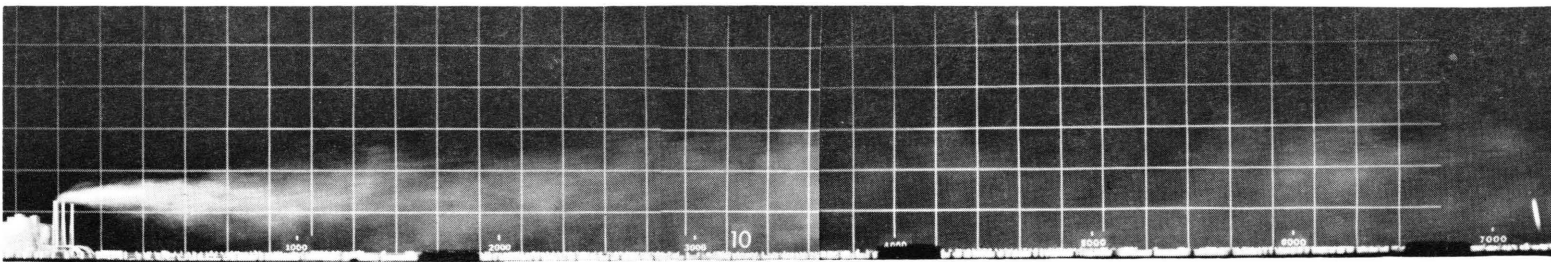
a



b

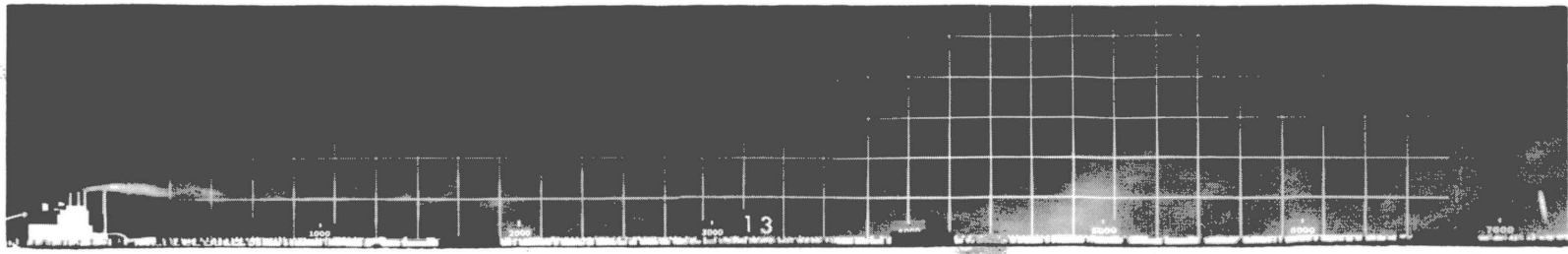


c

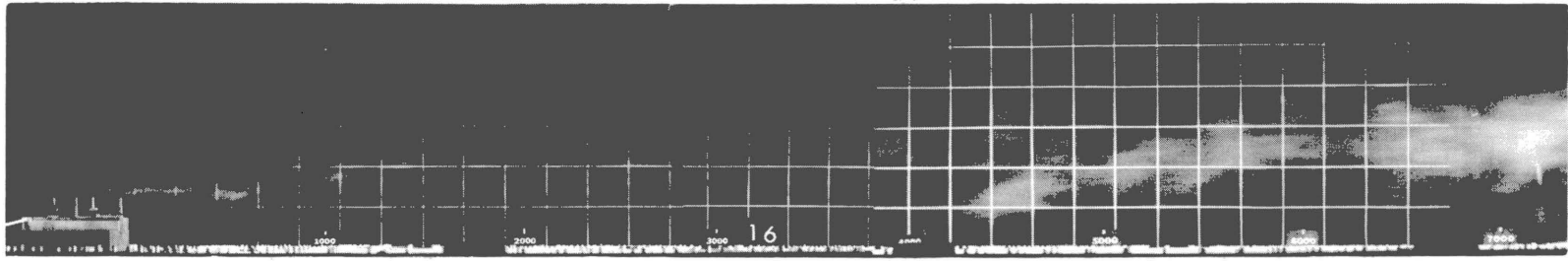


d

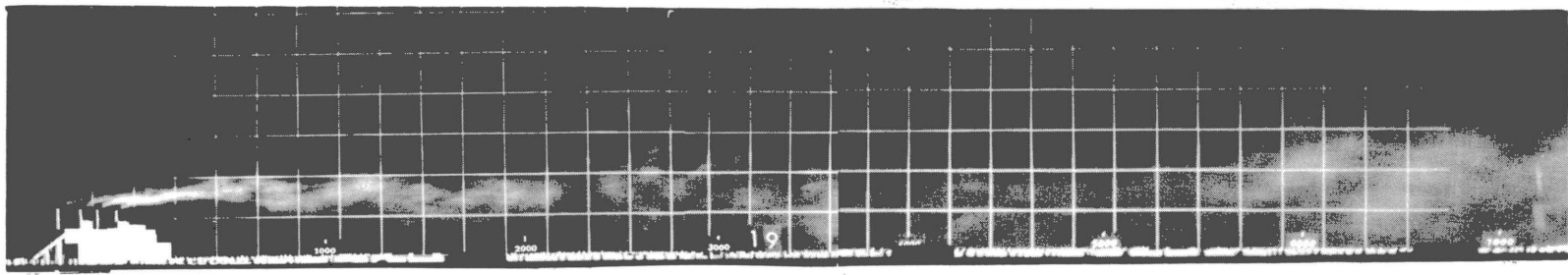
Figure 6.1-1. Plume visualization of BSPS for 100 percent load cases with the building present and wind directions of a) north, b) northeast, c) east, and d) southeast.



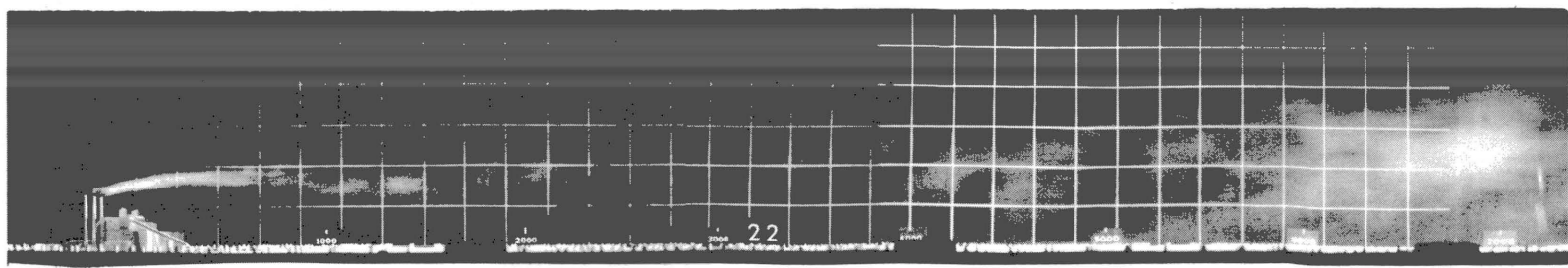
e



f



g



h

Figure 6.1-1 (continued). Plume visualization of BSPS for 100 percent load cases with the building present and wind directions of e) south, f) southwest, g) west, and h) northwest.

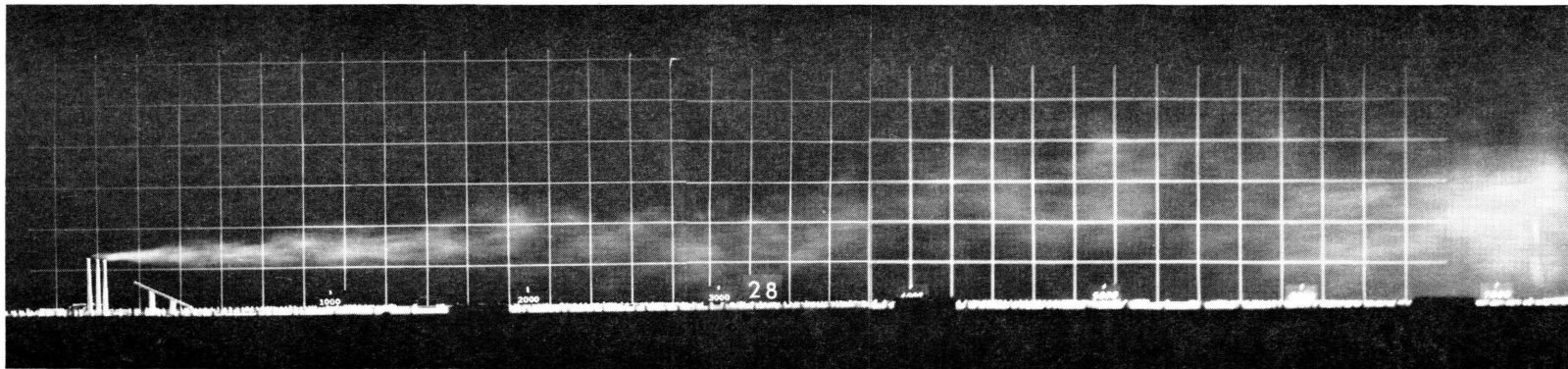
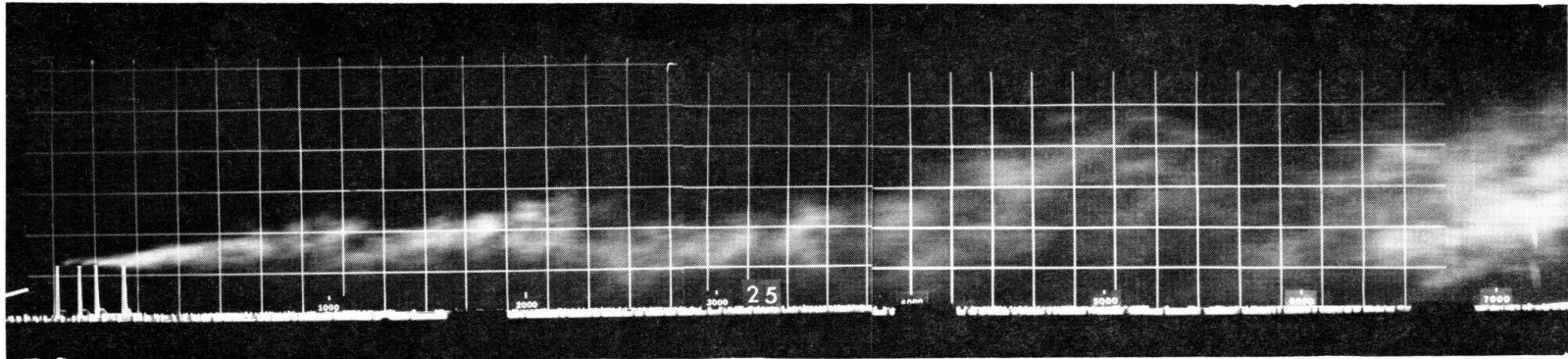


Figure 6.1-2. Plume visualization of BPS for 100 percent load cases without the building present for wind directions of a) southwest, and b) northwest.

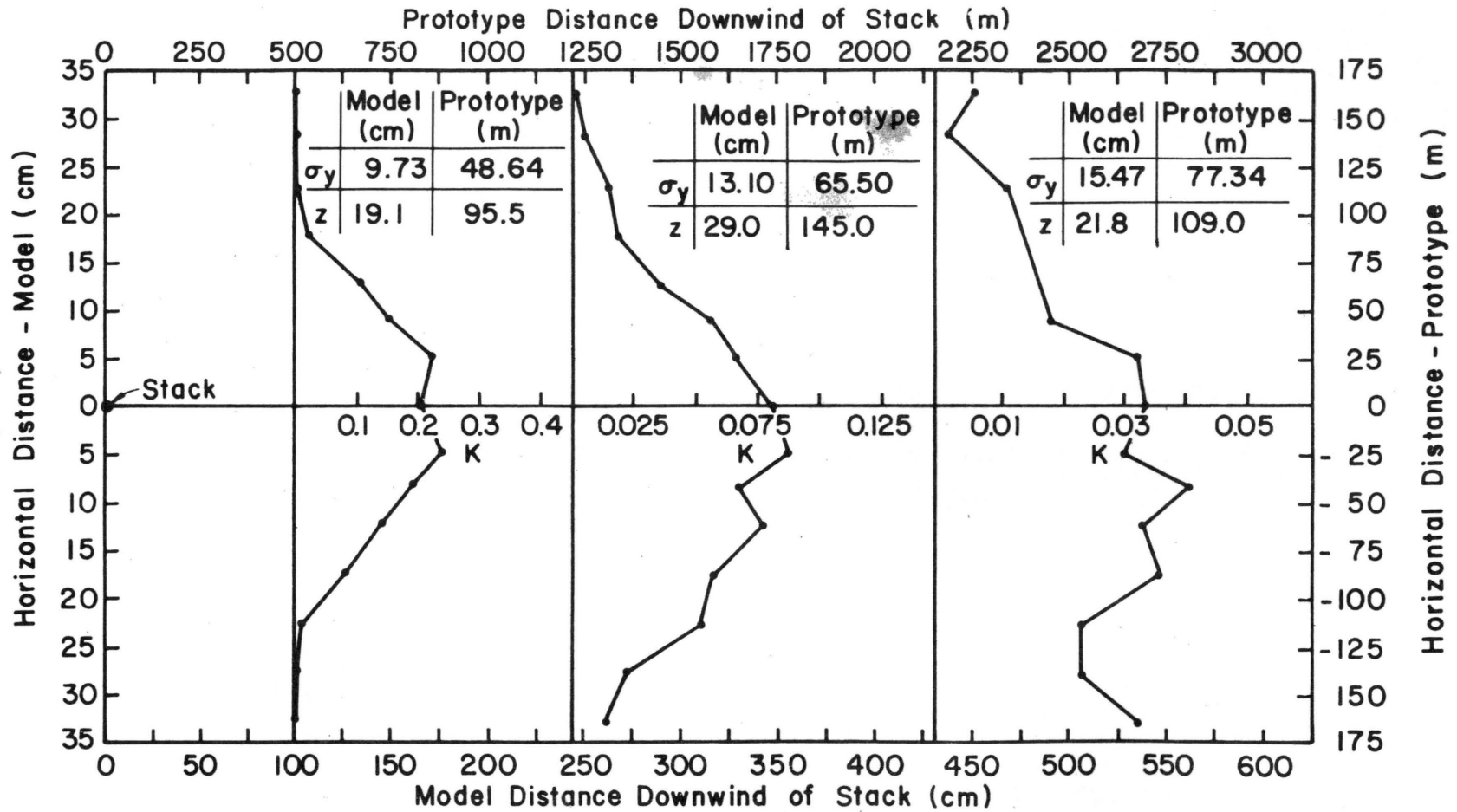


Figure 6.2-1a. Horizontal profiles of dimensionless concentration at the indicated height, z , above the tunnel floor for 100 percent load and a) northwest wind direction without buildings.

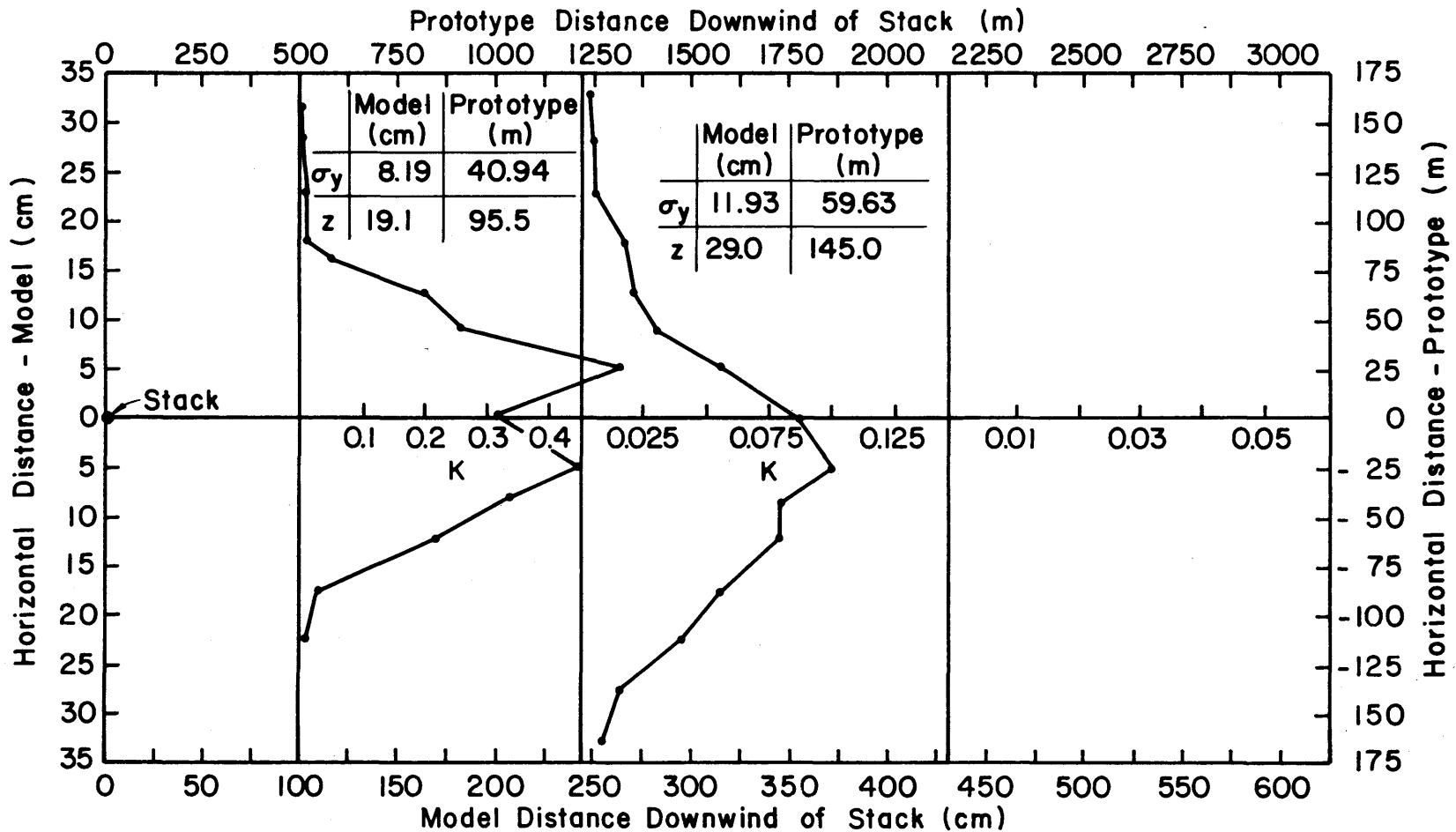


Figure 6.2-lb. Horizontal profiles of dimensionless concentration at the indicated height, z , above the tunnel floor for 100 percent load and b) southwest wind direction without the buildings.

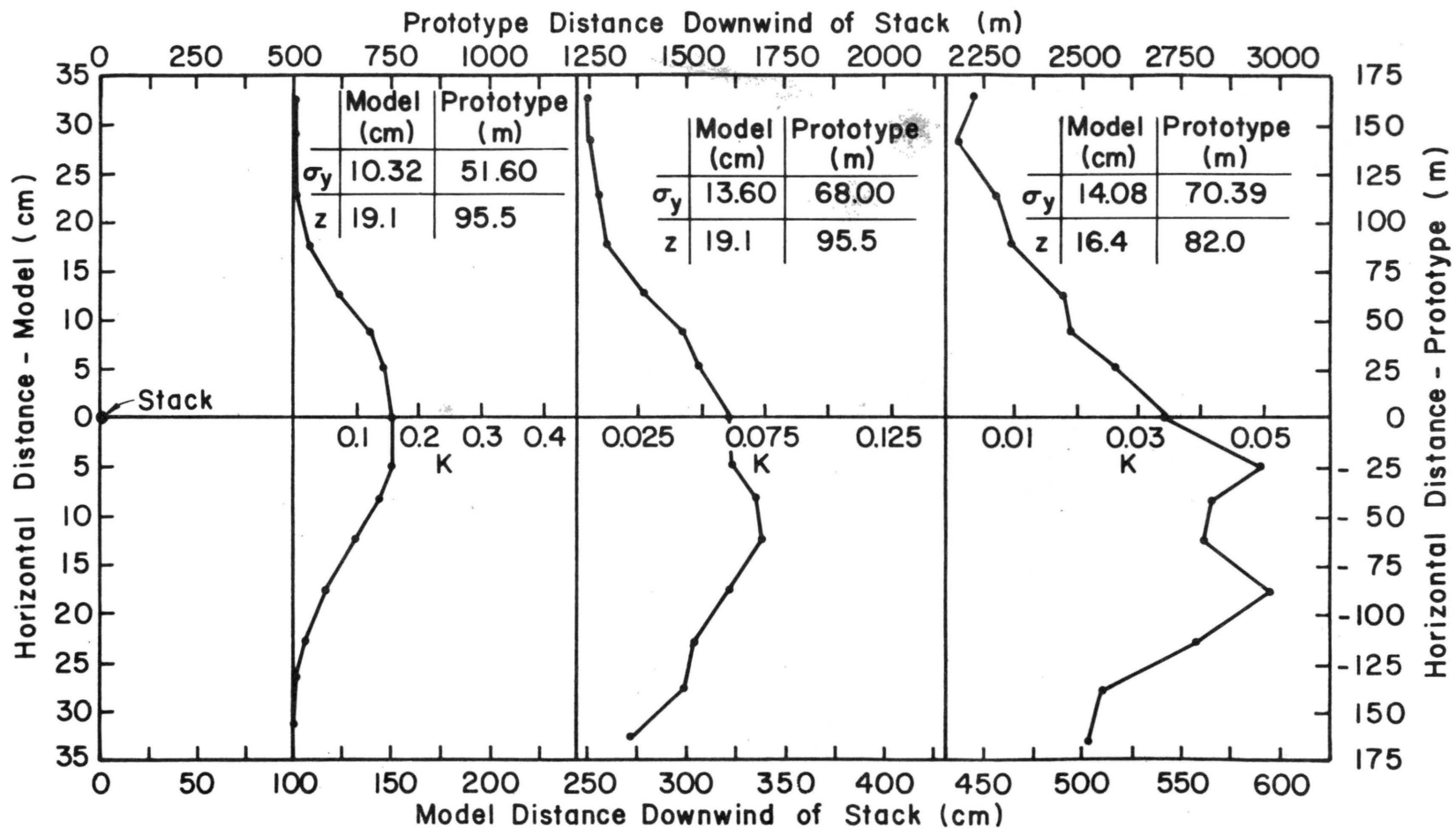


Figure 6.2-1c. Horizontal profiles of dimensionless concentration at the indicated height, z , above the tunnel floor for 100 percent load and c) southeast wind direction with the buildings.

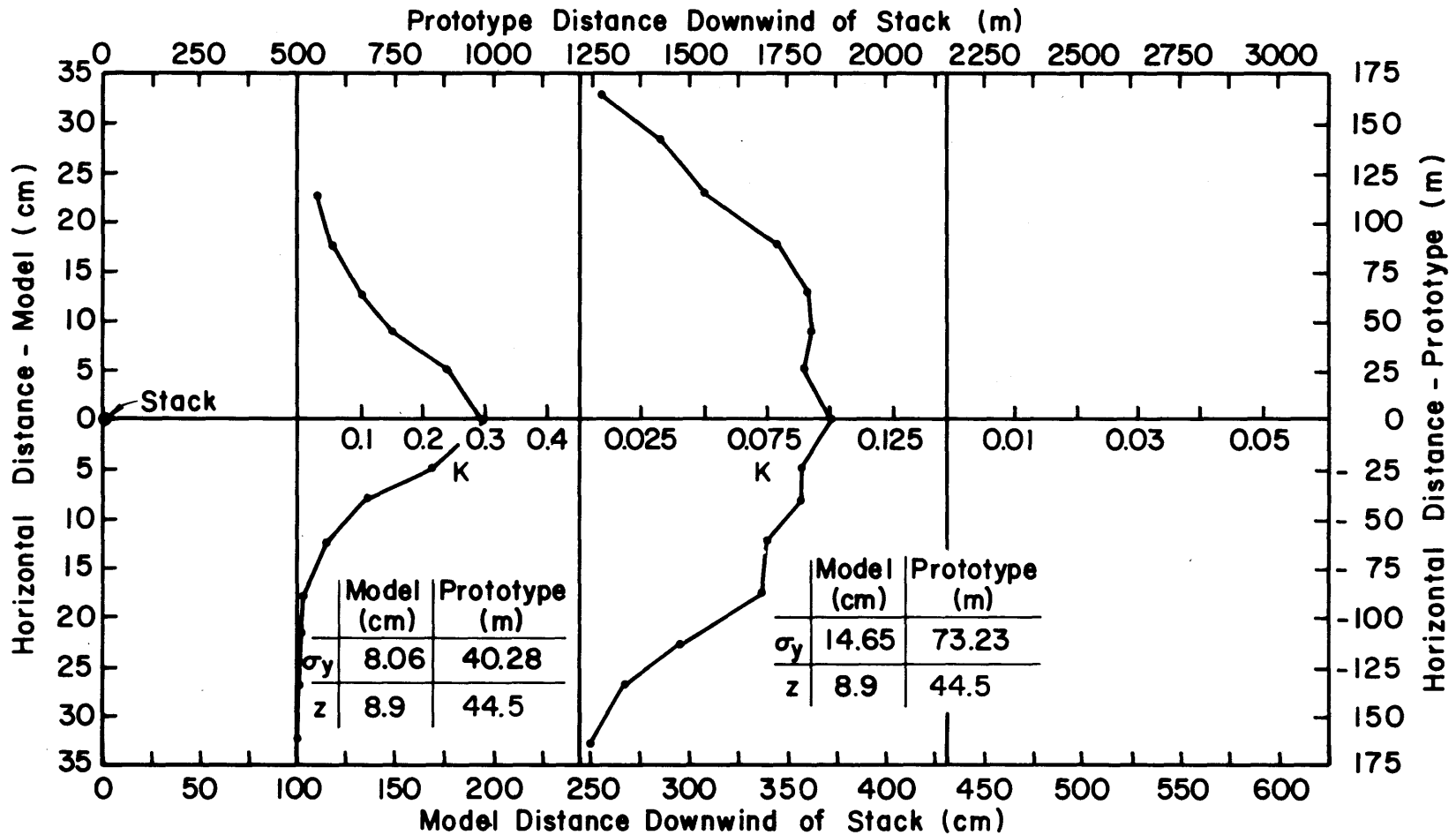


Figure 6.2-1d. Horizontal profiles of dimensionless concentration at the indicated height, z , above the tunnel floor for 100 percent load and d) south wind direction with the buildings.

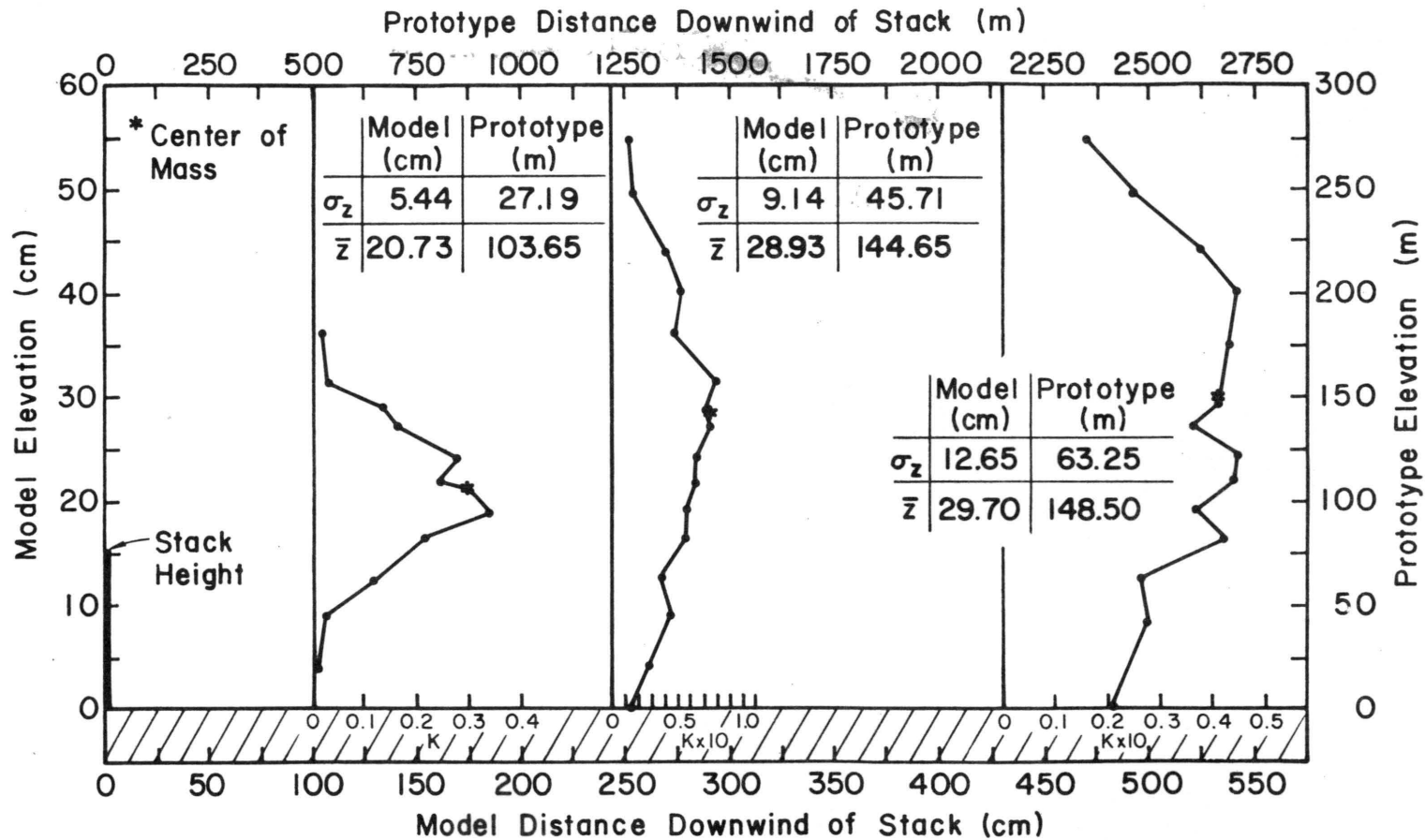


Figure 6.2-2a. Vertical profiles of dimensionless concentration at the indicated downwind distance for 100 percent load and a) northwest wind direction without the buildings.

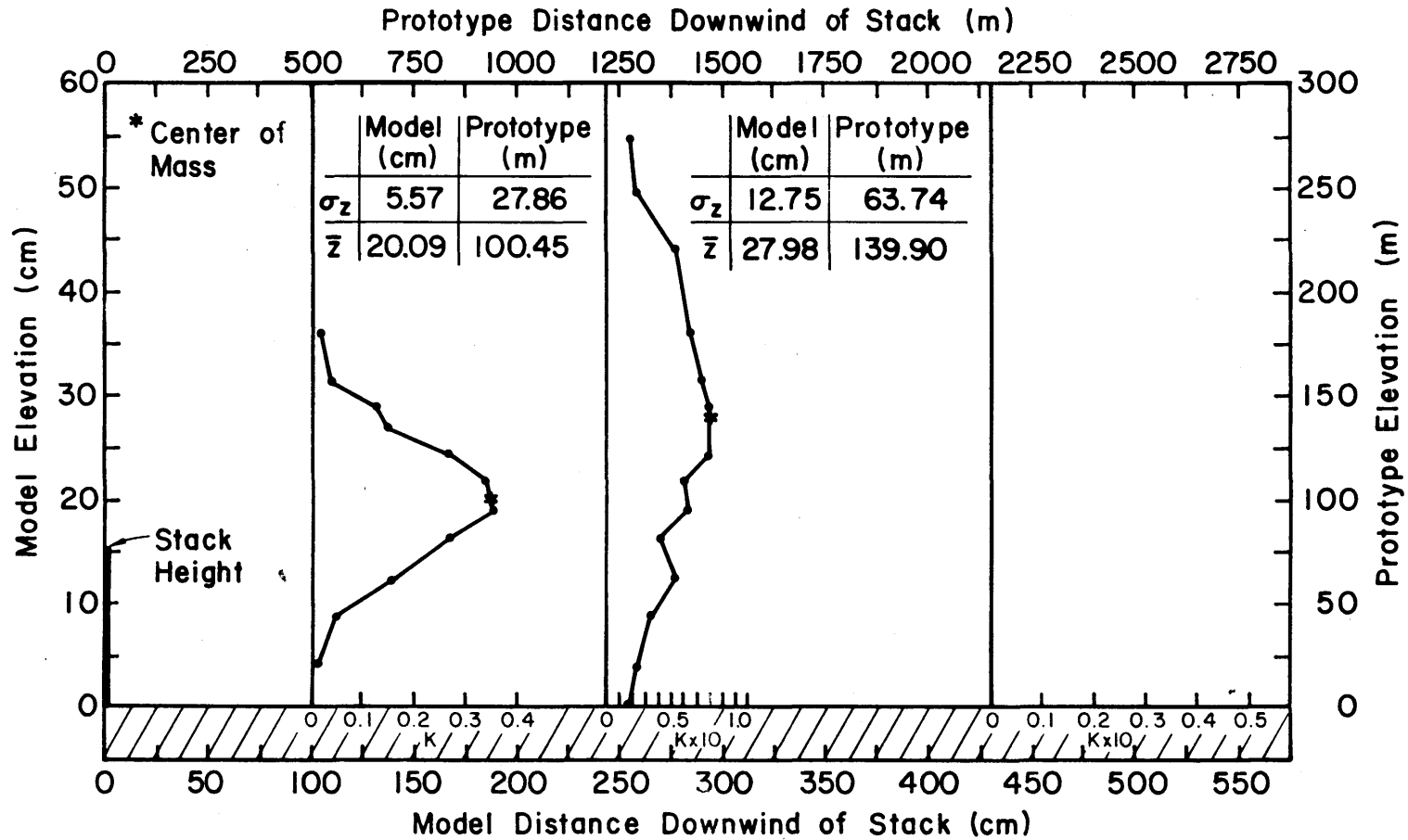


Figure 6.2-2b. Vertical profiles of dimensionless concentration at the indicated downwind distance for 100 percent load and b) southwest wind direction without buildings.

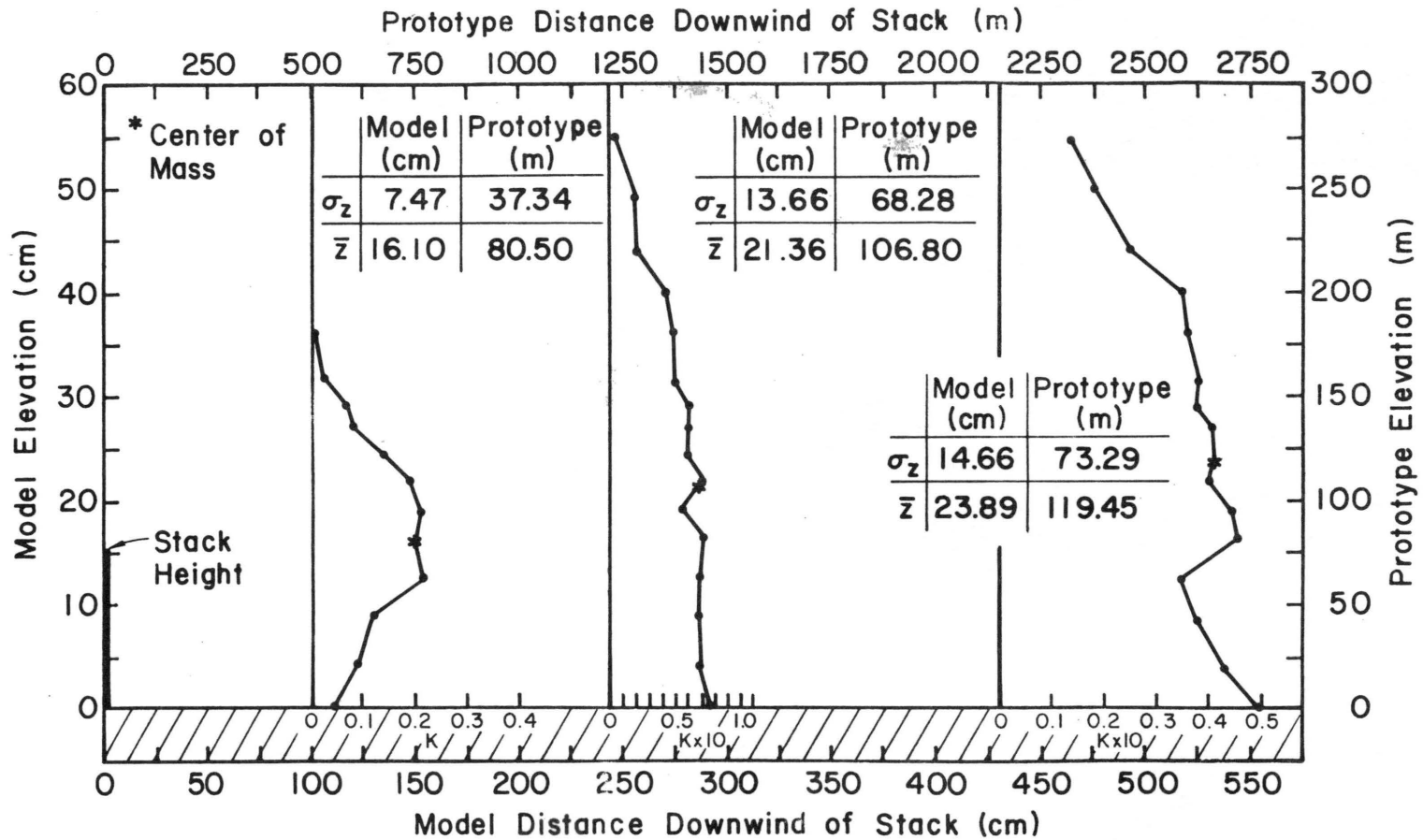


Figure 6.2-2c. Vertical profiles of dimensionless concentration at the indicated downwind distance for 100 percent load and c) southeast wind direction with the buildings.

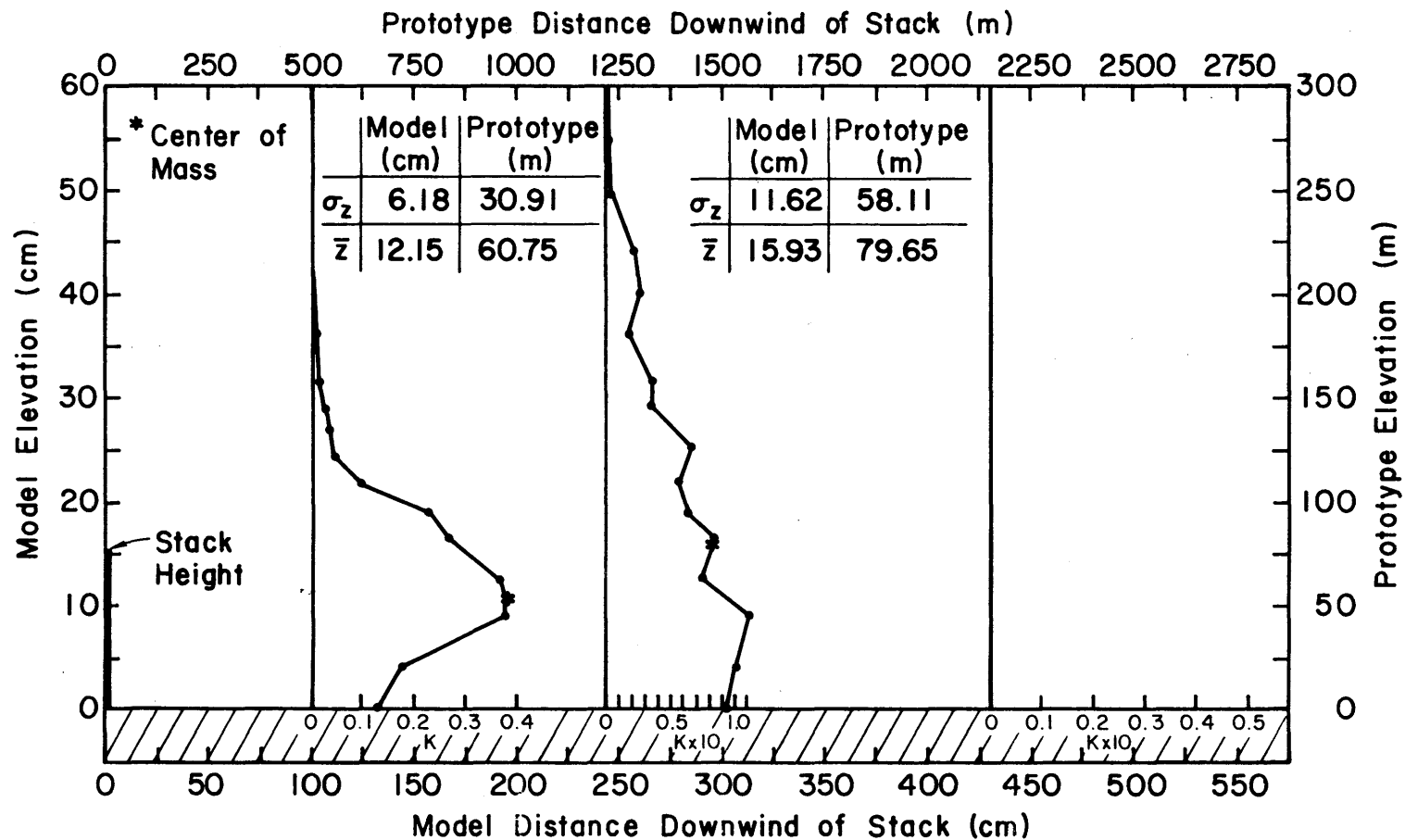


Figure 6.2-d. Vertical profiles of dimensionless concentration at the indicated downwind distance for 100 percent load and d) south wind direction with buildings.

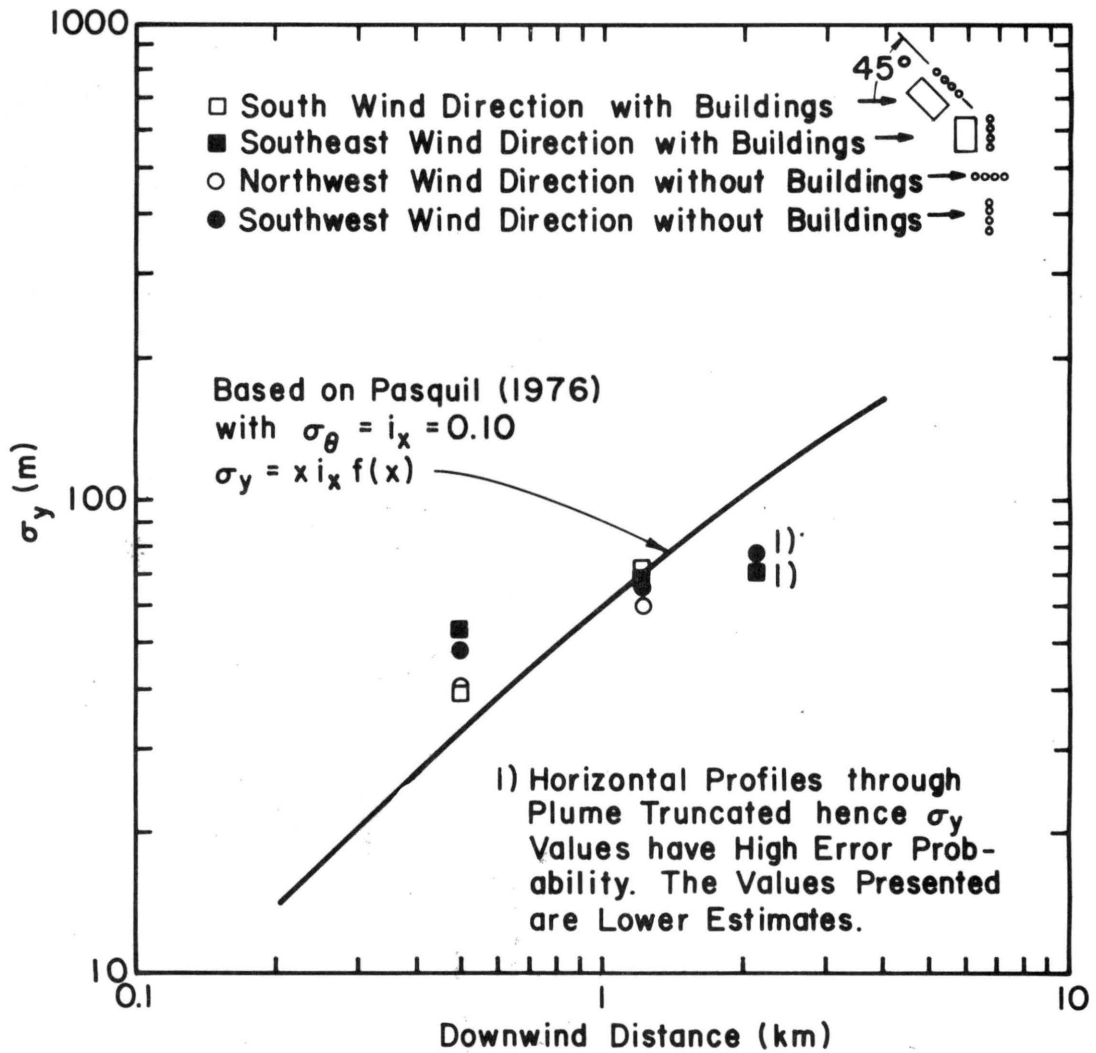


Figure 6.2-3. Atmospheric horizontal dispersion rate for neutral stability in comparison to wind tunnel results.

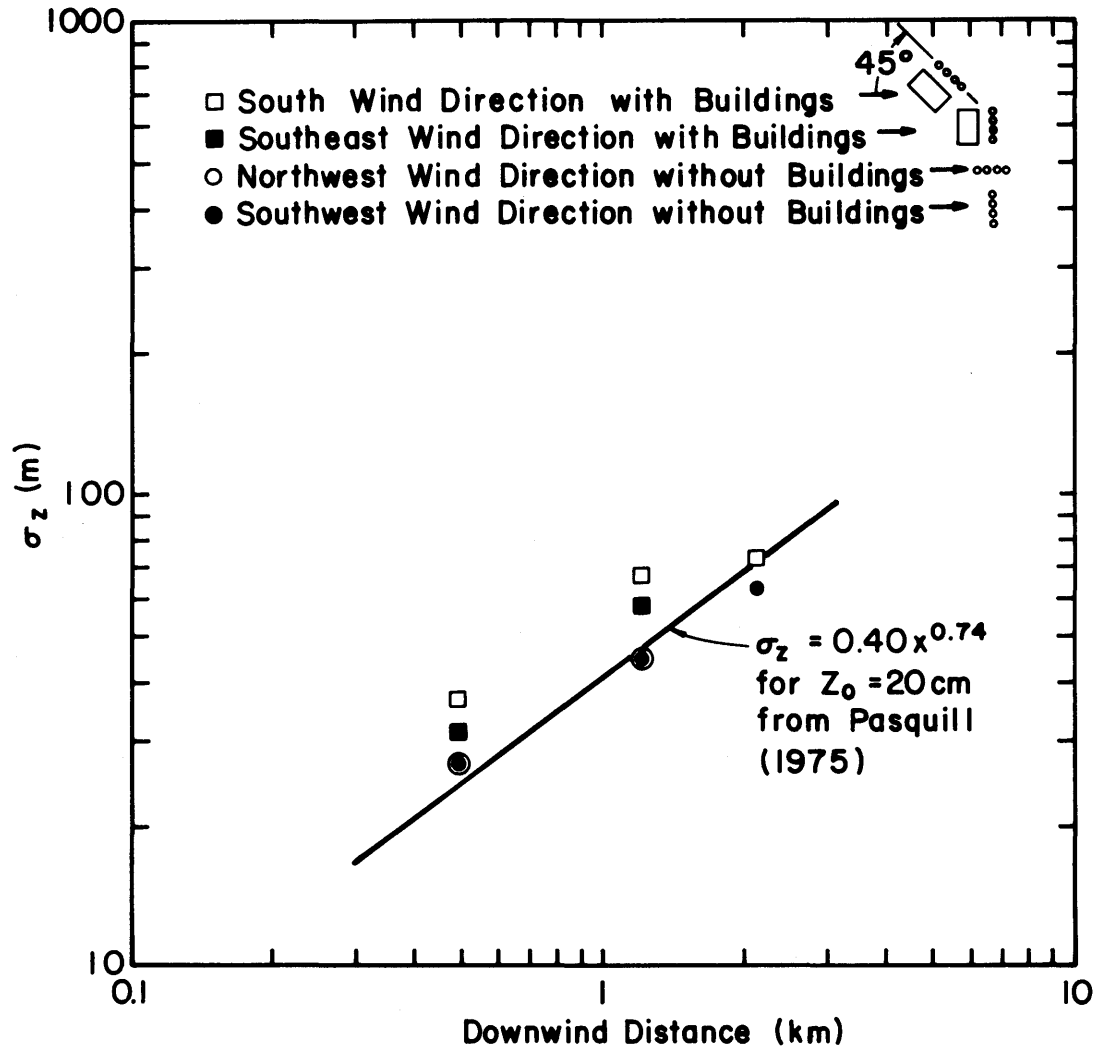


Figure 6.2-4. Atmospheric vertical dispersion rate for neutral stability in comparison to wind tunnel results.

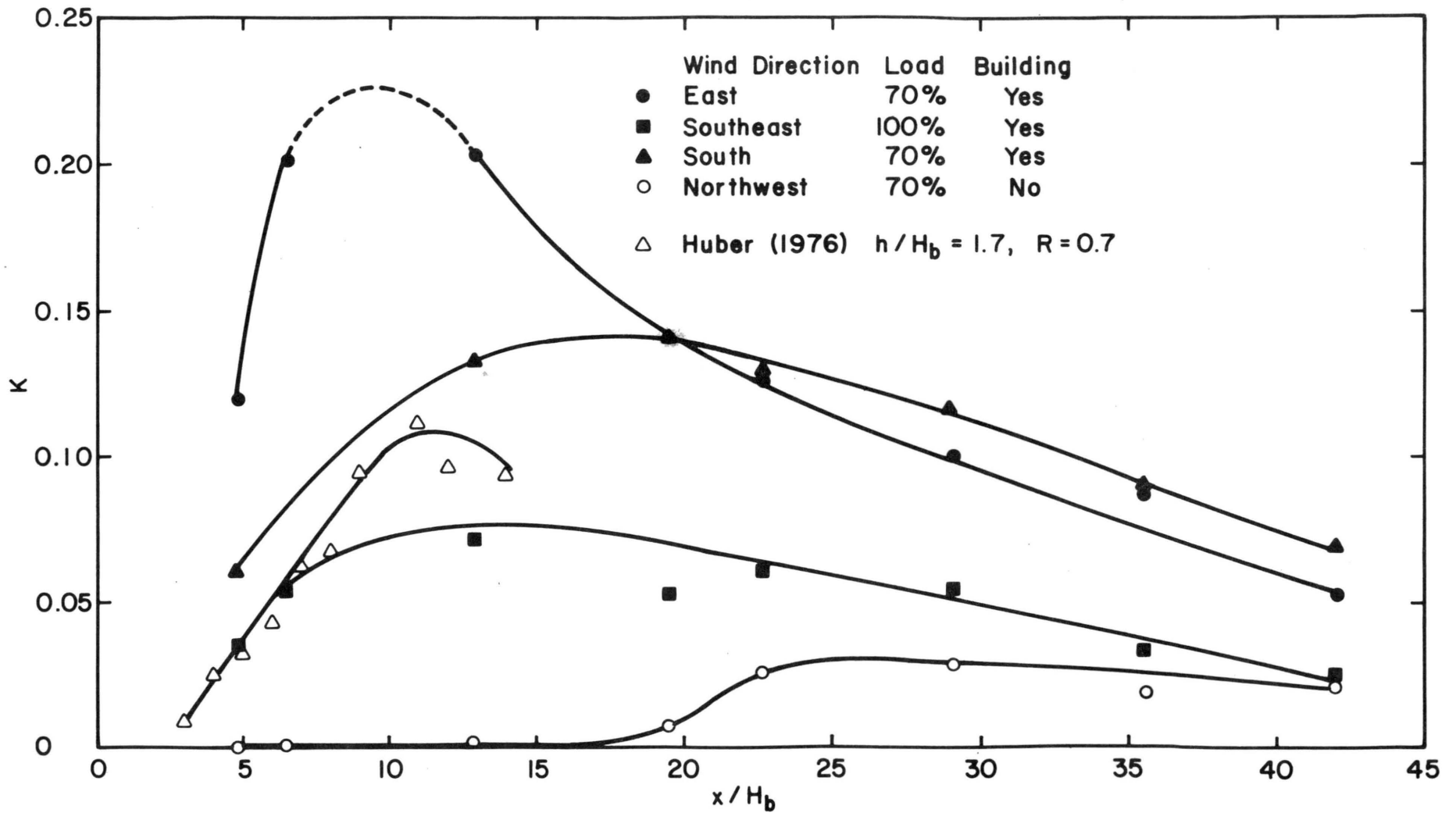


Figure 6.2-5. Plots of K versus x/H_b for three wind directions with the buildings, one case without the buildings and one case from Huber (1976).

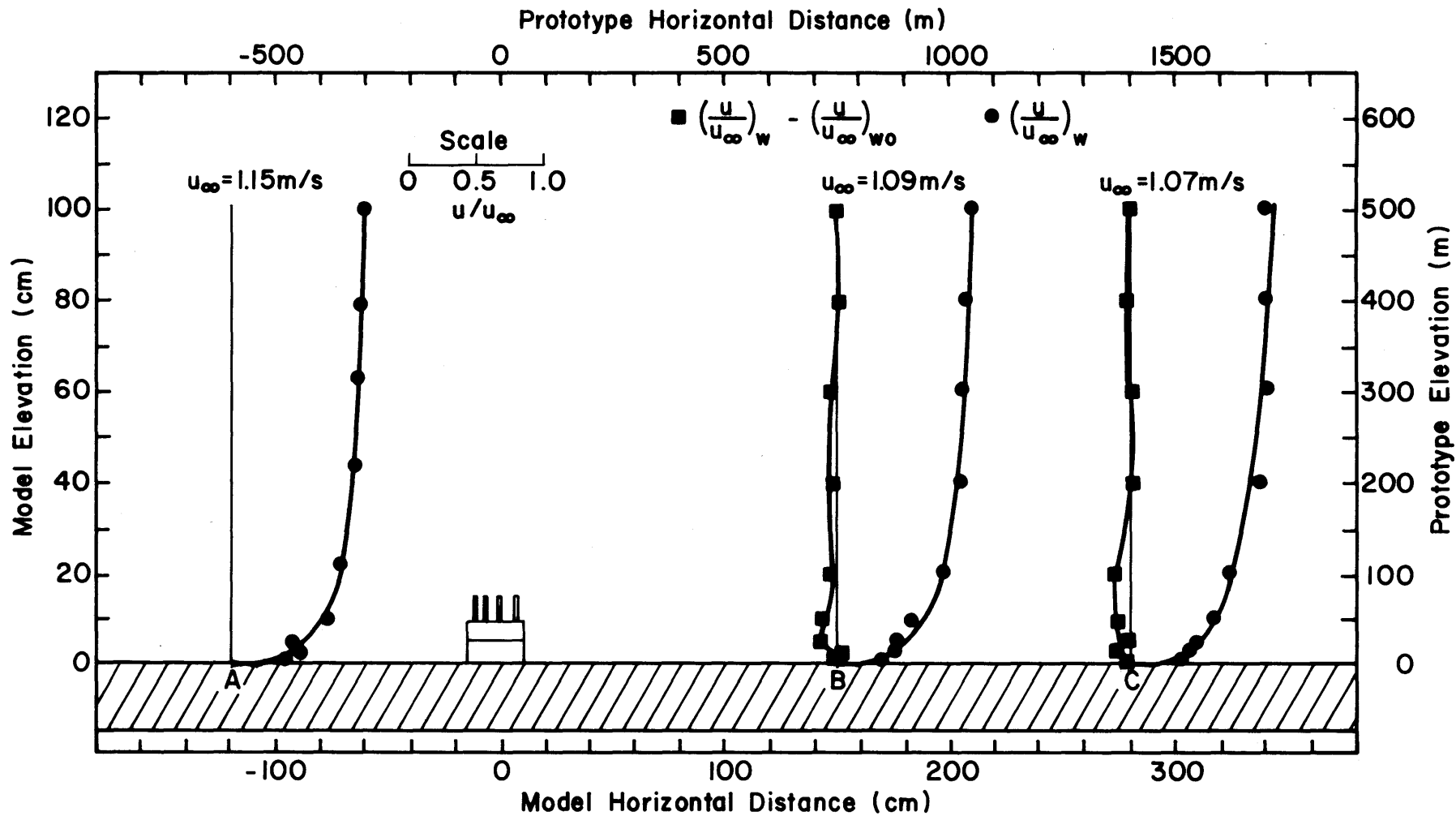


Figure 6.3-1. Vertical profiles of dimensionless velocity with the building present $[(\frac{u}{u_\infty})_w]$ and the difference in dimensionless velocity $[(\frac{u}{u_\infty})_w - (\frac{u}{u_\infty})_{w0}]$.

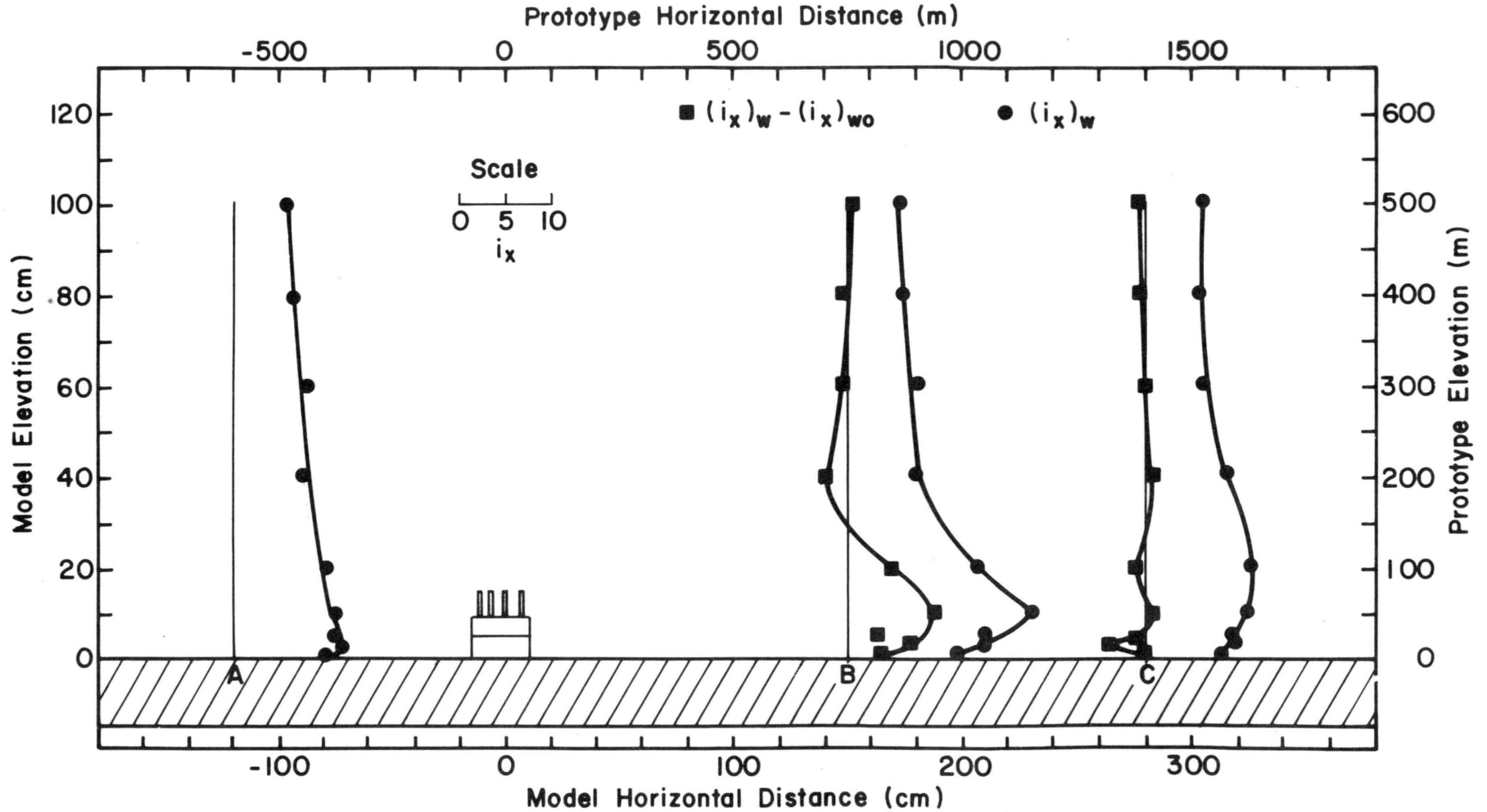


Figure 6.3-2. Vertical profiles of turbulence intensity with the building $[(i_x)_w]$ and turbulence intensity difference $[(i_x)_w - (i_x)_{wo}]$.

APPENDIX A

Concentration Data Tabulations

Note: The exit velocity tabulated is the equivalent exit velocity if all the effluent were emitted through a single stack of the indicated diameter.

CONCENTRATION DATA FOR RUN NO. 1 ON FEB. 20 1979 AT 11:37.
 WIND DIRECTION: 0 DEG. UNITS: 1 SCALE FACTOR: 500.
 DATA FOR TRACER GAS NO. 1, ETHANE BACKGROUND CONC. 1060.3 MV-SEC.
 CAL. FACTOR: .027 GAS FACTOR (PPM GAS/PPM METHANE): .533

VELOCITY (M/SEC) MODEL
 SOURCE STRENGTH (PPM) .812E+05
 VOLUME FLOW (CU. M/SEC) .334E-03
 STACK DIAMETER (M) .740E-02
 EXIT VELOCITY (M/SEC) .777E+01
 DENSITY RATIO .60
 BUILDING HEIGHT .0945

LOCATION	RAW DATA (MV-SEC)	NON-DIMENSIONAL CONCENTRATION COEFFICIENT(K)
1 *	1305.103	.102E-02
2 **	1324.970	.110E-02
4 **	3509.021	.102E-01
3 **	7665.927	.276E-01
5 **	2315.562	.524E-02
6 **	1440.700	.159E-02
7 **	9386.949	.348E-01
8 **	18460.50	.726E-01
9 **	12222.55	.466E-01
10 **	2795.939	.724E-02
11 **	1592.000	.222E-02
12 **	3767.346	.113E-01
13 **	15037.47	.583E-01
14 **	14162.02	.547E-01
15 **	8333.838	.304E-01
16 **	1184.611	.519E-03
17 **	10934.48	.412E-01
18 **	13210.59	.507E-01
19 **	12235.55	.466E-01
20 **	2002.260	.393E-02
21 **	1427.250	.153E-02
22 **	6568.204	.230E-01
23 **	14715.10	.570E-01
24 **	13804.28	.532E-01
25 **	4215.122	.132E-01
26 **	6253.204	.217E-01
27 **	2481.589	.593E-02
28 **	8088.292	.293E-01
29 **	8503.928	.311E-01
30 **	12648.11	.484E-01

CONCENTRATION DATA FOR RUN NO. 2 ON FEB. 20 1979 AT 13:40.
 WIND DIRECTION: 0 DEG. UNITS: 2 SCALE FACTOR: 500.
 DATA FOR TRACER GAS NO. 1, ETHANE BACKGROUND CONC. 449.25 MV-SEC.
 CAL FACTOR: .027 GAS FACTOR (PPM GAS/PPM METHANE): .533

	MODEL
VELOCITY (M/SEC)	.88
SOURCE STRENGTH (PPM)	.812E+05
VOLUME FLOW (CU. M/SEC)	.283E-03
STACK DIAMETER (M)	.740E-02
EXIT VELOCITY (M/SEC)	.658E+01
DENSITY RATIO	.60
BUILDING HEIGHT	.0945

LOCATION	RAW DATA (MV-SEC)	NON-DIMENSIONAL CONCENTRATION COEFFICIENT(K)
5 *	2257.799	.891E-02
3 *	5437.636	.246E-01
8 *	14409.34	.688E-01
14 *	14530.29	.694E-01
18 *	16518.32	.792E-01
23 *	11735.95	.556E-01
29 *	7932.815	.369E-01
30 *	9751.996	.458E-01

CONCENTRATION DATA FOR RUN NO. 3 ON FEB. 20 1979 AT 14:40.
 WIND DIRECTION: 0 DEG. UNITS: 3 SCALE FACTOR: 500.
 DATA FOR TRACER GAS NO. 1, ETHANE BACKGROUND CONC. 690.72 MV-SEC.
 CAL. FACTOR: .027 GAS FACTOR (PPM GAS/PPM METHANE): .533

MODEL
 VELOCITY (M/SEC) .88
 SOURCE STRENGTH (PPM) .812E+05
 VOLUME FLOW (CU. M/SEC) .234E-03
 STACK DIAMETER (M) .740E-02
 EXIT VELOCITY (M/SEC) .544E+01
 DENSITY RATIO .60
 BUILDING HEIGHT .0945

LOCATION	RAW DATA (MV-SEC)	NON-DIMENSIONAL CONCENTRATION COEFFICIENT(K)
5 *	2267.072	.939E-02
3 *	5642.861	.295E-01
8 *	16071.38	.916E-01
14 *	12278.43	.690E-01
18 *	13696.38	.775E-01
23 *	11261.82	.630E-01
29 *	8360.418	.457E-01
30 *	10129.65	.562E-01

CONCENTRATION DATA FOR RUN NO. 4 ON FEB. 20 1979 AT 15:30. SCALE FACTOR: 500.
 WIND DIRECTION: 45 DEG. UNITS: 1 BACKGROUND CONC. 699.08 MV-SEC.
 DATA FOR TRACER GAS NO. 1, ETHANE GAS FACTOR (PPM GAS/PPM METHANE): .533
 CAL. FACTOR: .027

VELOCITY (M/SEC) MODEL .88
 SOURCE STRENGTH (PPM) .812E+05
 VOLUME FLOW (CU. M/SEC) .334E-03
 STACK DIAMETER (M) .740E-02
 EXIT VELOCITY (M/SEC) .777E+01
 DENSITY RATIO .60
 BUILDING HEIGHT .0945

LOCATION	RAW DATA (MV-SEC)	NON-DIMENSIONAL CONCENTRATION COEFFICIENT(K)
1	858.5811	.666E-03
2	875.7382	.737E-03
3	1301.0333	.251E-02
4	1169.670	.196E-02
5	1094.7655	.165E-02
6	989.9746	.120E-02
7	1391.5330	.338E-02
8	2755.9331	.659E-02
9	1812.312	.465E-02
10	945.1270	.103E-02
11	1350.372	.272E-02
12	1018.276	.133E-02
13	4219.337	.147E-01
14	3537.004	.118E-01
15	3020.438	.969E-02
16	949.2643	.104E-02
17	1440.291	.309E-02
18	5790.451	.213E-01
19	3252.104	.107E-01
20	1090.710	.167E-02
21	995.9818	.124E-02
22	77.481	.638E-02
23	776.011	.279E-01
24	781.371	.869E-02
25	1545.433	.353E-02
26	4924.087	.176E-01
27	1091.550	.139E-02
28	798.754	.129E-01
29	602.493	.640E-02
30	600.450	.122E-01

CONCENTRATION DATA FOR RUN NO. 5 ON FEB. 20 1979 AT 17: 5.
 WIND DIRECTION: 45 DEG. UNITS: 2 SCALE FACTOR: 500.
 DATA FOR TRACER GAS NO. 1, ETHANE BACKGROUND CONC. 878.73 MV-SEC.
 CAL. FACTOR: .027 GAS FACTOR (PPM GAS/PPM METHANE): .533

	MODEL
VELOCITY (M/SEC)	.88
SOURCE STRENGTH (PPM)	.812E+05
VOLUME FLOW (CU. M/SEC)	.283E-03
STACK DIAMETER (M)	.740E-02
EXIT VELOCITY (M/SEC)	.658E+01
DENSITY RATIO	.60
BUILDING HEIGHT	.0945

LOCATION	RAW DATA (MV-SEC)	NON-DIMENSIONAL CONCENTRATION COEFFICIENT(K)
5 *	1115.773	.117E-02
3 **	1275.260	.195E-02
8 **	2407.932	.753E-02
15 **	1690.655	.400E-02
18 **	4674.147	.187E-01
23 **	4978.159	.202E-01
28 **	4084.628	.158E-01
30 *	4024.731	.155E-01

CONCENTRATION DATA FOR RUN NO. 6 ON FEB. 20 1979 AT 18:10.
 WIND DIRECTION: 45 DEG. UNITS: 3 SCALE FACTOR: 500.
 DATA FOR TRACER GAS NO. 1, ETHANE BACKGROUND CONC. 701.50 MV-SEC.
 CAL. FACTOR: .027 GAS FACTOR (PPM GAS/PPM METHANE): .533

	MODEL
VELOCITY (M/SEC)	.88
SOURCE STRENGTH (PPM)	.812E+05
VOLUME FLOW (CU. M/SEC)	.234E-03
STACK DIAMETER (M)	.740E-02
EXIT VELOCITY (M/SEC)	.544E+01
DENSITY RATIO	.60
BUILDING HEIGHT	.0945

LOCATION	RAW DATA (MV-SEC)	NON-DIMENSIONAL CONCENTRATION COEFFICIENT(K)
5 *	1114.239	.246E-02
3 *	1215.192	.306E-02
8 *	2968.747	.135E-01
15 *	2127.734	.850E-02
18 *	5645.517	.295E-01
23 *	5716.324	.299E-01
28 *	4219.815	.210E-01
30 *	4689.001	.238E-01

CONCENTRATION DATA FOR RUN NO. 07 ON FEB. 20 1979 AT 20:21
 WIND DIRECTION: 90 DEG. UNITS: 1 SCALE FACTOR: 500.
 DATA FOR TRACER GAS NO. 1, ETHANE BACKGROUND CONC. 1051.0 MV-SEC.
 CAL. FACTOR: .027 GAS FACTOR (PPM GAS/PPM METHANE): .533

VELOCITY (M/SEC) MODEL
 SOURCE STRENGTH (PPM) .812E+05
 VOLUME FLOW (CU. M/SEC) .334E-03
 STACK DIAMETER (M) .740E-02
 EXIT VELOCITY (M/SEC) .777E+01
 DENSITY RATIO .60
 BUILDING HEIGHT .0945

LOCATION	RAW DATA (MV-SEC)	NON-DIMENSIONAL CONCENTRATION COEFFICIENT(K)
1	1681.510	.263E-02
2	1063.760	.533E-04
3	5937.351	.204E-01
4	2780.662	.112E+00
5	12841.03	.492E-01
6	1047.688	.000E+00
7	6994.598	.248E-01
8	27352.41	.110E+00
9	36456.33	.148E+00
10	23022.58	.917E-01
11	11555.888	.438E-03
12	6072.147	.210E-01
13	25594.844	.104E+00
14	33399.45	.122E+00
15	33875.88	.137E+00
16	1314.330	.110E-02
17	4597.322	.148E-01
18	11390.34	.432E-01
19	24773.25	.990E-01
20	7898.020	.286E-01
21	1119.300	.285E-03
22	4351.544	.138E-01
23	14850.17	.576E-01
24	21819.00	.867E-01
25	13672.48	.527E-01
26	7987.332	.290E-01
27	1215.802	.688E-03
28	9712.213	.362E-01
29	19152.48	.756E-01
30	13184.20	.506E-01

CONCENTRATION DATA FOR RUN NO. 08 ON FEB. 20 1979 AT 22:46.
 WIND DIRECTION: 90 DEG. UNITS: 2 SCALE FACTOR: 500.
 DATA FOR TRACER GAS NO. 1, ETHANE BACKGROUND CONC. 503.09 MV-SEC.
 CAL. FACTOR: .027 GAS FACTOR (PPM GAS/PPM METHANE): .533

VELOCITY (M/SEC)	MODEL
SOURCE STRENGTH (PPM)	.89
VOLUME FLOW (CU. M/SEC)	.812E+05
STACK DIAMETER (M)	.283E-03
EXIT VELOCITY (M/SEC)	.740E-02
DENSITY RATIO	.658E+01
BUILDING HEIGHT	.60
	.0945

LOCATION	RAW DATA (MV-SEC)	NON-DIMENSIONAL CONCENTRATION COEFFICIENT (K)
5 *	17462.70	.835E-01
4 *	36160.23	.176E+00
9 *	38293.30	.186E+00
14 *	31129.11	.151E+00
19 *	25892.02	.125E+00
24 *	19493.72	.936E-01
29 *	17627.20	.844E-01
30 *	11933.75	.563E-01

CONCENTRATION DATA FOR RUN NO. 09 ON FEB. 20 1979 AT 23:43.
 WIND DIRECTION: 90 DEG. UNITS: 3 SCALE FACTOR: 500.
 DATA FOR TRACER GAS NO. 1, ETHANE BACKGROUND CONC. 790.51 MV-SEC.
 CAL. FACTOR: .027 GAS FACTOR (PPM GAS/PPM METHANE): .533

	MODEL
VELOCITY (M/SEC)	.88
SOURCE STRENGTH (PPM)	.812E+05
VOLUME FLOW (CU. M/SEC)	.234E-03
STACK DIAMETER (M)	.740E-02
EXIT VELOCITY (M/SEC)	.544E+01
DENSITY RATIO	.60
BUILDING HEIGHT	.0345

LOCATION	RAW DATA (MV-SEC)	NON-DIMENSIONAL CONCENTRATION COEFFICIENT(K)
5 *	20703.71	.119E+00
4 *	34568.22	.201E+00
9 *	36640.51	.214E+00
14 *	24325.63	.140E+00
19 *	21931.40	.126E+00
24 *	17611.36	.100E+00
29 *	15345.42	.867E-01
30 *	9520.652	.520E-01

CONCENTRATION DATA FOR RUN NO. 10 ON FEB. 10 1979 AT 17: 6.
 WIND DIRECTION: 135 DEG. UNITS: 1 SCALE FACTOR: 500.
 DATA FOR TRACER GAS NO. 1, ETHANE BACKGROUND CONC. 1776.4 MV-SEC.
 CAL. FACTOR: .025 GAS FACTOR (PPM GAS/PPM METHANE): .533

MODEL
 VELOCITY (M/SEC) .88
 SOURCE STRENGTH (PPM) .769E+05
 VOLUME FLOW (CU. M/SEC) .334E-03
 STACK DIAMETER (M) .740E-02
 EXIT VELOCITY (M/SEC) .777E+01
 DENSITY RATIO .60
 BUILDING HEIGHT .0945

LOCATION	RAW DATA (MV-SEC)	NON-DIMENSIONAL CONCENTRATION COEFFICIENT(K)
1 *	5207.450	.138E-01
2 *	4947.481	.127E-01
3 *	12216.24	.419E-01
4 *	15017.88	.532E-01
5 *	10538.28	.352E-01
6 *	2667.639	.358E-02
7 *	7033.554	.211E-01
8 *	14084.05	.494E-01
9 *	19507.91	.712E-01
10 *	5230.830	.139E-01
11 *	3042.300	.508E-02
12 *	9430.529	.307E-01
13 *	6228.161	.179E-01
14 *	15039.32	.533E-01
15 *	9387.275	.306E-01
16 *	1850.670	.298E-03
17 *	4568.752	.140E-01
18 *	14705.43	.519E-01
19 *	16890.49	.607E-01
20 *	4594.874	.113E-01
21 *	1871.522	.382E-03
22 *	8194.822	.258E-01
23 *	12567.33	.433E-01
24 *	15279.68	.542E-01
25 *	4438.276	.107E-01
26 *	8101.411	.254E-01
27 *	3212.990	.577E-02
28 *	6831.399	.203E-01
29 *	9922.455	.327E-01
30 *	10579.54	.354E-01

CONCENTRATION DATA FOR RUN NO. 11 ON FEB. 10 1979 AT 18:53.
 WIND DIRECTION: 135 DEG. UNITS: 2 SCALE FACTOR: 500.
 DATA FOR TRACER GAS NO. 1, ETHANE BACKGROUND CONC. 1677.5 MV-SEC.
 CAL. FACTOR: 025 GAS FACTOR (PPM GAS/PPM METHANE): .533

VELOCITY (M/SEC)	MODEL
SOURCE STRENGTH (PPM)	.80
VOLUME FLOW (CU. M/SEC)	.769E+05
STACK DIAMETER (M)	.283E-03
EXIT VELOCITY (M/SEC)	.740E-02
DENSITY RATIO	.658E+01
BUILDING HEIGHT	.60
	.0945

LOCATION	RAW DATA (MV-SEC)	NON-DIMENSIONAL CONCENTRATION COEFFICIENT(K)
5 *	13320.46	.552E-01
4 *	14852.41	.623E-01
9 *	12714.46	.523E-01
14 *	13905.82	.580E-01
19 *	14060.32	.587E-01
24 *	13414.00	.556E-01
30 *	8756.795	.336E-01

CONCENTRATION DATA FOR RUN NO. 12 ON FEB. 10 1979 AT 19:30.
 WIND DIRECTION: 135 DEG. UNITS: 3 SCALE FACTOR: 500.
 DATA FOR TRACER GAS NO. 1, ETHANE BACKGROUND CONC. 1497.8 MV-SEC.
 CAL. FACTOR: .025 GAS FACTOR (PPM GAS/PPM METHANE): .533

MODEL
 VELOCITY (M/SEC) .88
 SOURCE STRENGTH (PPM) .769E+05
 VOLUME FLOW (CU. M/SEC) .234E-03
 STACK DIAMETER (M) .740E-02
 EXIT VELOCITY (M/SEC) .544E+01
 DENSITY RATIO .60
 BUILDING HEIGHT .0945

LOCATION RAW DATA NON-DIMENSIONAL
 (MV-SEC) CONCENTRATION
 COEFFICIENT(K)

STAT NB	6	NB OF	PTS 4096	
RMS(MV)	.39843E+04		MEAN(MV)	-.22218E+03
5 *		12618.90		.638E-01
4 *		10922.61		.540E-01
9 *		11208.93		.557E-01
14 *		13563.16		.692E-01
19 *		11675.40		.584E-01
24 *		10600.92		.522E-01
30 *		8093.642		.378E-01

CONCENTRATION DATA FOR RUN NO. 111 ON FEB. 9 1979 AT 19:19
 WIND DIRECTION: 180 DEG. UNITS: 2 SCALE FACTOR: 500.
 DATA FOR TRACER GAS NO. 1, ETHANE BACKGROUND COND. 1564.9 MV-SEC.
 CAL. FACTOR: .025 GAS FACTOR (PPM GAS/PPM METHANE): .533

	MODEL
VELOCITY (M/SEC)	.88
SOURCE STRENGTH (PPM)	.769E+05
VOLUME FLOW (CU. M/SEC)	.283E-03
STACK DIAMETER (M)	.740E-02
EXIT VELOCITY (M/SEC)	.658E+01
DENSITY RATIO	.60
BUILDING HEIGHT	.0945

LOCATION	RAW DATA (MV-SEC)	NON-DIMENSIONAL CONCENTRATION COEFFICIENT(K)
1 *	9320.154	.377E-01
3 *	16105.78	.708E-01
7 *	18670.37	.832E-01
13 *	26691.76	.122E+00
18 *	24899.62	.114E+00
23 *	22412.35	.101E+00
28 *	15712.80	.688E-01
30 *	16329.91	.718E-01

CONCENTRATION DATA FOR RUN NO. 15 ON FEB. 9 1979 AT 20:22. SCALE FACTOR: 500.
WIND DIRECTION: 180 DEG. UNITS: 3
DATA FOR TRACER GAS NO. 1, ETHANE BACKGROUND CONC. 1458.4 MV-SEC.
CAL. FACTOR: .025 GAS FACTOR (PPM GAS/PPM METHANE): .533

MODEL
VELOCITY (M/SEC) .88
SOURCE STRENGTH (PPM) .769E+05
VOLUME FLOW (CU. M/SEC) .234E-03
STACK DIAMETER (M) .740E-02
EXIT VELOCITY (M/SEC) .544E+01
DENSITY RATIO .60
BUILDING HEIGHT .0945

LOCATION	RAW DATA (MV-SEC)	NON-DIMENSIONAL CONCENTRATION COEFFICIENT(K)
1 *	11767.96	.607E-01
3 *	18480.08	.100E+00
7 *	23927.68	.132E+00
13 *	25306.07	.140E+00
18 *	23580.63	.130E+00
23 *	21169.47	.116E+00
28 *	16675.60	.895E-01
30 *	13248.03	.694E-01

CONCENTRATION DATA FOR RUN NO. 16 ON FEB. 10 1979 AT 20: 7.
 WIND DIRECTION: 225 DEG. UNITS: 1 SCALE FACTOR: 500.
 DATA FOR TRACER GAS NO. 1, ETHANE BACKGROUND CONC. 1587.8 MV-SEC.
 CAL. FACTOR: .025 GAS FACTOR (PPM GAS/PPM METHANE): .533

MODEL
 VELOCITY (M/SEC) .89
 SOURCE STRENGTH (PPM) .427E+05
 VOLUME FLOW (CU. M/SEC) .334E-03
 STACK DIAMETER (M) .740E-02
 EXIT VELOCITY (M/SEC) .777E+01
 DENSITY RATIO .60
 BUILDING HEIGHT .0945

LOCATION	RAW DATA (MV-SEC)	NON-DIMENSIONAL CONCENTRATION COEFFICIENT(K)
2	1606.245	.133E-03
3	2440.121	.620E-02
4	1727.390	.101E-02
5	1773.218	.134E-02
6	1688.000	.725E-03
7	2146.373	.404E-02
8	4282.105	.195E-01
9	2842.109	.907E-02
10	1797.982	.152E-02
11	2005.967	.303E-02
12	4171.938	.187E-01
13	4946.080	.243E-01
14	5495.351	.283E-01
15	3412.719	.132E-01
16	1464.307	.000E+00
17	4813.104	.233E-01
18	5918.502	.313E-01
19	5172.691	.259E-01
20	1368.325	.000E+00
21	1458.549	.000E+00
22	2462.181	.633E-02
23	517.665	.260E-01
24	375.932	.157E-01
25	1549.947	.000E+00
26	325.783	.120E-01
27	1516.694	.000E+00
28	491.136	.240E-01
29	557.477	.289E-01
30	586.771	.310E-01
31	106.436	.200E-02

CONCENTRATION DATA FOR RUN NO. 17 ON FEB. 10 1979 AT 23: 4
 WIND DIRECTION: 225 DEG. UNITS: 2 SCALE FACTOR: 500
 DATA FOR TRACER GAS NO. 1, ETHANE BACKGROUND CONC. 1335.8 MV-SEC.
 CAL. FACTOR: .025 GAS FACTOR (PPM GAS/PPM METHANE) .533

VELOCITY (M/SEC)		MODEL	
SOURCE STRENGTH (PPM)		.80	
VOLUME FLOW (CU. M/SEC)		.684E+05	
STACK DIAMETER (M)		.283E-03	
EXIT VELOCITY (M/SEC)		.740E-02	
DENSITY RATIO		.658E+01	
BUILDING HEIGHT		.60	
.0945			

LOCATION	RAW DATA (MV-SEC)	NON-DIMENSIONAL CONCENTRATION COEFFICIENT(K)
1 *	1889.628	.295E-02
3 *	2935.154	.852E-02
8 *	4316.397	.159E-01
13 *	5387.314	.216E-01
19 *	4728.899	.181E-01
23 *	5751.366	.235E-01
28 *	4077.907	.146E-01
30 *	5726.896	.234E-01

CONCENTRATION DATA FOR RUN NO. 18 ON FEB. 10 1979 AT 23:45
WIND DIRECTION: 225 DEG. UNITS: 3 SCALE FACTOR: 500.
DATA FOR TRACER GAS NO. 1, ETHANE BACKGROUND CONC. 1226.0 MV-SEC.
CAL. FACTOR: .025 GAS FACTOR (PPM GAS/PPM METHANE) .533

VELOCITY (M/SEC)	MODEL
SOURCE STRENGTH (PPM)	.88
VOLUME FLOW (CU. M/SEC)	.684E+05
STACK DIAMETER (M)	.234E-03
EXIT VELOCITY (M/SEC)	.740E-02
DENSITY RATIO	.544E+01
BUILDING HEIGHT	.60
	.0945

LOCATION	RAW DATA (MV-SEC)	NON-DIMENSIONAL CONCENTRATION COEFFICIENT(K)
1 *	2096.319	.560E-02
3 *	3553.645	.150E-01
8 *	5645.031	.285E-01
13 *	5559.426	.279E-01
19 *	4597.258	.217E-01
23 *	5875.868	.299E-01
28 *	5687.997	.287E-01
30 *	5288.653	.262E-01

CONCENTRATION DATA FOR RUN NO. 19 ON FEB. 22 1979 AT 16:44
 WIND DIRECTION: 270 DEG. UNITS: 1 SCALE FACTOR: 500.
 DATA FOR TRACER GAS NO. 1, ETHANE BACKGROUND CONC. 183.49 MV-SEC.
 CAL. FACTOR: .217 GAS FACTOR (PPM GAS/PPM METHANE): .533

VELOCITY (M/SEC) MODEL
 SOURCE STRENGTH (PPM) .812E+05
 VOLUME FLOW (CU. M/SEC) .334E-03
 STACK DIAMETER (M) .740E-02
 EXIT VELOCITY (M/SEC) .777E+01
 DENSITY RATIO .60
 BUILDING HEIGHT .0945

LOCATION	RAW DATA (MV-SEC)	NON-DIMENSIONAL CONCENTRATION COEFFICIENT (K)
1	532.8549	.117E-01
2	574.6556	.131E-01
3	923.0485	.248E-01
4	2232.6725	.163E-02
5	258.4889	.252E-02
6	526.0814	.115E-01
7	1220.551	.348E-01
8	1872.176	.566E-01
9	846.3383	.202E-01
10	222.6556	.131E-02
11	553.0259	.124E-01
12	1232.8259	.352E-01
13	1863.4588	.564E-01
14	1405.6600	.410E-01
15	461.7869	.934E-02
16	273.0852	.301E-02
17	1059.754	.294E-01
18	1856.6600	.561E-01
19	1055.0000	.292E-01
20	209.7333	.880E-03
21	337.5888	.517E-02
22	1306.911	.377E-01
23	1513.926	.446E-01
24	1522.947	.449E-01
25	214.2322	.103E-02
26	1151.305	.325E-01
27	554.9224	.125E-01
28	1276.411	.367E-01
29	600.9333	.140E-01
30	1034.467	.285E-01

CONCENTRATION DATA FOR RUN NO. 20 ON FEB. 22 1979 AT 17:50.
 WIND DIRECTION: 270 DEG. UNITS: 2 SCALE FACTOR: 500.
 DATA FOR TRACER GAS NO. 1, ETHANE BACKGROUND CONC. 182.94 MV-SEC.
 CAL. FACTOR: .217 GAS FACTOR (PPM GAS/PPM METHANE): .533

MODEL
 VELOCITY (M/SEC) .88
 SOURCE STRENGTH (PPM) .812E+05
 VOLUME FLOW (CU. M/SEC) .283E-03
 STACK DIAMETER (M) .740E-02
 EXIT VELOCITY (M/SEC) .658E+01
 DENSITY RATIO .60
 BUILDING HEIGHT .0945

LOCATION

LOCATION	RAM DATA (MV-SEC)	NON-DIMENSIONAL CONCENTRATION COEFFICIENT (K)
1 *	605.3647	.167E-01
3 *	1144.394	.381E-01
8 *	2089.563	.755E-01
13 *	1841.622	.657E-01
18 *	1608.253	.564E-01
23 *	1499.790	.521E-01
28 *	1367.588	.469E-01
26 *	1033.256	.337E-01

CONCENTRATION DATA FOR RUN NO. 21 ON FEB. 22 1979 AT 22:22
 WIND DIRECTION: 270 DEG. UNITS: 3 SCALE FACTOR: 500.
 DATA FOR TRACER GAS NO. 1, ETHANE BACKGROUND CONC. 215.63 MV-SEC.
 CAL. FACTOR: .217 GAS FACTOR (PPM GAS/PPM METHANE): .533

VELOCITY (M/SEC)		MODEL	
SOURCE STRENGTH (PPM)		.89	
VOLUME FLOW (CU. M/SEC)		.812E+05	
STACK DIAMETER (M)		.234E-03	
EXIT VELOCITY (M/SEC)		.740E-02	
DENSITY RATIO		.544E+01	
BUILDING HEIGHT		.60	
		.0945	

LOCATION	RAW DATA (MV-SEC)	NON-DIMENSIONAL CONCENTRATION COEFFICIENT(K)
1 *	762.3850	.262E-01
3 *	1234.739	.488E-01
8 *	1881.821	.798E-01
13 *	1920.408	.816E-01
18 *	1485.330	.608E-01
23 *	1382.071	.559E-01
28 *	1099.076	.423E-01
26 *	987.1808	.369E-01

CONCENTRATION DATA FOR RUN NO. 22 ON FEB. 22 1979 AT 23:15.
 WIND DIRECTION: 315 DEG. UNITS: 1 SCALE FACTOR: 500.
 DATA FOR TRACER GAS NO. 1, ETHANE BACKGROUND CONC. 211.79 MV-SEC.
 CAL. FACTOR: .217 GAS FACTOR (PPM GAS/PPM METHANE): .533

VELOCITY (M/SEC) MODEL
 SOURCE STRENGTH (PPM) .812E+05
 VOLUME FLOW (CU. M/SEC) .334E-03
 STACK DIAMETER (M) .740E-02
 EXIT VELOCITY (M/SEC) .777E+01
 DENSITY RATIO .60
 BUILDING HEIGHT .0945

LOCATION	RAW DATA (MV-SEC)	NON-DIMENSIONAL CONCENTRATION COEFFICIENT (K)
1 *	297.7877	.288E-02
2 *	329.9333	.396E-02
3 *	607.3434	.133E-01
4 *	329.8483	.396E-02
5 *	337.0759	.420E-02
6 *	282.0445	.236E-02
7 *	1061.443	.285E-01
8 *	1340.313	.379E-01
9 *	1188.267	.328E-01
10 *	415.7109	.684E-02
11 *	797.2889	.196E-01
12 *	1235.520	.343E-01
13 *	1569.687	.456E-01
14 *	695.0435	.162E-01
15 *	562.6069	.118E-01
16 *	268.1264	.189E-02
17 *	810.1526	.201E-01
18 *	1391.269	.396E-01
19 *	1631.190	.476E-01
20 *	248.7146	.124E-02
21 *	297.9813	.289E-02
22 *	849.8879	.214E-01
23 *	1197.507	.331E-01
24 *	1121.874	.305E-01
25 *	420.0615	.699E-02
26 *	783.8558	.192E-01
27 *	429.7219	.731E-02
28 *	1151.627	.315E-01
29 *	879.7701	.224E-01
30 *	1206.848	.334E-01

CONCENTRATION DATA FOR RUN NO. 23 ON FEB. 23 1979 AT 01 9
WIND DIRECTION: 315 DEG. UNITS: 2 SCALE FACTOR: 500.
DATA FOR TRACER GAS NO. 1, ETHANE BACKGROUND CONC. 221.60 MV-SEC.
CAL. FACTOR: .217 GAS FACTOR (PPM GAS/PPM METHANE) .533

VELOCITY (M/SEC)	MODEL
SOURCE STRENGTH (PPM)	.812E+05
VOLUME FLOW (CU. M/SEC)	.283E-03
STACK DIAMETER (M)	.740E-02
EXIT VELOCITY (M/SEC)	.658E+01
DENSITY RATIO	.60
BUILDING HEIGHT	.0945

LOCATION	RAW DATA (MV-SEC)	NON-DIMENSIONAL CONCENTRATION COEFFICIENT (K)
3 *	670.4771	.178E-01
5 *	286.4730	.257E-02
8 *	1292.606	.424E-01
13 *	1575.368	.536E-01
18 *	1552.247	.527E-01
23 *	1288.486	.422E-01
28 *	1025.324	.318E-01
30 *	1055.836	.330E-01

CONCENTRATION DATA FOR RUN NO. 24 ON FEB. 23 1979 AT 0148.
 WIND DIRECTION: 315 DEG. UNITS: 3 SCALE FACTOR: 500.
 DATA FOR TRACER GAS NO. 1, ETHANE BACKGROUND CONC. 185.46 MV-SEC.
 CAL. FACTOR: 217 GAS FACTOR (PPM GAS/PPM METHANE): .533

			MODEL
VELOCITY (M/SEC)			.88
SOURCE STRENGTH (PPM)		.812E+05	
VOLUME FLOW (CU. M/SEC)		.234E-03	
STACK DIAMETER (M)		.740E-02	
EXIT VELOCITY (M/SEC)		.544E+01	
DENSITY RATIO		.60	
BUILDING HEIGHT		.0945	
LOCATION	RAW		NON-DIMENSIONAL
	DATA		CONCENTRATION
	(MV-SEC)		COEFFICIENT(K)
3 *	850.4929		.318E-01
5 *	328.0135		.683E-02
8 *	1396.214		.580E-01
13 *	1386.484		.575E-01
18 *	1180.000		.476E-01
23 *	1215.418		.493E-01
28 *	1151.886		.463E-01
30 *	990.7227		.386E-01

CONCENTRATION DATA FOR RUN NO. 25 ON FEB. 9 1979 AT 21:22
 WIND DIRECTION: 180 DEG. UNITS: 1 SCALE FACTOR: 500.
 DATA FOR TRACER GAS NO. 1, ETHANE BACKGROUND CONC. 1746.3 MV-SEC.
 CAL. FACTOR: .025 GAS FACTOR (PPM GAS/PPM METHANE): .533

MODEL
 VELOCITY (M/SEC) .88
 SOURCE STRENGTH (PPM) .769E+05
 VOLUME FLOW (CU. M/SEC) .334E-03
 STACK DIAMETER (M) .740E-02
 EXIT VELOCITY (M/SEC) .777E+01
 DENSITY RATIO .60
 BUILDING HEIGHT .0945

LOCATION	RAW DATA (MV-SEC)	NON-DIMENSIONAL CONCENTRATION COEFFICIENT(K)
1 *	1795.630	.258E-03
2 *	1582.119	.000E+00
3 *	1889.236	.589E-03
4 *	1649.051	.000E+00
5 *	2136.904	.161E-02
6 *	2148.713	.166E-02
7 *	1852.731	.439E-03
8 *	3061.912	.542E-02
9 *	1933.892	.773E-03
10 *	1755.658	.385E-04
11 *	1881.087	.556E-03
12 *	2531.834	.324E-02
13 *	3518.429	.731E-02
14 *	3342.882	.658E-02
15 *	2239.231	.203E-02
16 *	1796.736	.208E-03
17 *	2735.708	.408E-02
18 *	4696.421	.122E-01
19 *	4589.260	.117E-01
20 *	2100.875	.146E-02
21 *	1864.314	.486E-03
22 *	3373.637	.671E-02
23 *	5314.400	.147E-01
24 *	4635.940	.119E-01
26 *	2750.415	.414E-02
25 *	3688.557	.801E-02
27 *	1294.603	.000E+00
28 *	3611.896	.769E-02
29 *	5586.179	.158E-01
30 *	6959.824	.215E-01

CONCENTRATION DATA FOR RUN NO. 26 ON FEB. 9 1979 AT 22:34
 WIND DIRECTION: 180 DEG. UNITS: 2 SCALE FACTOR: 500.
 DATA FOR TRACER GAS NO. 1, ETHANE BACKGROUND CONC. 1748.3 MV-SEC.
 CAL. FACTOR: .025 GAS FACTOR (PPM GAS/PPM METHANE): .533

	MODEL
VELOCITY (M/SEC)	.88
SOURCE STRENGTH (PPM)	.769E+05
VOLUME FLOW (CU. M/SEC)	.283E-03
STACK DIAMETER (M)	.740E-02
EXIT VELOCITY (M/SEC)	.658E+01
DENSITY RATIO	.60
BUILDING HEIGHT	.0945

LOCATION	RAW DATA (MV-SEC)	NON-DIMENSIONAL CONCENTRATION COEFFICIENT(K)
8 *	2167.599	.204E-02
14 *	3830.066	.101E-01
18 *	5649.075	.190E-01
23 *	4887.160	.153E-01
29 *	6593.535	.236E-01
30 *	6087.413	.211E-01

CONCENTRATION DATA FOR RUN NO. 27 ON FEB. 9 1979 AT 23:17.
 WIND DIRECTION: 180 DEG. UNITS: 3 SCALE FACTOR: 500.
 DATA FOR TRACER GAS NO. 1, ETHANE BACKGROUND CONC. 1495.0 MV-SEC.
 CAL. FACTOR: .025 GAS FACTOR (PPM GAS/PPM METHANE): .533

	MODEL
VELOCITY (M/SEC)	.88
SOURCE STRENGTH (PPM)	.769E+05
VOLUME FLOW (CU. M/SEC)	.234E-03
STACK DIAMETER (M)	.740E-02
EXIT VELOCITY (M/SEC)	.544E+01
DENSITY RATIO	.60
BUILDING HEIGHT	.0945

LOCATION	RAW DATA (MV-SEC)	NON-DIMENSIONAL CONCENTRATION COEFFICIENT(K)
8 *	2516.465	.601E-02
14 *	4015.116	.148E-01
18 *	4306.936	.165E-01
23 *	4287.219	.164E-01
29 *	4092.735	.153E-01
30 *	4856.328	.198E-01

CONCENTRATION DATA FOR RUN NO. 28 ON FEB. 10 1979 AT 12:44
 WIND DIRECTION: 135 DEG. UNITS: 1 SCALE FACTOR: 500.
 DATA FOR TRACER GAS NO. 1, ETHANE BACKGROUND CONC. 1505.5 MV-SEC.
 CAL. FACTOR: .025 GAS FACTOR (PPM GAS/PPM METHANE): .533

VELOCITY (M/SEC) MODEL
 SOURCE STRENGTH (PPM) .769E+05
 VOLUME FLOW (CU. M/SEC) .334E-03
 STACK DIAMETER (M) .740E-02
 EXIT VELOCITY (M/SEC) .777E+01
 DENSITY RATIO .60
 BUILDING HEIGHT .0945

LOCATION	RAW DATA (MV-SEC)	NON-DIMENSIONAL CONCENTRATION COEFFICIENT(K)
1 *	1428.867	.000E+00
2 *	1645.851	.564E-03
3 *	1787.340	.113E-02
4 *	1774.263	.108E-02
5 *	1673.552	.675E-03
6 *	1787.335	.113E-02
7 *	1928.617	.170E-02
8 *	2252.374	.300E-02
9 *	2086.871	.234E-02
10 *	1899.347	.158E-02
11 *	1816.990	.125E-02
12 *	2602.892	.441E-02
13 *	3190.898	.677E-02
14 *	3352.771	.742E-02
15 *	2658.636	.463E-02
16 *	2127.906	.250E-02
17 *	1821.419	.127E-02
18 *	3319.048	.728E-02
19 *	5086.257	.144E-01
20 *	2095.064	.237E-02
21 *	1859.783	.142E-02
22 *	2486.107	.394E-02
23 *	4956.054	.139E-01
24 *	4436.684	.118E-01
25 *	2701.038	.480E-02
26 *	4605.937	.125E-01
27 *	2593.003	.437E-02
28 *	7042.059	.222E-01
29 *	4782.198	.132E-01
30 *	5787.169	.172E-01

CONCENTRATION DATA FOR RUN NO. 28 ON FEB. 10 1979 AT 12:44.
WIND DIRECTION: 135 DEG. UNITS: 2 SCALE FACTOR: 500.
DATA FOR TRACER GAS NO. 1, ETHANE BACKGROUND CONC. 1439.6 MV-SEC.
CAL. FACTOR: .025 GAS FACTOR (PPM GAS/PPM METHANE): .533

VELOCITY (M/SEC)	MODEL
SOURCE STRENGTH (PPM)	.88
VOLUME FLOW (CU. M/SEC)	.769E+05
STACK DIAMETER (M)	.283E-03
EXIT VELOCITY (M/SEC)	.740E-02
DENSITY RATIO	.658E+01
BUILDING HEIGHT	.60
	.0945

LOCATION	RAW DATA (MV-SEC)	NON-DIMENSIONAL CONCENTRATION COEFFICIENT (K)
5 *	1519.177	.939E-03
4 *	1676.006	.135E-02
7 *	1856.342	.198E-02
15 *	2302.367	.409E-02
19 *	5894.122	.211E-01
24 *	5662.068	.200E-01
25 *	6928.323	.260E-01
26 *	4513.425	.146E-01

CONCENTRATION DATA FOR RUN NO. 28 ON FEB. 10 1979 AT 12:44.
 WIND DIRECTION: 135 DEG. UNITS: 3 SCALE FACTOR: 500.
 DATA FOR TRACER GAS NO. 1, ETHANE BACKGROUND CONC. 1373.8 MV-SEC.
 CAL. FACTOR: .025 GAS FACTOR (PPM GAS/PPM METHANE): .533

VELOCITY (M/SEC)	MODEL
SOURCE STRENGTH (PPM)	.88
VOLUME FLOW (CU. M/SEC)	.769E+05
STACK DIAMETER (M)	.234E-03
EXIT VELOCITY (M/SEC)	.740E-02
DENSITY RATIO	.544E+01
BUILDING HEIGHT	.60
	.0945

LOCATION	RAW DATA (MV-SEC)	NON-DIMENSIONAL CONCENTRATION COEFFICIENT(K)
5 *	1411.934	.760E-03
4 *	1455.851	.590E-03
7 *	1719.600	.198E-02
15 *	2570.927	.686E-02
19 *	5777.438	.252E-01
24 *	6330.953	.284E-01
28 *	4625.412	.186E-01
26 *	5062.448	.211E-01

CONCENTRATION DATA FOR RUN NO. 6110 ON FEB. 17 1979 AT 12:24
 WIND DIRECTION: 135 DEG UNITS: 1 SCALE FACTOR: 500.
 DATA FOR TRACER GAS NO. 1, ETHANE BACKGROUND CONC. 1323.9 MV-SEC.
 CAL FACTOR: .028 GAS FACTOR (PPM GAS/PPM METHANE): .533

MODEL
 VELOCITY (M/SEC) .88
 SOURCE STRENGTH (PPM) .819E+05
 VOLUME FLOW (CU. M/SEC) .334E-03
 STACK DIAMETER (M) .740E-02
 EXIT VELOCITY (M/SEC) .777E+01
 DENSITY RATIO .60
 BUILDING HEIGHT .0945

LOCATION	RAW DATA (MV-SEC)	NON-DIMENSIONAL CONCENTRATION COEFFICIENT(K)
15 *	1379.798	.240E-03
23 *	2543.578	.523E-02
27 *	8422.346	.305E-01
31 *	19552.13	.782E-01
34 *	30330.37	.124E+00
37 *	35504.14	.147E+00
42 *	38784.34	.161E+00
45 *	34697.46	.143E+00
48 *	25170.29	.102E+00
52 *	13759.95	.534E-01
56 *	6649.584	.229E-01
60 *	3001.307	.720E-02
19 *	1963.934	.275E-02
V13 *	37562.18	.156E+00

CONCENTRATION DATA FOR RUN NO. 5310 ON FEB. 16 1979 AT 22: 9.
WIND DIRECTION: 135 DEG. UNITS: 1 SCALE FACTOR: 500.
DATA FOR TRACER GAS NO. 1, ETHANE BACKGROUND CONC. 2650.7 MV-SEC.
CAL. FACTOR: .028 GAS FACTOR (PPM GAS/PPM METHANE): .533

MODEL
VELOCITY (M/SEC) .88
SOURCE STRENGTH (PPM) .801E+05
VOLUME FLOW (CU. M/SEC) .334E-03
STACK DIAMETER (M) .740E-02
EXIT VELOCITY (M/SEC) .777E+01
DENSITY RATIO .60
BUILDING HEIGHT .0945

LOCATION	RAW DATA (MV-SEC)	NON-DIMENSIONAL CONCENTRATION COEFFICIENT(K)
1 *	12488.28	.432E-01
05 *	11257.20	.378E-01
08 *	10652.55	.351E-01
11 *	13132.04	.460E-01
13 *	12941.11	.452E-01
15 *	11887.44	.405E-01
17 *	12099.42	.415E-01
19 *	11999.65	.410E-01
21 *	11319.35	.380E-01
23 *	11397.57	.384E-01
26 *	10919.56	.363E-01
29 *	10689.99	.353E-01
30 *	8428.121	.254E-01
36 *	6930.528	.188E-01
40 *	5785.970	.138E-01
GN *	12004.06	.501E-01

CONCENTRATION DATA FOR RUN NO. 5228 ON FEB. 15 1979 AT 22:52
 WIND DIRECTION: 135 DEG. UNITS: 1 SCALE FACTOR: 500.
 DATA FOR TRACER GAS NO. 1, ETHANE BACKGROUND CONC. 2343.8 MV-SEC.
 CAL. FACTOR: .028 GAS FACTOR (PPM GAS/PPM METHANE): .533

VELOCITY (M/SEC) MODEL .88
 SOURCE STRENGTH (PPM) .801E+05
 VOLUME FLOW (CU. M/SEC) .334E-03
 STACK DIAMETER (M) .740E-02
 EXIT VELOCITY (M/SEC) .777E+01
 DENSITY RATIO .60
 BUILDING HEIGHT .0945

LOCATION	RAW DATA (MV-SEC)	NON-DIMENSIONAL CONCENTRATION COEFFICIENT(K)
1	8833.244	.279E-01
5	12533.633	.447E-01
8	10677.91	.366E-01
11	14762.89	.545E-01
13	14903.62	.551E-01
15	16600.71	.626E-01
17	16692.73	.630E-01
19	18979.25	.730E-01
21	18357.74	.703E-01
23	20091.11	.779E-01
25	12945.34	.465E-01
27	13892.82	.507E-01
29	11282.14	.392E-01
31	5885.726	.155E-01
33	4875.566	.111E-01
GN	5373.721	.133E-01

CONCENTRATION DATA FOR RUN NO. 5225 ON FEB. 15 1973 AT 15:22.
 WIND DIRECTION: 180 DEG. UNITS: 1 SCALE FACTOR: 500.
 DATA FOR TRACER GAS NO. 1, ETHANE BACKGROUND CONC. 2083.0 MV-SEC.
 CAL. FACTOR: .028 GAS FACTOR (PPM GAS/PPM METHANE): .535

VELOCITY (M/SEC) MODEL .88
 SOURCE STRENGTH (PPM) .801E+05
 VOLUME FLOW (CU. M/SEC) .334E-03
 STACK DIAMETER (M) .740E-02
 EXIT VELOCITY (M/SEC) .777E+01
 DENSITY RATIO .60
 BUILDING HEIGHT .0945

LOCATION	RAW DATA (MV-SEC)	NON-DIMENSIONAL CONCENTRATION COEFFICIENT (K)
1	7398.666	.233E-01
00	3597.473	.330E-01
11	14114.30	.520E-01
11	11487.27	.413E-01
11	16179.55	.619E-01
15	15492.21	.589E-01
17	19622.79	.770E-01
19	19713.60	.774E-01
21	20039.38	.788E-01
23	18738.86	.731E-01
26	16772.40	.645E-01
29	15171.14	.574E-01
32	14089.23	.527E-01
36	7447.372	.235E-01
40	6146.361	.178E-01
GN	5790.753	.163E-01

CONCENTRATION DATA FOR RUN NO. 5210 ON FEB. 15 1979 AT 21:50.
 WIND DIRECTION: 135 DEG. UNITS: 1 SCALE FACTOR: 500.
 DATA FOR TRACER GAS NO. 1, ETHANE BACKGROUND CONC. 2562.8 MV-SEC.
 CAL. FACTOR: .028 GAS FACTOR (PPM GAS/PPM METHANE): .533

VELOCITY (M/SEC) MODEL
 SOURCE STRENGTH (PPM) .801E+05
 VOLUME FLOW (CU. M/SEC) .334E-03
 STACK DIAMETER (M) .740E-02
 EXIT VELOCITY (M/SEC) .777E+01
 DENSITY RATIO .60
 BUILDING HEIGHT .0945

LOCATION	RAW DATA (MV-SEC)	NON-DIMENSIONAL CONCENTRATION COEFFICIENT (K)
1 *	18525.78	.701E-01
2 *	18247.42	.688E-01
3 *	18373.80	.694E-01
4 *	18265.78	.733E-01
5 *	15442.63	.565E-01
6 *	18909.11	.717E-01
7 *	16556.45	.614E-01
8 *	16754.11	.623E-01
9 *	16471.65	.610E-01
10 *	14037.02	.504E-01
11 *	13838.83	.495E-01
12 *	12669.54	.444E-01
13 *	7389.174	.212E-01
14 *	6950.699	.193E-01
15 *	3740.399	.517E-02
GN *	18540.64	.799E-01

CONCENTRATION DATA FOR RUK NO. 5128 ON FEB. 16 1979 AT 13:17.
 WIND DIRECTION: 135 DEG UNITS: 1 SCALE FACTOR: 500.
 DATA FOR TRACER GAS NO. 1, ETHANE BACKGROUND CONC. 1675.8 MV-SEC.
 CAL. FACTOR: .028 GAS FACTOR (PPM GAS/PPM METHANE): .533

VELOCITY (M/SEC) MODEL
 SOURCE STRENGTH (PPM) .801E+05
 VOLUME FLOW (CU. M/SEC) .334E-03
 STACK DIAMETER (M) .740E-02
 EXIT VELOCITY (M/SEC) .777E+01
 DENSITY RATIO .60
 BUILDING HEIGHT .0945

LOCATION	RAW DATA (MV-SEC)	NON-DIMENSIONAL CONCENTRATION COEFFICIENT (K)
1	2520.040	.371E-02
5	6858.010	.227E-01
8	28115.89	.116E+00
11	49644.21	.211E+00
15	78095.52	.335E+00
15	69542.69	.298E+00
17	62644.16	.268E+00
19	39968.89	.168E+00
22	31753.34	.132E+00
23	7775.384	.268E-01
26	4501.206	.124E-01
GN	496.5947	.355E-03

CONCENTRATION DATA FOR RUN NO. 5125 ON FEB. 16 1979 AT 14: 5.
 WIND DIRECTION: 180 DEG. UNITS: 1 SCALE FACTOR: 500.
 DATA FOR TRACER GAS NO. 1, ETHANE BACKGROUND CONC. 2047.4 MV-SEC.
 CAL FACTOR: .028 GAS FACTOR (PPM GAS/PPM METHANE): .533

VELOCITY (M/SEC) MODEL .88
 SOURCE STRENGTH (PPM) .801E+05
 VOLUME FLOW (CU M/SEC) .334E-03
 STACK DIAMETER (M) .740E-02
 EXIT VELOCITY (M/SEC) .777E+01
 DENSITY RATIO .60
 BUILDING HEIGHT .0945

LOCATION	RAW DATA (MV-SEC)	NON-DIMENSIONAL CONCENTRATION COEFFICIENT(K)
1 *	2920.646	.383E-02
5 *	13328.93	.495E-01
8 *	36431.96	.151E+00
11 *	63249.79	.269E+00
13 *	81871.02	.350E+00
15 *	78406.53	.335E+00
17 *	63291.97	.269E+00
19 *	35571.96	.147E+00
21 *	30850.35	.126E+00
23 *	10474.30	.370E-01
26 *	4408.395	.104E-01
GN *	2400.333	.155E-02

CONCENTRATION DATA FOR RUN NO. 5113 ON FEB. 16 1979 AT 14:45.
 WIND DIRECTION: 180 DEG. UNITS: 1 SCALE FACTOR: 500.
 DATA FOR TRACER GAS NO. 1, ETHANE BACKGROUND CONC. 2256.5 MV-SEC.
 CAL. FACTOR: .028 GAS FACTOR (PPM GAS/PPM METHANE): .333

MODEL
 VELOCITY (M/SEC) .88
 SOURCE STRENGTH (PPM) 801E+05
 VOLUME FLOW (CU. M/SEC) 334E-03
 STACK DIAMETER (M) 740E-02
 EXIT VELOCITY (M/SEC) 777E+01
 DENSITY RATIO .60
 BUILDING HEIGHT .0945

LOCATION	RAW DATA (MV-SEC)	NON-DIMENSIONAL CONCENTRATION COEFFICIENT(K)
1 *	41477.34	.172E+00
5 *	87221.66	.373E+00
8 *	84917.50	.363E+00
11 *	62880.73	.266E+00
13 *	53947.31	.227E+00
15 *	24325.62	.969E-01
17 *	11493.22	.405E-01
19 *	9282.660	.308E-01
21 *	6314.263	.178E-01
23 *	3808.076	.681E-02
26 *	2552.453	.130E-02
GN *	29719.75	0.126

CONCENTRATION DATA FOR RUN NO. 5110 ON FEB. 16 1979 AT 15:23.
 WIND DIRECTION: 135 DEG. UNITS: 1 SCALE FACTOR: 500.
 DATA FOR TRACER GAS NO. 1, ETHANE BACKGROUND CONC. 2540.9 MV-SEC.
 CAL. FACTOR: .028 GAS FACTOR (PPM GAS/PPM METHANE) .533

MODEL
 VELOCITY (M/SEC) .88
 SOURCE STRENGTH (PPM) .801E+05
 VOLUME FLOW (CU. M/SEC) .334E-03
 STACK DIAMETER (M) .740E-02
 EXIT VELOCITY (M/SEC) .777E+01
 DENSITY RATIO .60
 BUILDING HEIGHT .0945

LOCATION	RAW DATA (MV-SEC)	NON-DIMENSIONAL CONCENTRATION COEFFICIENT(K)
1 *	24283.89	.954E-01
5 **	30642.99	.123E+00
8 **	52799.42	.221E+00
11 **	48649.32	.202E+00
13 **	51124.39	.213E+00
15 **	47493.25	.197E+00
17 **	35723.22	.146E+00
19 **	22114.95	.859E-01
21 **	18778.19	.713E-01
23 **	8242.719	.250E-01
26 **	2825.372	.225E-02
GN *	14694.39	.556E-01

CONCENTRATION DATA FOR RUN NO. 5328 ON FEB. 16 1979 AT 20:20.
 WIND DIRECTION: 180 DEG. UNITS: 1 SCALE FACTOR: 500.
 DATA FOR TRACER GAS NO. 1, ETHANE BACKGROUND CONC. 2109.7 MV-SEC.
 CAL. FACTOR: .028 GAS FACTOR (PPM GAS/PPM METHANE): .533

MODEL
 VELOCITY (M/SEC) .88
 SOURCE STRENGTH (PPM) .801E+05
 VOLUME FLOW (CU. M/SEC) .334E-03
 STACK DIAMETER (M) .740E-02
 EXIT VELOCITY (M/SEC) .777E+01
 DENSITY RATIO .60
 BUILDING HEIGHT .0945

LOCATION	RAW DATA (MV-SEC)	NON-DIMENSIONAL CONCENTRATION COEFFICIENT(K)
5 *	8243.574	.269E-01
8 *	8287.221	.271E-01
11 *	11567.55	.415E-01
13 *	10372.95	.363E-01
15 *	13271.13	.490E-01
17 *	12220.82	.444E-01
19 *	10221.97	.356E-01
21 *	11278.42	.402E-01
23 *	11542.88	.414E-01
26 *	11912.69	.430E-01
29 *	12119.82	.439E-01
32 *	10603.86	.373E-01
36 *	7620.895	.242E-01
40 *	5585.439	.153E-01
3 *	7126.970	.220E-01
GN *	6850.071	.208E-01

CONCENTRATION DATA FOR RUN NO. 5213 ON FEB. 15 1979 AT 20:16.
 WIND DIRECTION: 180 DEG. UNITS: 1 SCALE FACTOR: 500.
 DATA FOR TRACER GAS NO. 1, ETHANE BACKGROUND CONC. 2219.6 MV-SEC.
 CAL. FACTOR: .028 GAS FACTOR (PPM GAS/PPM METHANE): .533

MODEL
 VELOCITY (M/SEC) .80
 SOURCE STRENGTH (PPM) .801E+05
 VOLUME FLOW (CU. M/SEC) .334E-03
 STACK DIAMETER (M) .740E-02
 EXIT VELOCITY (M/SEC) .777E+01
 DENSITY RATIO .60
 BUILDING HEIGHT .0945

LOCATION	RAW DATA (MV-SEC)	NON-DIMENSIONAL CONCENTRATION COEFFICIENT(K)
1 *	24584.41	.982E-01
17 *	14953.89	.559E-01
5 *	25308.38	.101E+00
8 *	18620.08	.720E-01
11 *	21107.67	.829E-01
13 *	16123.94	.610E-01
15 *	14452.68	.537E-01
19 *	11397.01	.403E-01
21 *	9518.820	.320E-01
23 *	10075.02	.345E-01
26 *	6012.828	.166E-01
29 *	5875.508	.160E-01
32 *	5532.648	.145E-01
36 *	2809.217	.259E-02
40 *	2350.609	.720E-03
GN *	23371-06	.928E-01

CONCENTRATION DATA FOR RUN NO. 6310 ON FEB. 17 1979 AT 21:23
 WIND DIRECTION: 135 DEG. UNITS: 1 SCALE FACTOR: 500.
 DATA FOR TRACER GAS NO. 1, ETHANE BACKGROUND CONC 2105.0 MV-SEC.
 CAL. FACTOR: .028 GAS FACTOR (PPM GAS/PPM METHANE) .533

MODEL
 VELOCITY (M/SEC) .88
 SOURCE STRENGTH (PPM) .819E+05
 VOLUME FLOW (CU. M/SEC) .334E-03
 STACK DIAMETER (M) .740E-02
 EXIT VELOCITY (M/SEC) .777E+01
 DENSITY RATIO .60
 BUILDING HEIGHT .0945

LOCATION	RAW DATA (MV-SEC)	NON-DIMENSIONAL CONCENTRATION COEFFICIENT(K)
15 *	3113.565	.433E-02
19 **	2566.443	.198E-02
23 **	3912.310	.776E-02
27 **	4431.435	.998E-02
31 **	6357.755	.183E-01
34 **	6719.890	.198E-01
37 **	8285.252	.265E-01
40 **	13580.68	.493E-01
45 **	11788.91	.416E-01
48 **	11511.59	.404E-01
50 **	14016.86	.511E-01
55 **	11249.29	.392E-01
60 **	7840.792	.246E-01
64 **	7223.884	.220E-01
V11 *	10132.08	.345E-01

CONCENTRATION DATA FOR RUN NO. 6228 ON FEB. 17 1973 AT 13:31.
 WIND DIRECTION: 180 DEG. UNITS: 1 SCALE FACTOR: 500.
 DATA FOR TRACER GAS NO. 1, ETHANE BACKGROUND CONC. 2254.7 MV-SEC.
 CAL. FACTOR: .028 GAS FACTOR (PPM GAS/PPM METHANE): .533

VELOCITY (M/SEC) MODEL
 SOURCE STRENGTH (PPM) .819E+05
 VOLUME FLOW (CU. M/SEC) .334E-03
 STACK DIAMETER (M) .740E-02
 EXIT VELOCITY (M/SEC) .777E+01
 DENSITY RATIO .60
 BUILDING HEIGHT .0945

LOCATION	RAW DATA (MV-SEC)	NON-DIMENSIONAL CONCENTRATION COEFFICIENT (K)
115 **	2708.210	.195E-02
119 **	3105.403	.365E-02
200 **	5439.523	.139E-01
201 **	6360.042	.176E-01
300 **	10457.06	.352E-01
304 **	15190.07	.557E-01
307 **	17412.75	.651E-01
400 **	22298.46	.860E-01
402 **	17815.67	.668E-01
408 **	20474.75	.782E-01
500 **	15222.71	.557E-01
506 **	14215.89	.513E-01
600 **	3185.557	.237E-01
604 **	6898.212	.199E-01
V21 *	20649.93	.790E-01

CONCENTRATION DATA FOR RUN NO. 6225 ON FEB. 17 1979 AT 18:30.
 WIND DIRECTION: 180 DEG. UNITS: 1 SCALE FACTOR: 500.
 DATA FOR TRACER GAS NO. 1, ETHANE BACKGROUND CONC. 2385.5 MV-SEC.
 CAL. FACTOR: .028 GAS FACTOR (PPM GAS/PPM METHANE): .533

MODEL
 VELOCITY (M/SEC) .88
 SOURCE STRENGTH (PPM) .819E+05
 VOLUME FLOW (CU. M/SEC) .334E-03
 STACK DIAMETER (M) .740E-02
 EXIT VELOCITY (M/SEC) .777E+01
 DENSITY RATIO .60
 BUILDING HEIGHT .0945

LOCATION	RAW DATA (MV-SEC)	NON-DIMENSIONAL CONCENTRATION COEFFICIENT(K)
15 *	2921.027	.230E-02
19 **	3524.527	.489E-02
23 **	3367.356	.421E-02
27 **	6307.216	.168E-01
31 **	9168.186	.291E-01
34 **	11445.19	.389E-01
37 **	14884.79	.536E-01
42 **	24618.94	.954E-01
45 **	20716.57	.787E-01
48 **	20473.89	.776E-01
52 **	15103.77	.546E-01
56 **	11169.47	.377E-01
60 **	5688.126	.142E-01
64 **	4410.476	.869E-02
V21 *	22302.23	.855E-01

CONCENTRATION DATA FOR RUN NO. 6213 ON FEB. 17 1979 AT 17: 0.
 WIND DIRECTION: 180 DEG. UNITS: 1 SCALE FACTOR: 500.
 DATA FOR TRACER GAS NO. 1, ETHANE BACKGROUND CONC. 2228.0 MV-SEC.
 CAL. FACTOR: .028 GAS FACTOR (PPM GAS/PPM METHANE): .533

MODEL
 VELOCITY (M/SEC) .88
 SOURCE STRENGTH (PPM) .819E+05
 VOLUME FLOW (CU. M/SEC) .334E-03
 STACK DIAMETER (M) .740E-02
 EXIT VELOCITY (M/SEC) .777E+01
 DENSITY RATIO .60
 BUILDING HEIGHT .0945

LOCATION	RAW DATA (MV-SEC)	NON-DIMENSIONAL CONCENTRATION COEFFICIENT(K)
15 *	4294.365	.887E-02
19 *	9534.941	.314E-01
23 *	13746.40	.494E-01
27 *	20586.35	.788E-01
31 *	23144.10	.898E-01
34 *	23807.60	.926E-01
37 *	23251.28	.902E-01
42 *	22652.09	.877E-01
45 *	23184.18	.899E-01
48 *	20144.75	.769E-01
52 *	19540.94	.743E-01
56 *	12122.66	.425E-01
60 *	6599.981	.188E-01
64 *	3377.440	.493E-02
V5 *	25808.45	.101E+00

CONCENTRATION DATA FOR RUN NO. 6210 ON FEB. 17 1979 AT 1535.
 WIND DIRECTION: 135 DEG UNITS: 1 SCALE FACTOR: 500.
 DATA FOR TRACER GAS NO. 1, ETHANE BACKGROUND CONC. 2039.0 MV-SEC.
 CAL FACTOR: .028 GAS FACTOR (PPM GAS/PPM METHANE): .533

MODEL
 VELOCITY (M/SEC) .88
 SOURCE STRENGTH (PPM) .819E+05
 VOLUME FLOW (CU. M/SEC) .334E-03
 STACK DIAMETER (M) .740E-02
 EXIT VELOCITY (M/SEC) .777E+01
 DENSITY RATIO .60
 BUILDING HEIGHT .0945

LOCATION	RAW DATA (MV-SEC)	NON-DIMENSIONAL CONCENTRATION COEFFICIENT(K)
15 *	2748.177	.304E-02
19 *	3201.054	.499E-02
23 *	3860.718	.782E-02
27 *	4724.244	.115E-01
31 *	8752.535	.288E-01
34 *	12298.00	.440E-01
37 *	13444.12	.489E-01
42 *	16929.83	.639E-01
45 *	19103.61	.732E-01
48 *	19351.41	.743E-01
52 *	16541.63	.622E-01
56 *	12988.62	.470E-01
60 *	12354.66	.443E-01
64 *	7234.215	.223E-01
V13 *	16440.41	.618E-01

CONCENTRATION DATA FOR RUN NO. 6128 ON FEB. 17 1979 AT 13: 9.
 WIND DIRECTION: 135 DEG. UNITS: 1 SCALE FACTOR: 500.
 DATA FOR TRACER GAS NO. 1, ETHANE BACKGROUND CONC. 1884.9 MV-SEC.
 CAL. FACTOR: .028 GAS FACTOR (PPM GAS/PPM METHANE): .533

MODEL
 VELOCITY (M/SEC) .88
 SOURCE STRENGTH (PPM) .819E+05
 VOLUME FLOW (CU. M/SEC) .334E-03
 STACK DIAMETER (M) .740E-02
 EXIT VELOCITY (M/SEC) .777E+01
 DENSITY RATIO .60
 BUILDING HEIGHT .0945

LOCATION	RAW DATA (MV-SEC)	NON-DIMENSIONAL CONCENTRATION COEFFICIENT (K)
19 *	1778.400	.000E+00
20 *	3822.553	.832E-02
21 *	7906.745	.258E-01
22 *	27600.98	.110E+00
23 *	37200.63	.152E+00
24 *	54842.70	.227E+00
25 *	58391.13	.243E+00
26 *	47847.29	.197E+00
27 *	36235.92	.147E+00
28 *	21967.21	.862E-01
29 *	4637.939	.118E-01
30 *	3691.544	.775E-02
31 *	2151.061	.114E-02
32 *	2388.723	.216E-02
V13 *	49193.64	.203E+00

CONCENTRATION DATA FOR RUN NO. 6125 ON FEB. 17 1979 AT 14:24
 WIND DIRECTION: 180 DEG. UNITS: 1 SCALE FACTOR: 500.
 DATA FOR TRACER GAS NO. 1, ETHANE BACKGROUND CONC. 1672 8 MV-SEC.
 CAL. FACTOR: .028 GAS FACTOR (PPM GAS/PPM METHANE) 533

VELOCITY (M/SEC) MODEL
 SOURCE STRENGTH (PPM) .819E+05
 VOLUME FLOW (CU. M/SEC) .334E-03
 STACK DIAMETER (M) .740E-02
 EXIT VELOCITY (M/SEC) .777E+01
 DENSITY RATIO .60
 BUILDING HEIGHT .0945

LOCATION	RAW DATA (MV-SEC)	NON-DIMENSIONAL CONCENTRATION COEFFICIENT(K)
15 *	1980.889	.132E-02
199 *	1816.359	.616E-03
207 *	3272.760	.687E-02
208 *	3903.829	.966E-02
11 *	4787.416	.198E+00
14 *	6145.972	.357E+00
17 *	1211.674	.513E+00
44 *	1653.863	.449E+00
44 *	7958.239	.334E+00
44 *	5240.652	.210E+00
62 *	8387.207	.288E-01
66 *	4631.267	.136E-01
V13 *	75985.77	.319E+00

CONCENTRATION DATA FOR RUK NO. 6328 ON FEB. 17 1979 AT 20:13.
 WIND DIRECTION: 180 DEG. UNITS: 1 SCALE FACTOR: 500.
 DATA FOR TRACER GAS NO. 1, ETHANE BACKGROUND CONC. 2096.5 MV-SEC.
 CAL. FACTOR: .028 GAS FACTOR (PPM GAS/PPM METHANE): .533

MODEL
 VELOCITY (M/SEC) .88
 SOURCE STRENGTH (PPM) .819E+05
 VOLUME FLOW (CU. M/SEC) .334E-03
 STACK DIAMETER (M) .740E-02
 EXIT VELOCITY (M/SEC) .777E+01
 DENSITY RATIO .60
 BUILDING HEIGHT .0945

LOCATION	RAW DATA (MV-SEC)	NON-DIMENSIONAL CONCENTRATION COEFFICIENT(K)
15 *	3559.485	.628E-02
19 **	2537.015	.189E-02
23 ***	4806.353	.116E-01
27 **	6299.348	.180E-01
31 **	3330.477	.530E-02
34 **	6332.079	.182E-01
37 **	3653.994	.524E-01
42 **	3133.113	.302E-01
45 **	11603.74	.408E-01
48 **	9865.049	.333E-01
52 **	10515.00	.361E-01
56 **	8979.506	.225E-01
60 **	3044.094	.228E-01
64 **	3568.725	.321E-01
V15 *	9828.322	.332E-01

CONCENTRATION DATA FOR RUK NO. 6113 ON FEB. 17 1973 AT 9:55.
 WIND DIRECTION: 180 DEG. UNITS: 1 SCALE FACTOR: 500.
 DATA FOR TRACER GAS NO. 1, ETHANE BACKGROUND CONC. 1975.8 MV-SEC.
 CAL. FACTOR: .028 GAS FACTOR (PPM GAS/PPM METHANE): .533

MODEL
 VELOCITY (M/SEC) .88
 SOURCE STRENGTH (PPM) .819E+05
 VOLUME FLOW (CU. M/SEC) .334E-03
 STACK DIAMETER (M) .740E-02
 EXIT VELOCITY (M/SEC) .777E+01
 DENSITY RATIO .60
 BUILDING HEIGHT .0945

LOCATION	RAW DATA (MV-SEC)	NON-DIMENSIONAL CONCENTRATION COEFFICIENT (K)
23 *	10191.65	.353E-01
27 *	14985.92	.558E-01
31 *	26745.13	.106E+00
34 *	37664.64	.153E+00
37 *	58460.60	.242E+00
42 *	52523.80	.217E+00
45 *	28023.39	.112E+00
48 *	12602.62	.456E-01
52 *	4280.445	.989E-02
60 *	1666.825	.246E-03
56 *	1998.265	.966E-04
64 *	1994.212	.792E-04
V5 *	71611.13	.299E+00

APPENDIX B

NUS Corporation Analysis of
Davis-Besse Nuclear Power Plant Wind Data



NORTHERN ENVIRONMENTAL SERVICES DIVISION

4 RESEARCH PLACE
ROCKVILLE, MARYLAND 20850
301/948-7010

NESD-79-178(MP)

May 3, 1979

Mr. Ken Mauer
Toledo Edison Company
Edison Plaza
300 Madison Avenue
Toledo, Ohio 43652

Subject: Wind Direction Persistence for 250-ft Wind by
 $\Delta T_{250'35'}$ Stability Class

- References: (1) Telephone Conversation between R. Peterson
(Colorado State University) and K. Timbre (NUS)
on March 29, 1979
- (2) Telephone Conversation between R. Peterson (CSU)
and M. Septoff (NUS) on March 30, 1979
- (3) Telephone Conversation between R. Peterson (CSU)
and K. Timbre (NUS) on April 30, 1979

Dear Mr. Mauer:

Enclosed you will find the information that was requested in the references. The attached tables present wind direction persistence as a function of atmospheric stability class based on data collected at the Davis-Besse Nuclear Power Plant. In addition, the wind persistence is presented as a function of stability class for "high" wind speeds, i.e., for wind speeds greater than or equal to 20.0 mph. The analysis was based on data collected for the period January to December 1978 and used the 8451 hourly observations of 250 foot level winds and stability class determined from ΔT (250 ft-35 ft). Wind direction was classified into 16 sectors. Each of the enclosed tables present the number of occurrences of wind direction persistence greater than or equal to 3 hours. No observations for these criteria were measured for either class A or B stability.

Tables 1 to 5 contain the wind direction persistence for all wind speeds and tables 6 and 7 contain the wind direction persistence for wind speeds \geq 20.0 mph. Wind speeds \geq 20.0 mph persisting \geq 3 hours occurred only for class D and E stability.

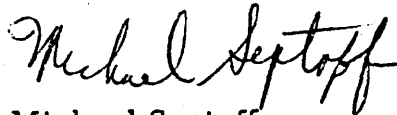
Mr. Ken Mauer
NESD-79-178(MP)
May 2, 1979
Page Two

As shown in the tables the greatest wind direction persistence was 25 hours associated with north-northeast winds and neutral (class D) stability. The largest wind direction persistence for winds greater than or equal to 20.0 mph was 18 hours associated with north-northeast and west-southwest winds and neutral conditions.

The results of the analysis were verbally transmitted to R. Peterson on April 30, 1979 (Reference 3). As the result of that conversation R. Peterson requested additional analyses. The analysis is to determine wind direction persistence as a function of stability class for winds in the range of 11 to 13 m/s. In addition, we were requested to provide analog strip charts for a few of the periods when the wind was persisting for 3 or more hours with speeds between 11 and 13 m/s. The results of the additional analyses will be completed and transmitted by the end of the week.

If you have any questions please call.

Very truly yours,



Michael Septoff
Staff Environmental Meteorologist

MS/ewd

Enclosures

cc: R. Peterson - Colorado State University

TABLE 1

NUMBER OF OCCURRENCES OF WIND DIRECTION PERSISTENCE
 FOR C STABILITY CLASS AND ALL WIND SPEEDS
 TECO DAVIS BESSE 250' WINDS 1/1/78 - 12/31/78

Hours of Persistence	N	NNE	NE	ENE	E	ESE	SE	SSE	S	SSW	SW	WSW	W	WNW	NW	NNW	Calm	Total
3	0	0	0	2	0	0	0	0	1	0	1	1	0	0	0	1	0	6
4				1					0		0	0				0		1
5				0														

TABLE 2

NUMBER OF OCCURRENCES OF WIND DIRECTION PERSISTENCE
 FOR D STABILITY CLASS AND ALL WIND SPEEDS
 TECO DAVIS BESSE 250' WINDS 1/1/78 - 12/31/78

Hours of Persistence	N	NNE	NE	ENE	E	ESE	SE	SSE	S	SSW	SW	WSW	W	WNW	NW	NNW	Calm	Total
3	69	105	184	80	150	58	7	4	16	27	27	98	101	53	34	31	0	1034
4	45	75	140	50	106	33	3	2	10	14	15	63	66	39	19	16		696
5	30	55	112	34	82	21	0	0	6	6	7	42	43	30	10	11		489
6	20	41	90	24	64	13			2	5	4	28	31	25	5	9		361
7	12	34	72	17	51	9			0	4	2	20	22	21	2	8		274
8	6	27	59	11	40	8				3	1	17	16	19	1	7		215
9	2	22	50	5	30	7				2	0	14	11	17	0	6		166
10	1	18	42	1	20	6				1		11	6	15		5		126
11	0	15	35	0	14	5				0		9	4	13		4		99
12		14	28		10	4						7	3	11		3		80
13		13	22		6	3						6	2	10		2		64
14		12	17		3	2						5	1	9		1		50
15		11	13		1	1						4	0	8		0		38
16		10	9		0	0						3		7				29
17		9	6									2		6				23
18		8	4									1		5				18
19		7	2									0		4				13
20		6	1											3				10
21		5	0											2				7
22		4												1				5
23		3												0				3
24		2																2
25		1																1
26		0																

TABLE 3

NUMBER OF OCCURRENCES OF WIND DIRECTION PERSISTENCE
 FOR E STABILITY CLASS AND ALL WIND SPEEDS
 TECO DAVIS BESSE 250' WINDS 1/1/78 - 12/31/78

Hours of Persistence	N	NNE	NE	ENE	E	ESE	SE	SSE	S	SSW	SW	WSW	W	WNW	NW	NNW	Calm	Total
3	5	5	0	1	5	3	10	3	5	30	45	34	27	21	5	2	0	201
4	3	2		0	2	1	5	1	1	19	28	19	14	15	2	1		113
5	2	0			1	0	2	0	0	11	16	10	5	10	0	0		57
6	1				0		0			7	9	6	2	7				32
7	0									5	3	3	0	4				15
8										4	0	1		2				7
9										3		0		0				3
10										2								2
11										1								1
12										0								

TABLE 4
 NUMBER OF OCCURRENCES OF WIND DIRECTION PERSISTENCE
 FOR F STABILITY CLASS AND ALL WIND SPEEDS
 TECO DAVIS BESSE 250' WINDS 1/1/78 - 12/31/78

Hours of Persistence	N	NNE	NE	ENE	E	ESE	SE	SSE	S	SSW	SW	WSW	W	WNW	NW	NNW	Calm	Total
3	1	0	0	0	0	1	3	11	9	4	3	7	12	0	3	0	0	54
4	0					0	2	7	4	2	2	4	6		0			27
5							1	5	2	1	1	3	3					16
6							0	3	1	0	0	2	1					7
7								2	0			1	0					3
8								1				0						1
9								0										

TABLE 5

NUMBER OF OCCURRENCES OF WIND DIRECTION PERSISTENCE
 FOR G STABILITY CLASS AND ALL WIND SPEEDS
 TECO DAVIS BESSE 250' WINDS 1/1/78 - 12/31/78

Hours of Persistence	N	NNE	NE	ENE	E	ESE	SE	SSE	S	SSW	SW	WSW	W	WNW	NW	NNW	Calm	Total
3	1	0	0	0	2	0	0	3	2	1	0	8	4	2	5	0	0	28
4	0				1			2	0	0		6	2	0	1			12
5					0			1				5	1		0			7
6								0				4	0					4
7												3						3
8												2						2
9												1						1
10												0						0

TABLE 6

NUMBER OF OCCURRENCES OF WIND DIRECTION PERSISTENCE
 FOR D STABILITY CLASS AND WIND SPEEDS ≥ 20.0 MPH
 TECO DAVIS BESSE 250' WINDS 1/1/78 - 12/31/78

Hours of Persistence	N	NNE	NE	ENE	E	ESE	SE	SSE	S	SSW	SW	WSW	W	WNW	NW	NNW	Total
3	11	26	29	9	43	14	0	0	0	5	10	47	47	23	10	3	277
4	7	22	25	6	30	9				2	5	35	33	15	6	1	196
5	4	19	22	5	22	7				0	2	27	22	11	4	0	145
6	2	16	19	4	16	5					1	20	15	7	3		108
7	1	13	16	3	10	4					0	17	11	5	2		82
8	0	11	14	2	6	3						15	8	4	1		64
9		10	12	1	2	2						13	5	3	0		48
10		9	10	0	0	1						11	2	2			35
11		8	8			0						9	0	1			26
12		7	5									7		0			19
13		6	4									6					16
14		5	3									5					13
15		4	2									4					10
16		3	1									3					7
17		2	0									2					4
18		1										1					2
19		0										0					0

TABLE 7
 NUMBER OF OCCURRENCES OF WIND DIRECTION PERSISTENCE
 FOR E STABILITY CLASS AND WIND SPEEDS ≥ 20.0 MPH
 TECO DAVIS BESSE 250' WINDS 1/1/78 - 12/31/78

Hours of Persistence	N	NNE	NE	ENE	E	ESE	SE	SSE	S	SSW	SW	WSW	W	WNW	NW	NNW	Total
3	0	0	0	0	0	0	1	0	2	10	16	10	1	7	2	0	49
4							0		1	8	10	6	0	4	1	0	30
5										6	6	3		2	0		17
6										5	4	2		1			12
7										4	2	1		0			7
8										3	0	0					3
9										2							2
10										1							1
11										0							0



NORTHERN ENVIRONMENTAL SERVICES DIVISION

4 RESEARCH PLACE
ROCKVILLE, MARYLAND 20850
301/948-7010

142

NESD-79-195(MP)
May 4, 1979

Mr. Ken Mauer
Toledo Edison Company
Edison Plaza
300 Madison Avenue
Toledo, Ohio 43652

Subject: Wind Direction Persistence For 250-ft Wind By $\Delta T_{250'-35'}$ Stability Class For Wind Speeds Between 11 and 13 mps

- Reference: (1) Telephone conversation between R. Peterson (Colorado State University) and K. Timbre (NUS) on April 30, 1979
- (2) Letter to K. Mauer from M. Septoff dated May 2, 1979 (NESD-79-178(MP))

Dear Mr. Mauer:

The following presents the results of the analysis requested by R. Peterson (Reference 1). This analysis is similar to that provided to Dr. Peterson in Reference 2 with the addition of the determination of the occurrences of wind persistence as a function of atmospheric stability class for wind speeds greater than or equal to 24.5 mph (11 mps) and less than or equal to 29.5 mph (13 mps). The analysis was based on data collected at the Davis-Besse Nuclear Power Plant during the period January to December 1978 and used the 8451 hourly observations of 250 foot level winds with stability class determined from $\Delta T(250ft-35ft)$. Wind direction was classified into 16 sectors. The attached tables present the number of occurrences of wind direction persistence greater than or equal to 3 hours. These conditions existed only for class D and E stability.

The greatest wind direction persistence for wind speeds ≥ 24.5 mph and ≤ 29.5 mph was 6 hours associated with north-northeast winds and neutral (D) stability.

Mr. Ken Mauer
NESD-79-195(MP)
May 4, 1979
Page Two

Also attached as requested in reference 1 are copies of the analog strip charts for the 250 foot level wind speed and direction which illustrate three examples of wind direction persistence ≥ 3 hours with moderate wind speeds. The wind speed scale for the chart is 0 to 50 mph with a chart speed of 2 inches per hour.

If you have any questions, please call.

Very truly yours,



Keith Timbre
Assistant Environmental Meteorologist

/dat
attch

cc: R. Peterson - Colorado State University
M. Septoff

TABLE 1-1
 NUMBER OF OCCURRENCES OF WIND DIRECTION PERSISTENCE
 FOR D STABILITY CLASS AND WIND SPEEDS ≥ 24.5 MPH AND ≤ 29.5 MPH
 TECO DAVIS BESSE 250' WINDS 1/1/78 - 12/31/78

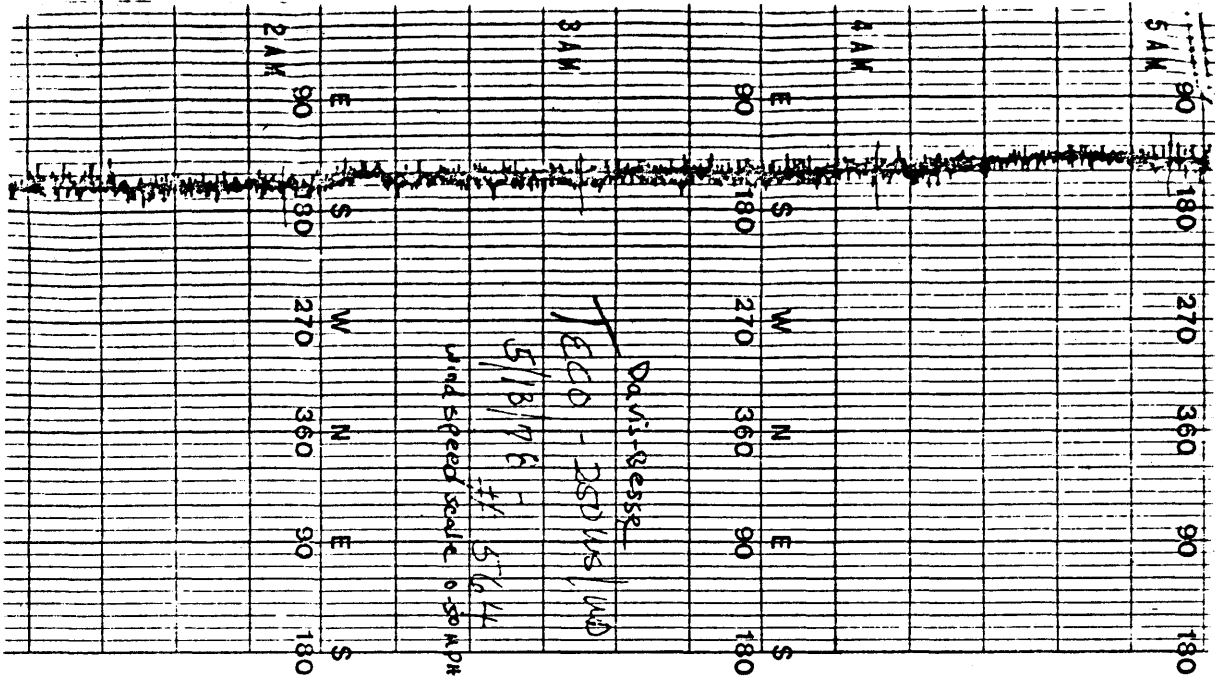
Hours of Persistence	N	NNE	NE	ENE	E	ESE	SE	SSE	S	SSW	SW	WSW	W	WNW	NW	NNW	Total
3	0	9	5	0	8	1	0	0	0	0	0	6	6	3	1	1	40
4		6	2		4	0						2	2	1	0	0	17
5		3	1		2							0	0	0			6
6		1	0		0												1
7		0															0

TABLE 2-1

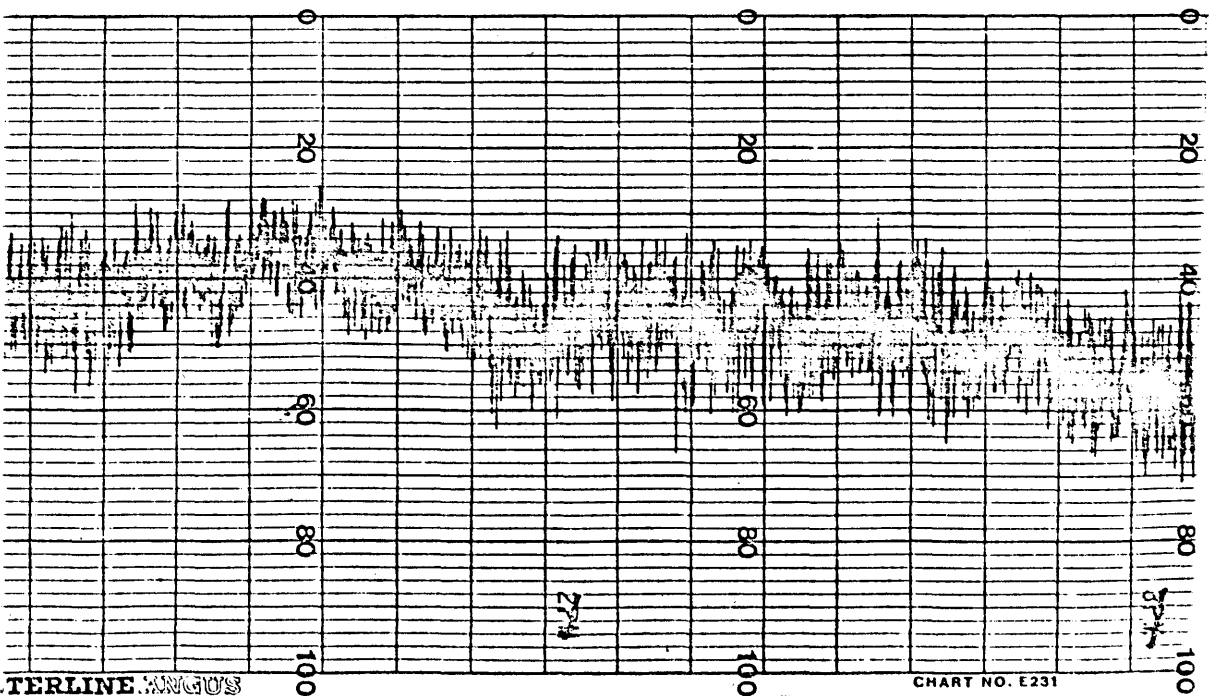
NUMBER OF OCCURRENCES OF WIND DIRECTION PERSISTENCE
 FOR E STABILITY CLASS AND WIND SPEEDS ≥ 24.5 MPH AND ≤ 29.5 MPH
 TECO DAVIS BESSE 250' WINDS 1/1/78 - 12/31/78

Hours of Persistence	N	NNE	NE	ENE	E	ESE	SE	SSE	S	SSW	SW	WSW	W	WNW	NW	NNW	Total
3	0	0	0	0	0	0	0	0	0	3	7	2	0	2	0	0	14
4										2	4	0		0			6
5										1	1						2
6										0	0						0

USE THIS TIME SCALE (2"/HR)



DAVIS-RESSK
TECD - 250 W/S / W/D
5/18/76
#1 5644
Wind speed scale 0-50 MPH



TERLINE WINDUS
DIANAPOLIS, IND., U.S.A.

CHART NO. E231

USE THIS TIME SCALE (2"/HR)

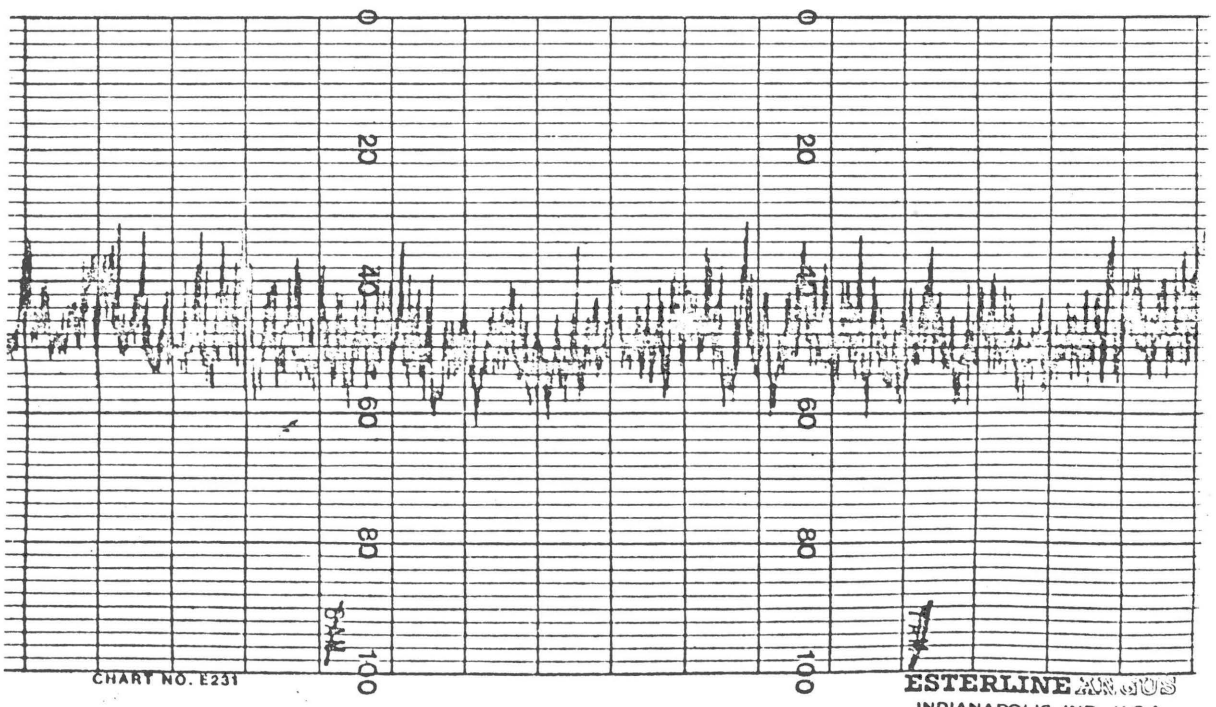
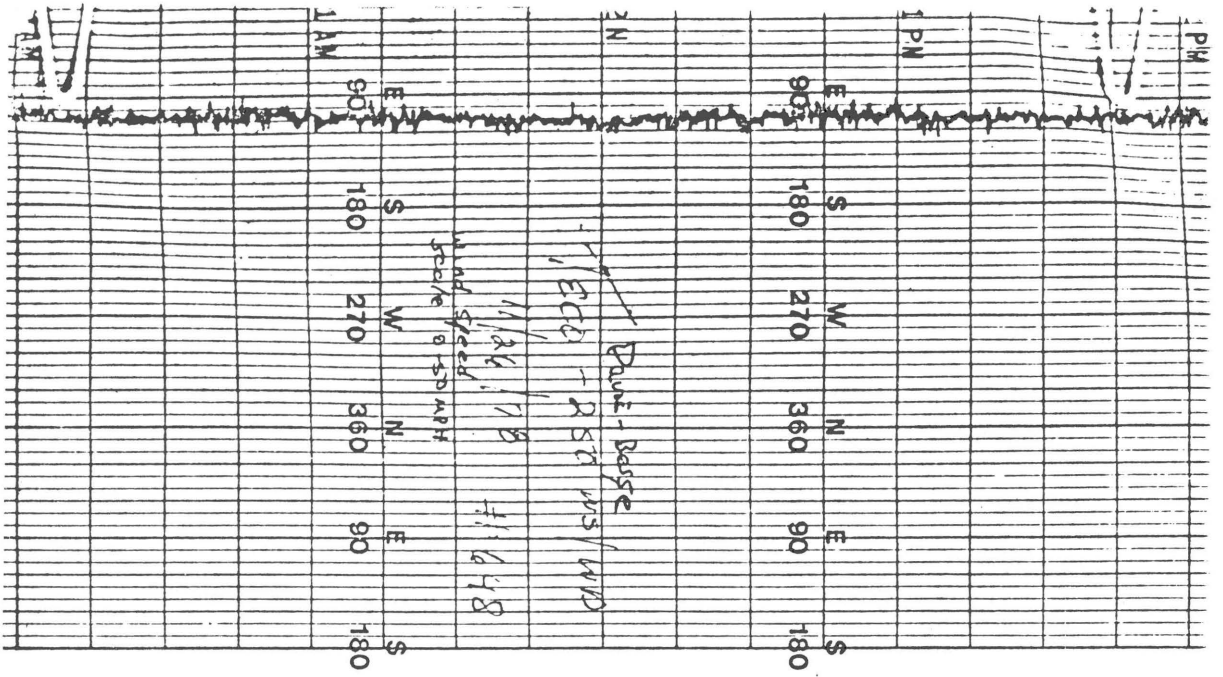
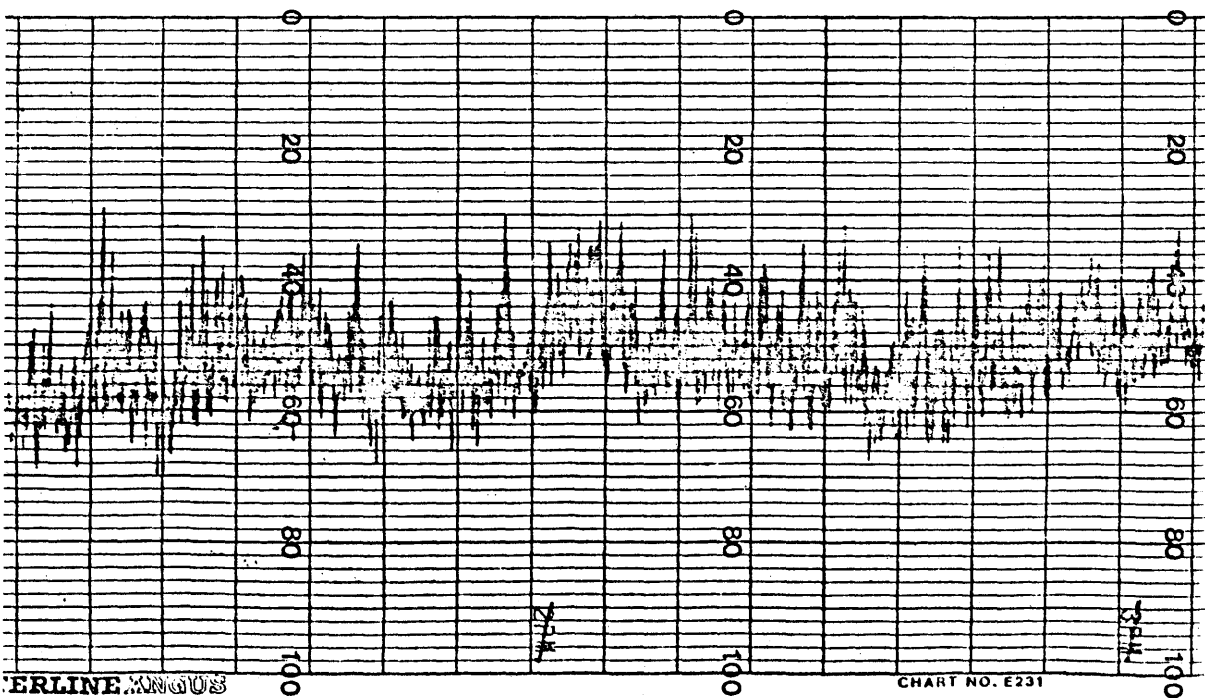
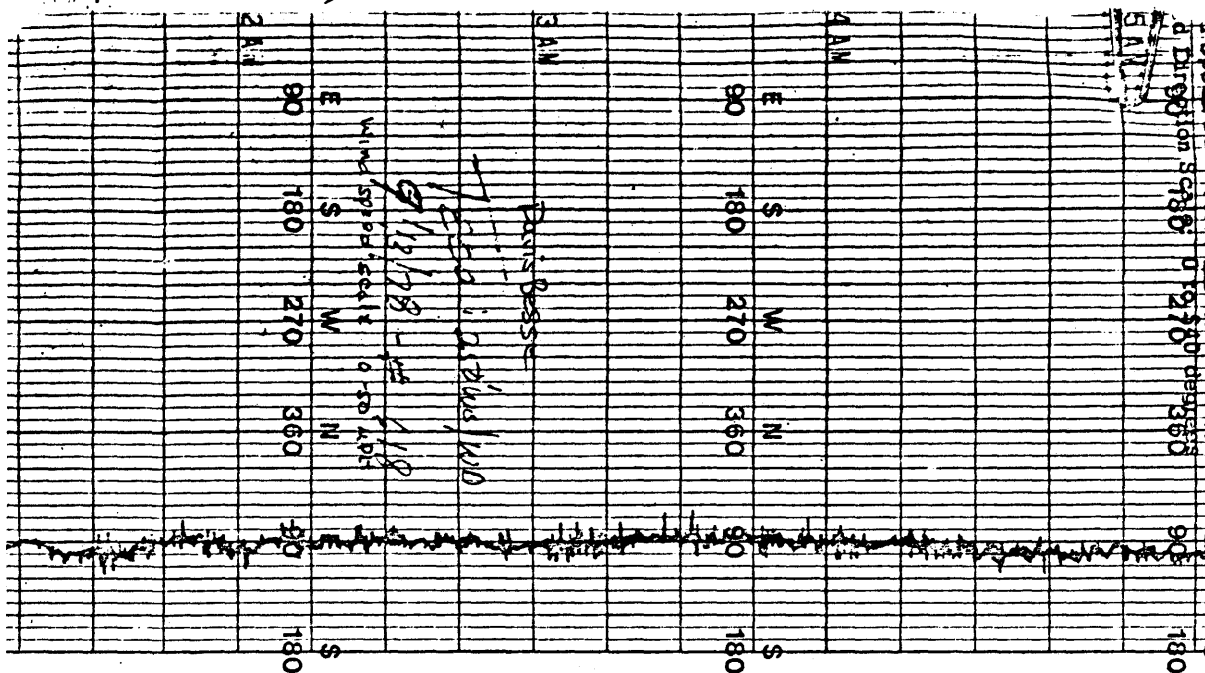


CHART NO. E231

ESTERLINE RECORDS
INDIANAPOLIS, IND., U.S.A.

USE THIS TIME SCALE (2"/HR)



ERLINE KINGS
ANAPOLIS, IND., U.S.A.

CHART NO. E231